For Alec, Jack, Nick and Paul Greene.

research skills. Through his advisement and unwavering commitment to my success, Dr. Xi has helped me to develop confidence and independence in scientific research. I thank him for his guidance and continued support throughout the years.

I could not have asked for better lab-mates than Dr. Jianfeng Wu and Kevin Boehnke. I am eternally obliged to Jianfeng, who has mentored me in the lab, collaborated with me at every level, and coached me through many failed and successful experiments. In addition to his wealth of research expertise, Jianfeng's patience and humor has rescued me more times than I can recall. I thank Kevin Boehnke for always being an intellectual sounding board, for the many times he happily reviewed my slides and abstracts, and for always being available to share a genuine smile, or a tasty lunch. I also appreciate Gayathri Vadlamudi for the hours she spent listening to me and for her assistance in the lab. Her comfort and support was critical to my progress.

I thank Ting Luo for providing me with Rep-PCR methods and for his gracious help with the confocal microscope and rendering biofilm images. I am grateful to my colleagues Christine West, Deana Thomas, Hae-Ryung Park, Kelly Hogan and Kate Thompson for their emotional support.

I am thankful for the writing support and consultation I have received from Kirsten Herald through the Writing Lab and for the statistical support and advice provided by the staff at the Center for Statistical Consultation and Research (CSCAR).

TABLE OF CONTENTS

LIST OF FIGURES

LIST OF TABLES

ABSTRACT

Healthcare-associated infections (HAIs) are a serious problem globally and device-associated infections accounted for more than 25% of all HAIs in the U.S. A*cinetobacter baumannii*, a gram-negative opportunistic pathogen, is commonly associated with HAIs and biofilm-related infections worldwide. Factors contributing to the clinical persistence of *A. baumannii* include biofilm formation, multiple drug resistance (MDR) mechanisms and a tenacious ability to survive in the environment. Understanding how the interaction of these virulence factors impact environmental persistence will allow for more effective infection control and help minimize environmentally mediated transmission of *A. baumannii.*

For this study, 132 clinical isolates from 115 patients and 54 environmental isolates were collected from the University of Michigan Hospital from August 2012-January 2014. Rep-PCR banding patterns, antibiotic susceptibility profiles, biofilm formation and desiccation tolerance were determined. The objective of the first study was to compare the trade-offs in fitness imposed by the ability to form biofilms, tolerate desiccation and MDR between *A. baumannii* environmental and clinical strains. This study demonstrated that the MDR positive phenotype was deleterious for environmental strains and the high biofilm phenotype was critical for survival, providing evidence of a trade-off between antibiotic resistance and desiccation tolerance, driven by condition-dependent adaptation. This is important because it increases current understanding of the association of the MDR phenotype with persistence, and demonstrates that the association is mediated by environmental conditions.

Biofilm cells are able to detach from the biofilm and promote rapid recontamination. The second study investigated the hypothesis that detached biofilm cells revert to the planktonic

phenotype by comparing the antibiotic susceptibilities of *A. baumannii* planktonic, biofilm and detached sessile cells, and found that the detached sessile cells were phenotypically distinct from planktonic cells with respect to antibiotic susceptibilities. This is significant because it suggests that antibiotic therapies should be sufficient to target the detached cell population rather than planktonic cells for the treatment of biofilm-related infections. In addition, I compared the ability for *A. baumannii* to form biofilm on six different surface types and found that *A. baumannii* cells did not attach well to glass; polycarbonate followed by brushed stainless steel was the substrata best suited for biofilm growth. This is important because polycarbonate is a material commonly used to in medical implants and therefore should be avoided.

Currently, an assumption used to simplify mathematical modeling of pathogen transport is that the exchange of contamination between the skin and surfaces is symmetrical. The third study challenged this assumption by measuring the bi-directional transfer efficiencies of *A. baumannii*, with and without latex glove use. Then, I developed a fate and transport mathematical model to determine if the realistic relaxation of the simplifying assumption of symmetry changed the risk of pathogen transport between patients and rooms. These studies demonstrated that the transfer efficiencies of *A. baumannii* were asymmetrical and the simplifying assumption of symmetry inflated the role of the environment while minimizing the true impact of healthcare worker-mediated transmission between patients.

This research is the first to evaluate the fitness cost of desiccation tolerance due to biofilm formation and multidrug resistance among clinical as well as environmental *A. baumannii* isolates. It is the first study to investigate the hypothesis that detached biofilm cells revert to the planktonic phenotype and is the first to compare *A. baumannii* biofilms across a range of material types. In addition, this is the first study to address the current simplifying

assumption of bacterial transfer symmetry in mathematical modeling. Areas identified for future research include genetic studies identifying targets to explain the variation in survival observed between MDR clinical and environmental isolates and research characterizing the full nature of the detached biofilm cell population, which may provide more clues for the treatment, and control of biofilm-related infections. In addition, the fate-and-transport mathematical model developed in this study should be expanded to incorporate the data collected in this research, with a realistic relaxation of the simplifying assumptions, allowing for robust estimates of the risk of environmental transmission of *A. baumannii* between patients.

In conclusion, this dissertation advances our understanding of the association between resistance, biofilms, and persistence. Results of my investigations will improve the accuracy of environmental mediated infectious disease transmission systems and can be used to strengthen current guidelines to control healthcare-associated infections. Further, the results provide new insights, that I hope will stimulate innovative approaches to reduce the risk of biofilm-related infections and curtail the environmental persistence and transmission of *A. baumannii*.

CHAPTER I

Background and Overview of Dissertation Thesis

1.1.0 HEALTHCARE-ASSOCIATED INFECTIONS

Healthcare-associated infections (HAIs), or infections incurred by a patient during their hospital stay that was not present at the time of hospital admittance, is a significant problem and affects millions of patients every year worldwide (1). In 2002, approximately 99,000 deaths in the United States alone were attributed to HAIs. The implementation of improved infection control practices and surveillance methods have led to a reduction in HAIs in the U.S., but the incidence of HAIs remains high; in 2011, approximately 1 in every 25 hospitalized patients had at least one HAI and more than 10% of the approximately 722,000 HAIs in U.S. hospitals resulted in death (2). The overall economic burden of HAI's in the U.S. is huge, costing the healthcare industry roughly $6.5 billion in 2004 alone. . In addition to increased costs and excess mortality, HAI's result in increased patient hospital stays, increased development of multidrug resistant microorganisms and overall increased healthcare costs for the patient and their families (1), (3).

Risk factors for acquiring an HAI during hospitalization include admittance into a critical care unit, use of indwelling catheters/devices and long hospital stays (1), (2), (4). Device-associated infections, particularly those associated with central lines, urinary catheters and ventilators accounted for more than 25% of all HAIs in 2011(2), (5), (6). Most common

infection types are pneumonia and surgical-site infections (2) and the microorganisms culpable

in HAIs are diverse. Commonly associated pathogen in HAIs include *S. aureus, K. pneumonia,*

A. baumannii, and *P. aeruginosa,* among others (2), (4).

1.2.0 *ACINETOBACTER BAUMANNII*: AN EMERGING NOSOCOMIAL PATHOGEN

The Genus *Acinetobacter* is a group of non-motile, non-fermentative, strictly aerobic,

gram-negative coccobacillary rods that belong to the family Moraxellaceae. While most of the

32 taxonomically distinct species are not associated with disease, one in particular, *Acinetobacter*

baumannii, has emerged over the past 10 years as a clinically significant, nosocomial pathogen

(7), (8), (9). Risk factors for acquiring *A. baumannii* infections include previous antibiotic

treatment, indwelling device/catheter use, critical illness, prolonged hospital stay and ICU

residency (10), (11), (12), (13). Although known for its role in healthcare-associated pneumonia

– particularly ventilator-associated pneumonia - *A. baumannii* has also been implicated in many

other infections including urinary tract infections, bacteremia, surgical infections, device-related

infections, decubitus ulcers and secondary meningitis (12), (14). Of all the nosocomial

infections that result in death in the U.S., up to 3% are due to *A. baumannii* infections. Within

the ICU, up to 10% of the nosocomial infection-related deaths are due to *A. baumannii* infections

(8), (14).

1.2.1 Antibiotic resistance of A. baumannii

Worldwide, *Acinetobacter baumannii* has been shown to exhibit a high level of resistance

to most antibiotics. Historically, carbapenems were the preferred treatment, but they are no

longer consistently effective against *A. baumannii* infections (10), (15), (16). The increasing

prevalence of multidrug resistant *A. baumannii* has led to many cases where colistin (which is

highly nephrotoxic) is the only remaining effective treatment (17). Multidrug-resistance (MDR) is defined as being non-susceptible to three or more classes of antibiotics (16). A more specific definition of MDR for *A. baumannii* was provided by Manchanda, et al. as non-susceptibility to at least three of the following classes of antibiotics: cephalosporins, fluroquinolones, and aminoglycosides (18). *A. baumannii* can also be described as extensively drug resistant (XDR) or pan-drug resistant (PDR); XDR describes isolates that are MDR plus resistant to carbapenems and PDR describes isolates that are XDR plus resistant to polymyxins and tigecycline (18). Clinically relevant strains have a higher level of drug resistance than non-clinically significant strains (19), (20).

Of great concern is *A. baumannii's* ability to rapidly develop antibiotic resistance. A 2006 study by Fournier, et al. identified 45 acquired resistance genes in *A. baumannii* strain AYE (7). Known *A. baumannii* resistance mechanisms include enzymes that inactivate or modify antimicrobials, multidrug efflux pumps, decreased outer membrane permeability, alteration of target sites, ribosomal mutations/modifications, metabolic bypass, and a lipopolysaccharide mutation (13), (18), (21). The low permeability of the outer membrane of *A. baumannii* provides an inherent resistance to certain antibiotics. *A. baumannii* are also able to take up and incorporate plasmids, transposons and integrons, genetic elements that can confer drug resistance. Forming a biofilm also confers resistance (19).

1.3.0 BIOFILMS: A GENERAL OVERVIEW

Biofilms are a collection of bacteria, fungi, or other microorganisms in which the cells adhere to a surface and each other and are embedded in a self-produced matrix of extracellular polymeric substances (EPS). This EPS, which contains cellular components such as extracellular

DNA, proteins, lipids and polysaccharides, acts as a glue-like substance to keep the cells anchored together to a surface. Biofilm formation occurs in four cyclic phases: reversible and irreversible attachment, micro-colony formation, macro-colony formation of complex, three-dimensional structure formation and detachment (22), (23). The detachment step is critical for the biofilm cells to be able to disseminate and cause subsequent infection (6). Biofilm detachment occurs by two mechanisms; erosion, which is the continual detachment of individual cells or minute fragments of the biofilm and sloughing, which is a rapid, substantial loss of biofilm fragments (24). The cells of the biofilm are physiologically different from their planktonic counterparts (23). Planktonic cells, which are free-floating cells, begin the initial stages of biofilm formation; once they attach to a surface, they undergo transcriptional regulation changes and convert from the planktonic phenotype to the biofilm (community) phenotype (25). This natural conversion to the biofilm phenotype has only recently come to light. Detached biofilm cells are often regarded as planktonic cells in the literature (23).

A key feature of the biofilm is the genetic and phenotypic diversity of the microbial populations within the biofilm. This community of interdependent microorganisms are able to communicate with each other via quorum sensing (25), (26). Quorum sensing regulates many physiological processes within the biofilm and occurs in response to cell-population density levels and environmental stress. For example, as population density changes, the bacteria release pheromones and other chemical signaling molecules for communicating and regulating many important processes such as conjugation, motility, biofilm formation and virulence (27), (28).

1.3.1 Biofilms and infectious diseases

Biofilm formation is a documented mechanism of pathogenesis in device-related infections. Biofilms promote the survival of microorganisms on device surfaces such as

prostheses, heart valves and catheters (29), (30). Biofilms can cause disseminated infections or environmental contamination via detachment of cells or aggregates of cells during the lifecycle of the biofilm (24). The Centers for Disease Control and Prevention estimates that more than 65% of all infections are biofilm-related.

The biofilm serves as a protective, hydrated barrier between the cells and the external environment. In the body, biofilms can persist on both dead and living tissue (i.e. endocarditis). Biofilms facilitate survival under harsh conditions and physiochemical stresses, providing a protective environment within which the infective cells can survive, detach and reseed (31). In the open environment, the biofilm protects cells from low nutrient resources and harsh conditions such as desiccation and disinfection (25), (28), (32).

The biofilm matrix also provides protection from antibiotics. Biofilm cells can be hundreds or thousands of times more resistant to antibiotics compared to their planktonic counterparts (33), (34) and *in vitro* antibiotic susceptibility testing only considers planktonic cells. Furthermore, the biofilm phenotype can result in viable cells that cannot be cultured. This is a problem for identifying the cause of a biofilm-associated infection and for determination of antibiotic susceptibilities (25), (35), (36).

The mechanisms of antibiotic protection conferred by biofilms are poorly understood. Putative processes that have been identified include impeding the diffusion of the drug into the matrix, arresting positively charged antibiotics via binding by negatively charged polymers and the inherent slow growth rate of sessile cells (37), (38). The ability for cells to detach from the biofilm and colonize new locations explains how biofilms can serve as the source of persistent infections. The heterogeneous genotypic and phenotypic characteristics of detaching sessile cells likely promote their ability to survive in changing environmental conditions (39).

1.4.0 *A. BAUMANNII* AND BIOFILM FORMATION

Acinetobacter baumannii is a known biofilm former. Biofilm formation by *A. baumannii* is regulated by quorum sensing via the AbaR-AbaI paired system (27) and is encouraged by many factors including the possession of bacterial appendages such as pili and flagella and bacterial surface components such as outer membrane proteins and adhesins (28). The ability for any pathogen to adhere to a surface is a critical first step in the formation of biofilm. *A. baumannii* mediate attachment to abiotic surfaces via pili, encoded by the *csu*A/BABCDE chaperone-usher pilus assembly operon (40). Attachment to epithelial cells occurs by means of the PER-1 extended-spectrum *β*-lactamase via the *bla*PER-1 gene, which is widespread among cefepime-resistant *A. baumannii* (30). Loehfelm and colleagues reported the identification of a biofilm-associated protein (Bap) in *A. baumannii*, which is believed to play a role in the initial adherence on medically relevant surfaces and may also play a role in adherence to host tissue and in biofilm formation (41), (42).

1.5.0 *A. BAUMANNII* AND ENVIRONMENTAL SURVIVAL

The prevention of *A. baumannii* infection is challenging, because *A. baumannii* has a remarkable ability to survive in/on medical devices and within the hospital environment; it is resistant to some sanitizers, dehydration, UV radiation, detergents and most antibiotics (10), (43). The tenacity of *A. baumannii* is underscored by its ability to survive in conditions that other pathogens, such as *Staphylococcus aureus* (MSRA) cannot survive. Research by Constanze Wendt, et al. found that *A. baumannii* can survive in dry conditions for prolonged periods of time, contributing to the ability of this pathogen to persist in hospitals endemically (44). A study by Jawad and colleagues subjected 39 clinical isolates to desiccation on glass

coverslips and found that the mean survival time was 27 days (45). Biofilm formation was not considered in this 1998 study, which likely explains such extended environmental survival. Biofilms also provide protection from disinfection. Standard hospital biocides, e.g. against MRSA and *Pseudomonas aeruginosa,* may be effective at eradicating planktonic cells from surfaces but not all are effective at killing pathogens that propagate as biofilms (46), (47).

There are several proposed mechanisms by which *A. baumannii* are able to survive in the open environment, all of which have only recently been addressed. The most studied is the ability of *A. baumannii* cells to enter a dormant state, particularly within the biofilm. In dormancy, proteins associated with the dormant state are overexpressed and those that are not associated have decreased expression and heightened post-translational regulation of protein synthesis. Another strategy is tighter packing of the chromosome when under environmental stress, which provides added protection to the genetic code (48).

1.6.0 *A. BAUMANNII* TRANSMISSION

Transmission of *A. baumannii* can occur from person-to-person and via the environment (i.e. fomites). *Acinetobacter* contaminated surfaces play an important role in the transmission of this pathogen in hospitals (8), (49), (50). Transmission of *Acinetobacter* species may occur from moist vectors and the desiccated cells can remain viable constituents suspended in dust (51). *A. baumannii* is known to colonize the skin in warmer, moist climates; skin colonization of *A. baumannii* occurs within healthcare institutions (52).

Direct contact of the healthcare worker (HCW) with contaminated patients and contaminated environments is the most likely mechanism of transport of *A. baumannii* in the hospital setting. Griffith et al. found that patient wounds can become contaminated with *A.*

baumannii once in the healthcare setting. A review published by Moultrie et al. concur with this finding reporting that hospitalized patients with wound injuries, and those using invasive devices are at high risk for acquiring nosocomial *A. baumannii* infection (52), (53). A case-control study conducted in 2000 found that, after controlling for confounding factors, those who developed *A. baumannii* infection were exposed to more *A. baumannii* infected patients than controls (Odds ratio, 1.1, 95% CI, 1.01-1.2; p=0.02). The reservoir of the outbreak could not be determined, further supporting the author's hypothesis that cross-transmission between patients, via healthcare workers and fomites promoted the spread of the infection within this outbreak (54).

The gloves and gowns of healthcare workers can be a source of contamination and spread of *A. baumannii* in hospitals. A 2010 study by Morgan et al. looked at the frequency of colonization of *A. baumannii* and *Pseudomonas aeruginosa* on the gloves and gowns of healthcare workers. Using workers who were culture negative for both *A. baumannii* and *P. aeruginosa*, the frequency of transmission of these microorganisms to gloves, gowns and hands, after having cared for an infection positive patient, was observed. The frequency of contamination was higher for *A. baumannii* than for *P. aeruginosa* with 38.7% of contacts producing detectible levels. This is higher than that observed in previous studies by this group for *S. aureus* (18.5%) and vancomycin-resistant *Enterococcus* (8.5%). They also found that gloves were contaminated more frequently than gowns; hands were contaminated with *A. baumannii* even after the gloves were removed and the hands were washed in 4.5% of contacts (55). This study suggests that compared to other important nosocomial pathogens, *A. baumannii* is transmitted to healthcare worker garb or protective barriers at a higher frequency. In addition to gloves and gowns, *A. baumannii* survives on many other environmental surfaces including

pillows, mattresses, bed rails, ventilator tubing, intravascular catheters, resuscitation equipment and patient room keyboards (12), (56), (57), (58).

1.7.0 KNOWLEDGE GAPS

It is widely accepted that biofilms are a mechanism of pathogenesis, providing pathogens protection from the harsh environment, protection from many antibiotics and promoting environmental survival. Some antibiotic resistance mechanisms, such as colistin resistance, concurrently confer desiccation tolerance, an important environmental survival mechanism. However, much of what we have learned has been studied primarily in clinical strains and these characteristics have only been examined individually or in pairs with one another. Environmental pressures can cause variations in the expression of different phenotypes (59). The trade-offs in fitness imposed by the ability to form biofilms, tolerate desiccation and multidrug resistance are potentially different for *A. baumannii* strains that live primarily in the environment, compared to clinical strains adapted to living in the human host. In the environment, it may be more beneficial to resist desiccation by forming biofilms and in the human host more beneficial to maintain resistance to multiple antibiotics than resist desiccation. Research into whether these trade-offs occur and direct comparisons between clinical and environmental *A. baumannii* strains is lacking. To our knowledge, no studies have evaluated the fitness cost of antibiotic resistance in environmental strains.

The individual stages of the biofilm life cycle have different roles in aiding the security and pathogenesis provided by the collective biofilm. These stages are potential targets for prevention and control. Using materials that repel cells from the surface can limit biofilm formation, but few studies have assessed whether *A. baumannii* biofilm formation varies by

surface (60), (61), (62). Despite evidence that the biofilm is phenotypically and genetically heterogeneous, cells that detach from the biofilm are typically regarded as planktonic cells. Whether the detached sessile cells revert to the planktonic phenotype or maintain the biofilm phenotype is not known. Lastly, the transfer efficiencies of *A. baumannii* have never been measured, nor has the effect of glove use on pathogen transfer efficiency been quantified. Specific pathogen transmission parameters are needed to fill current knowledge gaps of environmentally mediated infectious disease transmission systems. Further, the simplifying assumption of symmetry in the transfer of pathogens during a touch with the environment lacks justification.

1.8.0 RESEARCH OBJECTIVES AND SUMMARY OF STUDIES

The objective of this research was to evaluate the major factors contributing to the clinical success of *A. baumannii* in hospitals: namely biofilm formation, multidrug resistance and environmental persistence, with an emphasis on the role of biofilms. By understanding how environment surface types, multidrug resistance and biofilm formation contributes to the environmental survival and transmission of *A. baumannii*, advancements can be made in the prevention and control of biofilm-related infections and in environmentally mediated pathogen transmission. Additionally, it is the goal of this research to derive data to develop a more robust mathematical fate-and-transport model to examine *A. baumannii* transmission patterns and quantify the risk of exposure to patients.

1.10.0 REFERENCES

1.   Allegranzi B, Bagheri Nejad S, Combescure C, Graafmans W, Attar H, Donaldson L, et al. Burden of endemic health-care-associated infection in developing countries: systematic review and meta-analysis. Lancet 2011;377(9761):228-41.

2.   Magill SS, Edwards JR, Bamberg W, Beldavs ZG, Dumyati G, Kainer MA, et al. Multistate point-prevalence survey of health care-associated infections. N Engl J Med 2014;370(13):1198-208.

3.   Sievert DM, Ricks P, Edwards JR, Schneider A, Patel J, Srinivasan A, et al. Antimicrobial-resistant pathogens associated with healthcare-associated infections: summary of data reported to the National Healthcare Safety Network at the Centers for Disease Control and Prevention, 2009-2010. Infect Control Hosp Epidemiol 2013;34(1):1-14.

4.   Zorgani A, Abofayed A, Glia A, Albarbar A, Hanish S. Prevalence of Device-associated Nosocomial Infections Caused By Gram-negative Bacteria in a Trauma Intensive Care Unit in Libya. Oman Medical Journal 2015;30(4):270-5.

5.   Dohnt K, Sauer M, Muller M, Atallah K, Weidemann M, Gronemeyer P, et al. An in vitro urinary tract catheter system to investigate biofilm development in catheter-associated urinary tract infections. J Microbiological Methods 2011;87(3):302-8.

6.   Donlan RM, Costerton JW. Biofilms: survival mechanisms of clinically relevant microorganisms. Clin Microbiol Reviews 2002;15(2):167-93.

7.   Fournier PE, Richet H. The epidemiology and control of Acinetobacter baumannii in health care facilities. Clin Infect Dis 2006;42(5):692-9.

8.   Weber DJ, Rutala WA, Miller MB, Huslage K, Sickbert-Bennett E. Role of hospital surfaces in the transmission of emerging health care-associated pathogens: norovirus, Clostridium difficile, and Acinetobacter species. Am J Infect Control 2010;38(5 Suppl 1):S25-33.

9.   Gordon NC, Wareham DW. Multidrug-resistant Acinetobacter baumannii: mechanisms of virulence and resistance. Intl J Antimicrobial Agents 2010;35(3):219-26.

10.   Sunenshine RH, Wright MO, Maragakis LL, Harris AD, Song X, Hebden J, et al. Multidrug-resistant Acinetobacter infection mortality rate and length of hospitalization. Emerg Infect Dis 2007;13(1):97-103.

11.   Falagas ME, Karveli EA, Siempos, II, Vardakas KZ. Acinetobacter infections: a growing threat for critically ill patients. Epidemiol and Infect 2008;136(8):1009-19.

12.   Bergogne-Berezin E, Towner KJ. Acinetobacter spp. as nosocomial pathogens: microbiological, clinical, and epidemiological features. Clin Microbiol Reviews 1996;9(2):148-65.

13.   Lin MF, Lan CY. Antimicrobial resistance in Acinetobacter baumannii: From bench to bedside. World J Clin Cases 2014;2(12):787-814.

14.   Russo TA, Luke NR, Beanan JM, Olson R, Sauberan SL, MacDonald U, et al. The K1 capsular polysaccharide of Acinetobacter baumannii strain 307-0294 is a major virulence factor. Infection and Immunity 2010;78(9):3993-4000.

15.   Tacconelli E, Cataldo MA, De Pascale G, Manno D, Spanu T, Cambieri A, et al. Prediction models to identify hospitalized patients at risk of being colonized or infected with multidrug-resistant Acinetobacter baumannii calcoaceticus complex. J Antimicrobial Chemother 2008;62(5):1130-7.

16.   Neonakis IK, Spandidos DA, Petinaki E. Confronting multidrug-resistant Acinetobacter baumannii: a review. Intl J Antimicrobial Agents 2011;37(2):102-9.

17.   Moffatt JH, Harper M, Harrison P, Hale JD, Vinogradov E, Seemann T, et al. Colistin resistance in Acinetobacter baumannii is mediated by complete loss of lipopolysaccharide production. Antimicrob Agents Chemother 2010;54(12):4971-7.

18.   Manchanda V, Sanchaita S, Singh N. Multidrug resistant acinetobacter. J Global Infect Dis 2010;2(3):291-304.

19.   de Breij A, Dijkshoorn L, Lagendijk E, van der Meer J, Koster A, Bloemberg G, et al. Do biofilm formation and interactions with human cells explain the clinical success of Acinetobacter baumannii? PLoS One 2010;5(5):e10732.

20.   King LB, Swiatlo E, Swiatlo A, McDaniel LS. Serum resistance and biofilm formation in clinical isolates of Acinetobacter baumannii. FEMS Immunol and Med Micro 2009;55(3):414-21.

21.   Lee K, Yong D, Jeong SH, Chong Y. Multidrug-resistant Acinetobacter spp.: increasingly problematic nosocomial pathogens. Yonsei Medical Journal 2011;52(6):879-91.

22.   McQueary CN, Actis LA. Acinetobacter baumannii biofilms: variations among strains and correlations with other cell properties. J Microbiol 2011;49(2):243-50.

23.   Rollet C, Gal L, Guzzo J. Biofilm-detached cells, a transition from a sessile to a planktonic phenotype: a comparative study of adhesion and physiological characteristics in Pseudomonas aeruginosa. FEMS Microbiol Letters 2009;290(2):135-42.

24.   Stoodley P, Wilson S, Hall-Stoodley L, Boyle JD, Lappin-Scott HM, Costerton JW. Growth and detachment of cell clusters from mature mixed-species biofilms. Appl Environ Microbiol 2001;67(12):5608-13.

25.   Wolcott RD, Ehrlich GD. Biofilms and chronic infections. JAMA 2008;299(22):2682-4.

26.   Davey ME, O'Toole G A. Microbial biofilms: from ecology to molecular genetics. Microbiol and Molec Biol Reviews 2000;64(4):847-67.

27.   Jung J, Park W. Acinetobacter species as model microorganisms in environmental microbiology: current state and perspectives. Appl Microbiol Biotechnol 2015;99(6):2533-48.

28.   Gaddy JA, Actis LA. Regulation of Acinetobacter baumannii biofilm formation. Future Microbiol 2009;4(3):273-8.

29.   Lewis K. Persister cells. Annual Review of Microbiol 2010;64:357-72.

30.   Lee HW, Koh YM, Kim J, Lee JC, Lee YC, Seol SY, et al. Capacity of multidrug-resistant clinical isolates of Acinetobacter baumannii to form biofilm and adhere to epithelial cell surfaces. Clin Microbiol Infect 2008;14(1):49-54.

31.   Costerton JW, Stewart PS, Greenberg EP. Bacterial biofilms: a common cause of persistent infections. Science 1999;284(5418):1318-22.

32.   Branda SS, Vik S, Friedman L, Kolter R. Biofilms: the matrix revisited. Trends in Microbiol 2005;13(1):20-6.

33.   Lewis K. Riddle of biofilm resistance. Antimicrob Agents Chemother 2001;45(4):999-1007.

34.   Bardouniotis E, Huddleston W, Ceri H, Olson ME. Characterization of biofilm growth and biocide susceptibility testing of Mycobacterium phlei using the MBEC assay system. FEMS Microbiol Letters 2001;203(2):263-7.

35.   Ceri H, Olson M, Morck D, Storey D, Read R, Buret A, et al. The MBEC Assay System: multiple equivalent biofilms for antibiotic and biocide susceptibility testing. Methods in enzymology 2001;337:377-85.

36.   El-Azizi M, Rao S, Kanchanapoom T, Khardori N. In vitro activity of vancomycin, quinupristin/dalfopristin, and linezolid against intact and disrupted biofilms of staphylococci. Annals of Clin Microbiol and Antimicrobials 2005;4:2.

37.   Mah TF, O'Toole GA. Mechanisms of biofilm resistance to antimicrobial agents. Trends in Microbiol 2001;9(1):34-9.

38.   Stewart PS. Mechanisms of antibiotic resistance in bacterial biofilms. Intl J Med Microbiol 2002;292(2):107-13.

39.   Hall-Stoodley L, Stoodley P. Biofilm formation and dispersal and the transmission of human pathogens. Trends in Microbiol 2005;13(1):7-10.

40.   Tomaras AP, Dorsey CW, Edelmann RE, Actis LA. Attachment to and biofilm formation on abiotic surfaces by Acinetobacter baumannii: involvement of a novel chaperone-usher pili assembly system. Microbiology 2003;149(Pt 12):3473-84.

41.   Loehfelm TW, Luke NR, Campagnari AA. Identification and characterization of an Acinetobacter baumannii biofilm-associated protein. J Bacteriology 2008;190(3):1036-44.

42.   Brossard KA, Campagnari AA. The Acinetobacter baumannii biofilm-associated protein plays a role in adherence to human epithelial cells. Infection and Immunity 2012;80(1):228-33.

43.   Yang H, Liang L, Lin S, Jia S. Isolation and characterization of a virulent bacteriophage AB1 of Acinetobacter baumannii. BMC Microbiol 2010;10:131.

44.   Wendt C, Dietze B, Dietz E, Ruden H. Survival of Acinetobacter baumannii on dry surfaces. J Clin Microbiol 1997;35(6):1394-7.

45.   Jawad A, Seifert H, Snelling AM, Heritage J, Hawkey PM. Survival of Acinetobacter baumannii on dry surfaces: comparison of outbreak and sporadic isolates. J Clin Microbiol 1998;36(7):1938-41.

46.   Rao RS, Karthika RU, Singh SP, Shashikala P, Kanungo R, Jayachandran S, et al. Correlation between biofilm production and multiple drug resistance in imipenem resistant clinical isolates of Acinetobacter baumannii. Indian J Med Microbiol 2008;26(4):333-7.

47.   Smith AW. Biofilms and antibiotic therapy: is there a role for combating bacterial resistance by the use of novel drug delivery systems? Advanced drug delivery reviews 2005;57(10):1539-50.

48.   Gayoso CM, Mateos J, Mendez JA, Fernandez-Puente P, Rumbo C, Tomas M, et al. Molecular mechanisms involved in the response to desiccation stress and persistence in Acinetobacter baumannii. J Proteome Research 2014;13(2):460-76.

49.   Fontana C, Favaro M, Minelli S, Bossa MC, Testore GP, Leonardis F, et al. Acinetobacter baumannii in intensive care unit: a novel system to study clonal relationship among the isolates. BMC Infect Dis 2008;8:79.

50.   Markogiannakis A, Fildisis G, Tsiplakou S, Ikonomidis A, Koutsoukou A, Pournaras S, et al. Cross-transmission of multidrug-resistant Acinetobacter baumannii clonal strains causing

episodes of sepsis in a trauma intensive care unit. Infect Control Hosp Epidemiol 2008;29(5):410-7.

51.   Jawad A, Heritage J, Snelling AM, Gascoyne-Binzi DM, Hawkey PM. Influence of relative humidity and suspending menstrua on survival of Acinetobacter spp. on dry surfaces. J Clin Microbiol 1996;34(12):2881-7.

52.   Griffith ME, Lazarus DR, Mann PB, Boger JA, Hospenthal DR, Murray CK. Acinetobacter skin carriage among US army soldiers deployed in Iraq. Infect Control Hosp Epidemiol 2007;28(6):720-2.

53.   Moultrie D, Hawker J, Cole S. Factors associated with multidrug-resistant Acinetobacter transmission: an integrative review of the literature. AORN Journal 2011;94(1):27-36.

54.   D'Agata EM, Thayer V, Schaffner W. An outbreak of Acinetobacter baumannii: the importance of cross-transmission. Infect Control Hosp Epidemiol 2000;21(9):588-91.

55.   Morgan DJ, Liang SY, Smith CL, Johnson JK, Harris AD, Furuno JP, et al. Frequent multidrug-resistant Acinetobacter baumannii contamination of gloves, gowns, and hands of healthcare workers. Infect Control Hosp Epidemiol 2010;31(7):716-21.

56.   Catalano M, Quelle LS, Jeric PE, Di Martino A, Maimone SM. Survival of Acinetobacter baumannii on bed rails during an outbreak and during sporadic cases. J Hosp Infect 1999;42(1):27-35.

57.   Neely AN, Maley MP, Warden GD. Computer keyboards as reservoirs for Acinetobacter baumannii in a burn hospital. Clin Infect Dis 1999;29(5):1358-60.

58.   Rebmann T, Rosenbaum PA. Preventing the transmission of multidrug-resistant Acinetobacter baumannii: an executive summary of the Association for Professionals in infection control and epidemiology's elimination guide. Am J Infect Control 2011;39(5):439-41.

59.   Luo TL, Rickard AH, Srinivasan U, Kaye KS, Foxman B. Association of blaOXA-23 and bap with the persistence of Acinetobacter baumannii within a major healthcare system. Front Microbiol 2015;6:182.

60.   Vidal R, Dominguez M, Urrutia H, Bello H, Gonzalez G, Garcia A, et al. Biofilm formation by Acinetobacter baumannii. Microbios 1996;86(346):49-58.

61.   Orsinger-Jacobsen SJ, Patel SS, Vellozzi EM, Gialanella P, Nimrichter L, Miranda K, et al. Use of a stainless steel washer platform to study Acinetobacter baumannii adhesion and biofilm formation on abiotic surfaces. Microbiology 2013;159(Pt 12):2594-604.

62.   Longo F, Vuotto C, Donelli G. Biofilm formation in Acinetobacter baumannii. The New Microbiologica 2014;37(2):119-27.

CHAPTER II

The Impact of Biofilm Formation and Multidrug Resistance on Environmental Survival of Clinical and Environmental Isolates of *Acinetobacter baumannii*

2.0.0 ABSTRACT

Objectives: *Acinetobacter baumannii,* a gram-negative bacterium, is an opportunistic pathogen capable of living in multiple environments. The increasing multidrug resistance of *A. baumannii* and its ability to form biofilms present challenges for treatment and infection control. A better understanding of the impact of biofilm formation and antibiotic resistance on environmental persistence of *A. baumannii* in hospital settings is needed for more effective infection prevention and control.

Methods: We compared biofilm formation, antibiotic resistance profiles and desiccation tolerance in a collection of *A. baumannii* strains isolated from patients (n=115) and the hospital environment (n=30). MALDI-TOF and Vitek® 2 systems were used for isolate identification and to determine antibiotic resistance; isolates were genotyped using repetitive extragenic palindromic-PCR. Biofilm forming capacity was quantified using the microtiter plate method and desiccation tolerance was determined up to 56 days. Hazard ratios of cell death due to desiccation were estimated using a Cox proportional hazards model.

Results: Half of our isolate collection shared a single rep-type. Of these, 64% were MDR positive compared to 8% of isolates with different rep-types. High biofilm forming, clinical, MDR positive strains were 50% less likely to die of desiccation than low biofilm, non-MDR

strains. In contrast, environmental, MDR positive, low biofilm forming strains had a 2.7 times *increase* in risk of cell death due to desiccation compared to their MDR negative counterparts. MDR negative, high biofilm forming environmental strains had a 60% *decrease* in risk compared to their low biofilm forming counterparts.

Conclusions: The MDR positive phenotype was deleterious for environmental isolates and the high biofilm phenotype was critical for survival. This study provides evidence of the trade-off between antibiotic resistance and desiccation tolerance, driven by condition-dependent adaptation, and establishes rationale for research into the genetic basis of the variation in fitness cost between clinical and environmental isolates.

2.1.0 INTRODUCTION[1]

Acinetobacter baumannii, a gram-negative bacterium, is an opportunistic pathogen

capable of living in multiple environments that is an increasing problem in hospital settings.

Once infection is established, risk of mortality is high: up to 26% for in-hospital patients (1) and

up to 43% for intensive care unit (ICU) patients (2). Multidrug resistant (MDR) A. baumannii

strains are increasingly reported worldwide (1), (3), and A. baumannii express several

mechanisms which confer this resistance: multidrug efflux pumps, β-lactamases,

aminoglycoside-modifying enzymes and the alteration of targets (4). It is also challenging to

control, as A. baumannii can survive in the hospital environment for prolonged periods of time

(5) and environmental contamination has been linked to hospital outbreaks (6).

The capacity of A. baumannii to persist in the environment may be due, in part, to its

ability to form biofilms on both abiotic and biological surfaces (7), (8). Biofilm formation is also

a mechanism of pathogenesis in device-related infections and provides a source of repeated

transmission by prolonging survival on inanimate objects (9), (10). Under harsh environmental

conditions, A. baumannii cells deep in the biofilm can undergo dormancy, becoming

metabolically inactive and robust to environmental stress (11), (12). The multiple antibiotic

resistance mechanisms found in A. baumannii also may play a role in its environmental survival.

Boll, et al. demonstrated that resistance to cationic antimicrobial peptide drugs, such as colistin,

also increases A. baumannii tolerance to desiccation (13). In MDR A. baumannii infections,

colistin (or polymyxin E) is often the last remaining effective treatment (14). Gayoso et al.

demonstrated that some antibiotic resistant associated proteins -- which are also associated with

---

[1] Information in this chapter has been prepared for publication with co-authors Duane Newton, PhD, Gayathri
Vadlamudi, Betsy Foxman, PhD, and Chuanwu Xi, PhD.

increased tolerance to detergents -- were over-expressed in *A. baumannii* under desiccation-stress (12). These findings suggest that some drug resistance mechanisms leverage the cells ability to survive in the open environment.

Antibiotic resistance in bacteria generally incurs a fitness cost, often manifested as reduced growth rates or a compromised competitive ability (15). Environmental pressures have been implicated for variations in phenotypic expressions (16). The trade-offs in fitness imposed by the ability to form biofilms, tolerate desiccation and multidrug resistance are potentially different for *A. baumannii* strains that live primarily in the environment compared to clinical strains adapted to living in the human host. In the environment, it may be more beneficial to resist desiccation by forming biofilms and in the human host more beneficial to maintain resistance to multiple antibiotics than resist desiccation. To test whether these trade-offs occur, we compared the biofilm formation, antibiotic susceptibility profiles and desiccation tolerance in a collection of *A. baumannii* strains isolated from patients and the hospital environment. Our results suggest that a trade-off between antibiotic resistance and desiccation tolerance occurs, and biofilm formation contributes significantly to the survival of these isolates.

2.2.0 MATERIALS AND METHODS

2.2.1 Collection of A. baumannii isolates

The study protocol was approved by the University of Michigan IRBMED (HUM00075484). We collected 132 clinical isolates from 115 patients and 54 environmental isolates from the University of Michigan Hospital (Ann Arbor, MI) between August 2012 and January 2014. Only the first isolate obtained from any patient was included. For environmental isolates that were collected on the same day, from the same fomite, sharing the same rep-type

banding pattern, only one was randomly chosen for inclusion; out of the 54 isolates collected, 30 environmental isolates met these criteria.

Clinical isolates were obtained from patients presenting with *Acinetobacter baumannii* infection, and were cultured and identified using MALDI-TOF mass spectrometer (Bruker Daltonics, Bellerica, MA) by the hospital microbiology laboratory. Environmental isolates were obtained by swabbing nonporous, high and low touch areas within and outside of the infected patient's room using sterile, individually wrapped, CultureSwab[TM] (Becton, Dickinson and Co., Sparks, MD) swabs, moistened in 3 mL of brain-heart infusion broth (Becton, Dickinson & Co., Sparks, MD). Excess broth was first pressed out of the swab and areas of approximately 2-3 cm^2 were swabbed in both a forward-back and a side-to-side motion while rotating the swab tip and returned to the tube containing the broth for immediate processing. Bacteria were recovered from swabs by first inoculating directly onto CHROMagar[TM] *Acinetobacter* plates (Hardy Diagnostics, Santa Maria, CA), which were incubated overnight at 37°C and evaluated for pink colonies. Bacteria were also recovered by homogenizing the swab with corresponding liquid using Omni-Tip™ disposable rotor stator generator probes (OMNI International, Kennesaw, GA) for 30 sec to remove any remaining cells from the swab. The homogenate was incubated at 37°C for 18 h on a rotating shaker table (150-180 rpm) during which time a 1 mL aliquot was removed at 2 hours and 18 hours, serial diluted to 10^{-3}, plated onto CHROMagar[TM] plates and grown for 24 hours at 37°C. Colonies that were identified as positive for *Acinetobacter* on the CHROMagar[TM] plates were subcultured onto blood agar plates (Thermal Fisher Scientific, Waltham, MA) and transferred to the University of Michigan Hospital Microbiology lab for MALDI-TOF identification and VITEK®2 susceptibility testing. Samples confirmed as *A.*

baumannii were grown in BBL^{TM} Mueller Hinton II (MHII) broth (Becton, Dickinson and Co., Sparks, MD) and stored at -70°C in 15% glycerol.

2.2.2 *Preparation of initial inoculums*

For each experiment, initial inoculums were prepared by transferring a frozen aliquot into 2.5 mL of MHII broth and incubating at 37°C for 18±2 h on a rotating shaker table (150-180 rpm). The culture was inoculated onto BBL^{TM} MHII agar (Becton, Dickinson and Co., Sparks, MD) and grown at 37°C. An isolated colony was transferred to MHII broth and incubated at 37°C with shaking at 150-180 rpm for 15-18 hours. From this, a starting culture with an optical density at a wavelength of 600 nm (OD_{600}) of 0.200 ± 0.01 (Synergy™ HT Multi-Mode Microplate Reader, BioTek® Instruments, Inc.), which approximates 10^8 CFU/mL, was used.

2.2.3 *Repetitive extragenic palindromic polymerase chain reaction (rep-PCR) genotyping*

Genomic DNA was extracted using a commercially available whole genome extraction kit (QIAamp® DNA Mini Kit by Qiagen, Valencia, CA). DNA quantification was performed by nanodrop (NS-1000, Thermo Scientific, Wilmington, DE) and DNA purity was evaluated by the absorbance ratio at 260 and 280 nm (A260/A280). Rep-PCR oligonucleotide primer sets published by Vila et al. (17) were prepared by Invitrogen (Carlsbad, CA). Rep-PCR conditions were followed as previously described (16), (18). Amplified products were stained using EZ-Vision® Three, DNA Dye and Buffer 6X (AMRESCO®, Solon, OH) and aliquots (10μL) of each sample were subjected to elecrophoresis in 1.2% agarose gel. A 1 Kb GeneRuler DNA Ladder Mix (#SM0333, Thermo Scientific, City, ST) was used in the first and every 4th lane of the gel. Gels were imaged using a UV trans-illuminator and imager. BioNumerics® Version 7.5 Software (Applied Maths, Inc., Austin, TX) was used to detect lanes and bands and to build

phylogenetic trees using the Neighbor Joining clustering method with the Jaccard similarity coefficient (19).

2.2.4 Antibiotic susceptibility testing

Antibiotic susceptibility profiles were determined using VITEK®2 (bioMérieux, Inc., Durham NC). Isolates were considered to be multidrug resistant (MDR) if they were resistant to the following three drug classes, or resistant to two and intermediate to one (20): cephalosporins, fluoroquinolones, and aminoglycosides.

2.2.5 Quantification of biofilm formation:

Each isolate was grown as described above and diluted 1:100 in MHII broth. Biofilm forming capacity was quantified in triplicate using the microtiter plate method as previously described (21), (22) using 0.1% crystal violet Gram stain solution (CAS no. 10114-58-6, Fisher Science Education, Nazareth, PA). The OD_{600} was measured using a microplate reader to obtain relative biofilm biomass measurements. The average of each triplicate was calculated and *A. baumannii* ATCC 17978 (American Type Culture Collection, Manassas, VA) was used to normalize data.

2.2.6 Environmental survivability

Environmental survivability is defined as desiccation tolerance over time and was tested over a period of 56 days as described previously (23). Each isolate was grown as described above, subcultured onto MHII agar and grown at 37°C overnight. An isolated colony was transferred to 2 mL MHII broth and incubated at 37°C with shaking at 150-180 rpm for 15-18 hours. From this, a 1 mL aliquot, with an OD_{600} of 0.200 ± 0.01, which approximates 10^8 CFU/mL, was used. Cells from each culture were pelleted using a mini centrifuge (5415R, Eppendorf, Hauppauge, NY) at $8600 \times g$ for 5 min and the pellet was re-suspended in 1 mL of

1× PBS buffer. This was repeated twice to thoroughly wash the cells. Samples were then

serially diluted in 1× PBS buffer to obtain an OD_{600} of 0.001, which approximates 10^6 CFU/mL.

In duplicate, 10 μl of each culture was inoculated into the wells of a 96-well plate, preparing one

for each time period of 1, 3, 7, 14, 28, and 56 days as shown in Figure 2-1. The plates were

covered with a semi-permeable membrane and incubated at approximately 72°F (22°C) with a

relative humidity level of approximately 40% for the designated time period. At each time

interval, the cells were revived by adding 100 uL of MHII broth to wells with gentle pipetting up

and down. Samples were serial diluted 1000 fold, spread plated onto MHII agar and incubated

overnight at 37°C for colony enumeration.

Figure 2.1: Desiccation Tolerance Method
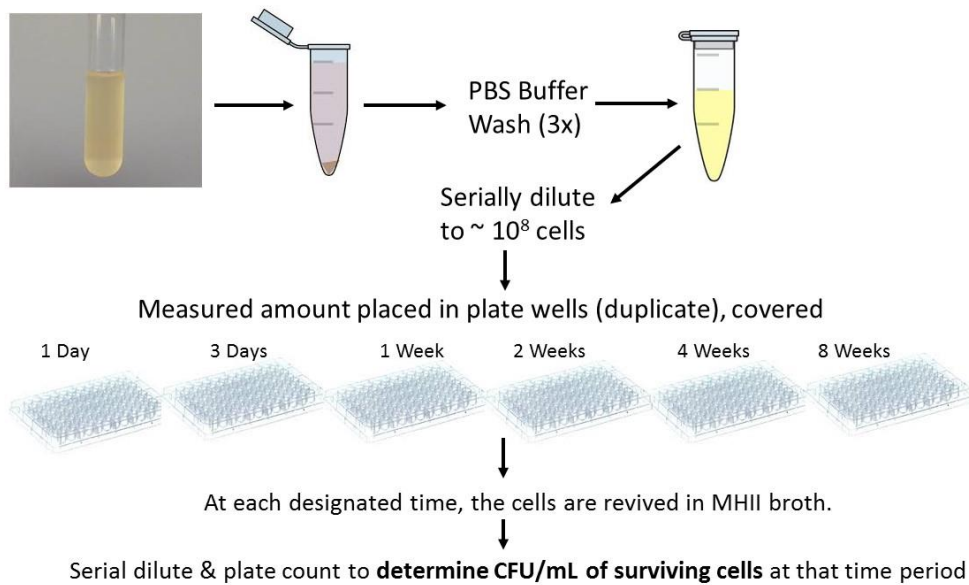
2.2.7 Statistical Analysis

Cox proportional hazards regression analysis was performed using R: A language and environment for statistical computing (R Foundation for Statistical Computing, Vienna, Austria). All other statistical analyses were performed using GraphPad Prism 6 for Windows (Version 6.01, Graph Pad Software, Inc., La Jolla, CA). Statistical significance was assessed using the paired and unpaired t tests (as appropriate), the Holm-Šídák test and one-way ANOVA, Log-rank and log-likelihood ratio with a significance level of $\alpha \leq 0.05$.

2.3.0 RESULTS

2.3.1 Epidemiology/Isolate collection

We obtained 132 clinical isolates from 115 different patients over an 18-month period. Only the first isolate obtained from any one patient was included. Clinical isolates were equally likely to be obtained from ICU, non-ICU and outpatient locations (Table 2.1). *A. baumannii* was successfully recovered from 54 of the 314 environmental samples for an overall recovery rate of 17%. Of these 54 isolates, 30 independent isolates were included (see methods). Eighty percent (24/30) of the environmental isolates were collected from patient rooms and the remaining 20% (6/30) were obtained from non-patient areas such as nurses' stations and medical supply areas. Clinical isolates were recovered primarily from urinary tract and respiratory tract specimens. Environmental isolates were mostly recovered from sink areas. Although some of the environmental isolates were collected from the room of an infected patient, only 10% (3/30) of the environmental isolates shared the exact same REP-type as the corresponding patient occupying that room. Distribution of isolation sites of all 132 clinical and 54 environmental isolates that were collected are shown in Appendix 2-B.

Table 2.1: Study isolate characteristics stratified by rep-type of 115 clinical and 30 environmental Acinetobacter baumannii isolates obtained from a University hospital between Aug 2012 and Jan 2014.

	Clinical		Environmental		Population Total n (%)
	Dominant† n (%)	Sporadic‡ n (%)	Dominant† n (%)	Sporadic‡ n (%)	
Total (n)	52 (100)	63 (100)	21 (100)	9 (100)	145 (100)
Patient characteristics					
Mean Age (years)	52.7	41.5	n/a	n/a	47.1
Males	24 (46)	38 (60)	n/a	n/a	62 (54)
Females	28 (53)	25 (40)	n/a	n/a	53 (46)
Hospital Location					
ICU Unit	24 (46)	4 (7)	17 (81)	4 (44)	49 (34)
Non-ICU Unit	11 (21)	26 (41)	4 (19)	5 (56)	46 (32)
Outpatient	17 (33)	33 (52)	n/a	n/a	50 (34)
Site of Isolation					
Urinary	19 (36)	29 (46)	n/a	n/a	48 (33)
Respiratory	17 (33)	17 (27)	n/a	n/a	34 (23)
Soft Tissue	10 (19)	9 (14)	n/a	n/a	19 (13)
Blood	4 (8)	3 (5)	n/a	n/a	7 (5)
*Other Body Site	2 (4)	5 (8)	n/a	n/a	7 (5)
Keypad	n/a	n/a	4 (19)	2 (22)	6 (4)
Sink Area	n/a	n/a	7 (33)	3 (33)	10 (7)
Floor	n/a	n/a	4 (19)	1 (11)	5 (3)
Computer Area	n/a	n/a	2 (9.5)	1 (11)	3 (2)
Bed Rail	n/a	n/a	2 (9.5)	0 (0)	2 (1)
**Other Fomite	n/a	n/a	2 (9.5)	2 (22)	4 (3)

†Dominant rep-type strains are those with a common banding pattern (Figs 1A).
‡Sporadic rep-type strains are those with banding patterns highly dissimilar from the dominant type (Figs 1B).
*Other body sites include CSF, drainage, para fluid, and bone.
**Other fomites include hallway ledge, phone, bed-side table, and counter top.

2.3.2 Rep-PCR genotyping

We identified a common banding pattern that had 8 distinct bands, with a prominent band at approximately 4000 base-pairs. Of the145 isolates, 64 displayed the common banding pattern exactly and 9 differed only by 1 band; we will refer to these 73 strains as the "dominant rep-type" for the remainder of this paper (Figure 2.2). The remaining 72 isolates displayed banding patterns highly dissimilar from the dominant type (Figure 2.3). We will refer to this set of strains as "sporadic rep-type". We identified 59 unique banding patterns among the sporadic rep-types.

The distribution of dominant and sporadic rep-types varied by isolate source. Urinary isolates were predominantly of the sporadic rep-type (29/48, 60%) but half of respiratory isolates were comprised of the dominant-type. One-third of the environmental isolates (10/30) were isolated from the sink area and these were predominantly of the dominant type (7/10, 70%).

2.3.3 Antibiotic Susceptibility

Table 2.3 shows the number of strains resistant to each antibiotic, stratified by clinical/environmental status and rep-type. Nearly half of the clinical isolates (54/115) were resistant to the fluoroquinolone ciprofloxacin, followed by the aminoglycoside gentamicin where 34% (39/115) were resistant. Environmental isolates were almost 3 times more likely to be resistant to 3 or more antibiotic classes (MDR) than clinical isolates (odds ratio 2.87, p=0.02; 57% (17/30) vs. 31% (36/115), Figure 2.4A). Table 2.3 and Figure 2.4C shows the percentage of clinical and environmental isolates that were MDR, stratified by rep-type. The higher percentages of resistance seen among both the clinical and environmental isolates can be attributed to the dominant rep-type. The most commonly observed resistance among the dominant rep-type was to ciprofloxacin, with 97% (71/73) resistant compared to 12.5% (9/72) of the sporadic rep-type isolates. Overall, isolates of the dominant rep-type were almost 20 times more likely to be MDR than sporadic rep-type strains (64% (47/73) vs. 8% (6/72), odds ratio=19.88, Fisher's exact test p<0.0001).

Clinical isolates collected from patients in the ICU were also more likely to be MDR than those collected from patients outside the ICU: (67.5% (19/28) vs. 16.2% (6/37), odds ratio= 9.05, Fisher's exact test p=0.0001). Although the numbers of environmental isolates were small, they show a similar trend (ICU: 62% (13/21) were MDR vs. 44% (4/9) non-ICU). Clinical and environmental isolates collected from the ICU were more likely to be of the dominant rep-type

(chi-square p-value <0.0001) compared to those collected outside the ICU but there was no difference in MDR prevalence by isolate source (t-test p=0.99).

2.3.4 Biofilm Formation

Mean OD_{600} values for environmental and clinical isolates were 1.17 and 0.88 respectively (t-test p=0.03) (*Figure 2.4*). Environmental isolates produced more biofilm biomass than clinical isolates, regardless of rep-type. For the dominant rep-type, the mean OD_{600} values for clinical and environmental strains were 0.92 and 1.10 respectively (t-test p=0.30) and for the sporadic-type, clinical and environmental strains mean OD_{600} values were 0.84 and 1.55 respectively (t-test p=0.006). The mean biofilm OD_{600} values of non-ICU environmental isolates (n=9) and ICU derived environmental isolates (n=21) were 1.35 and 1.18 respectively, (t-test p=0.50).

2.3.5 Desiccation tolerance

Overall, there was no statistical difference in survival between clinical and environmental isolates with respect to desiccation tolerance (Figure 2.4). When stratified by rep-type, dominant-type clinical strains survived better than dominant-type environmental strains. By contrast, sporadic-type environmental strains survived better than sporadic-type clinical strains. We used the Cox proportional hazards model to examine the effect of MDR and biofilm phenotypes of clinical and environmental isolates as explanatory variables, after accounting for rep-type, for risk of cell death due to desiccation after 56 days of follow-up (Table 2.2). Biofilm formation capacity and MDR phenotype were statistically significant and each had a statistically significant interaction terms with clinical/environmental status. However, the source of isolation (clinical versus environmental) was not statistically significant, and therefore does not affect

survival without the added effect of biofilm formation or MDR phenotype. Die-off rates due to

desiccation for each time-period are presented in Appendix 2-C).

Table 2.2: Fitted results of the Cox proportional hazard model for risk of cell death due to desiccation after 56 days follow-up of 73 dominant-type and 72 sporadic-type A. baumannii isolates. Risk comparisons with hazard ratios are also presented.

Cox Proportional Hazards Model Summary				
†Covariate	β coef	Hazard Rate	95% CI	*P* value
Rep-type	0.558	1.75	1.10-2.77	0.018
Clinical/Environmental Status	-0.269	0.76	0.25-2.34	0.637
MDR phenotype	0.927	2.53	1.13-5.65	0.024
Biofilm OD_{600}	-0.845	0.43	0.22-0.84	0.013
Clinical/Environmental Status*MDR	-1.398	0.25	0.10-0.63	0.004
Clinical/Environmental Status*Biofilm	0.733	2.08	1.01-4.29	0.047
Likelihood ratio	22.13 on 6 degrees freedom			0.001
Concordance	0.618, (standard error = 0.044)			
‡Fitted Cox Model Comparisons	Subject at risk (n)	Hazard Ratio	95% CI	*P* value
Dominant Rep-type	73	1.75	1.02-2.57	0.017
Reference Group: Sporadic Rep-type	72	--	--	--
Clinical, MDR-	79	1.60	0.95-2.70	0.071
Reference Group: Clinical, MDR+	36	--	--	--
Environmental, MDR-	13	0.40	0.18-0.88	0.023
Reference Group: Environmental, MDR+	17	--	--	--
Environmental, MDR-, *High Biofilm*	9	0.40	0.17-0.93	0.034
Environmental, MDR+, *Low Biofilm*	4	2.68	1.2-5.97	0.016
Environmental, MDR+, *High Biofilm*	13	1.07	0.34-3.33	0.904
Reference Group: Environmental, MDR-, *Low Biofilm*	4	--	--	--
Clinical, MDR-, *High Biofilm*	30	0.86	0.59-1.27	0.322
Clinical, MDR+, *Low Biofilm*	23	0.58	0.35-0.97	0.038
Clinical, MDR+, *High Biofilm*	13	0.50	0.26-0.97	0.039
Reference Group: Clinical, MDR-, *Low Biofilm*	48	--	--	--

†Covariate reference groups: Rep-Type, Sporadic type; Group, Environmental; MDR phenotype, MDR negative. * interaction. CI, confidence interval.
‡For each comparison, the reciprocal of the hazard ratio (HR) provides the HR of the reference group. High and low biofilm was determined using the overall mean OD_{600} value of 0.95 where high biofilm $OD_{600} \geq 0.95$ and low biofilm < 0.95.

*Figure 2.2: Dendogram of 73 dominant rep-type strains consisting of 52 clinical and 21 environmental isolates with corresponding gel lanes and antibiotic susceptibility profiles for each isolate. Antibiotic susceptibility is indicated as green=susceptible, yellow=intermediate, red=resistant. *Environmental isolates.*
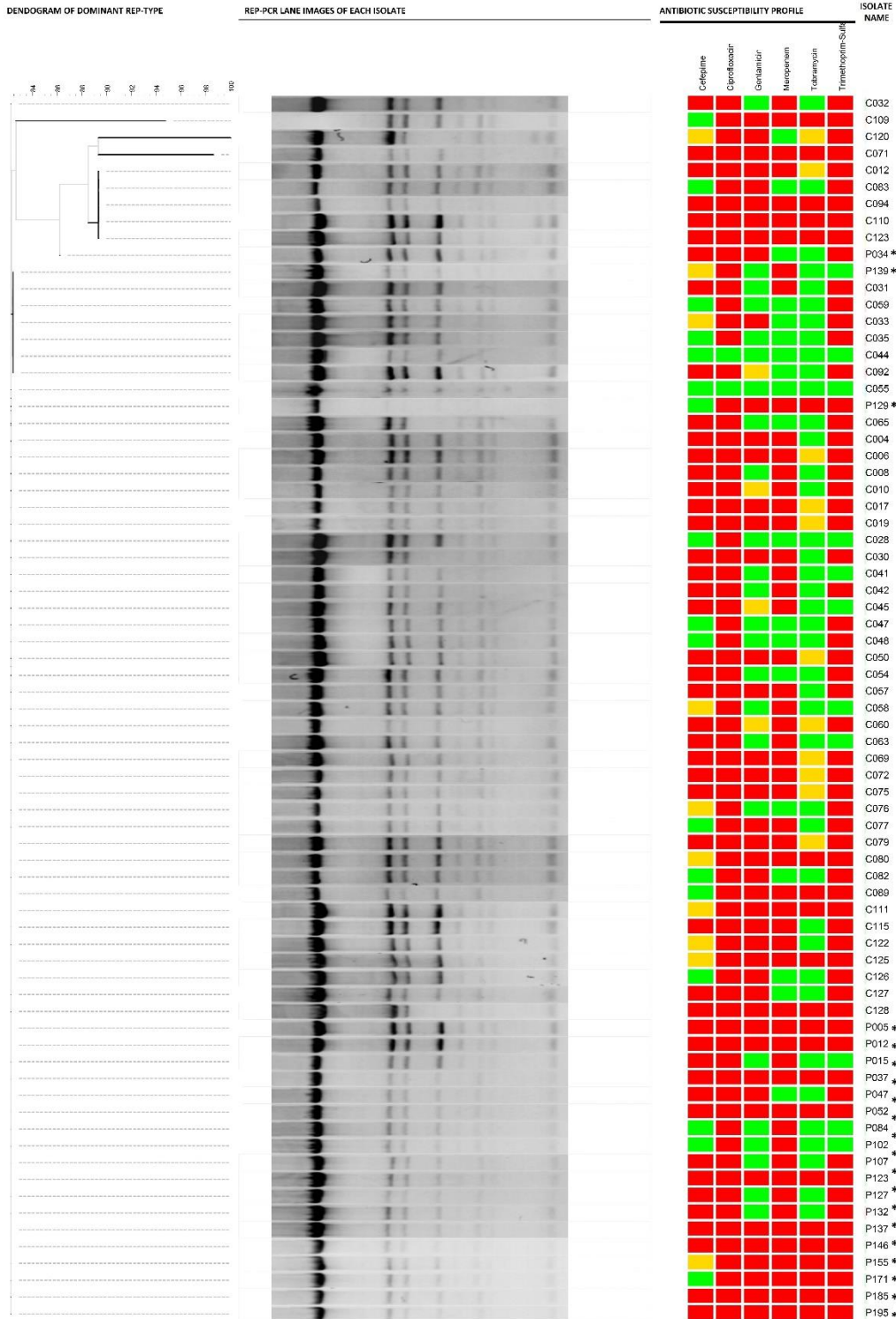
*Figure 2.3: Dendogram of 72 sporadic rep-type strains consisting of 63 clinical and 9 environmental isolates with corresponding gel lanes and antibiotic susceptibility profiles for each isolate. Antibiotic susceptibility is indicated as green=susceptible, yellow=intermediate, red=resistant. *Environmental isolates.*
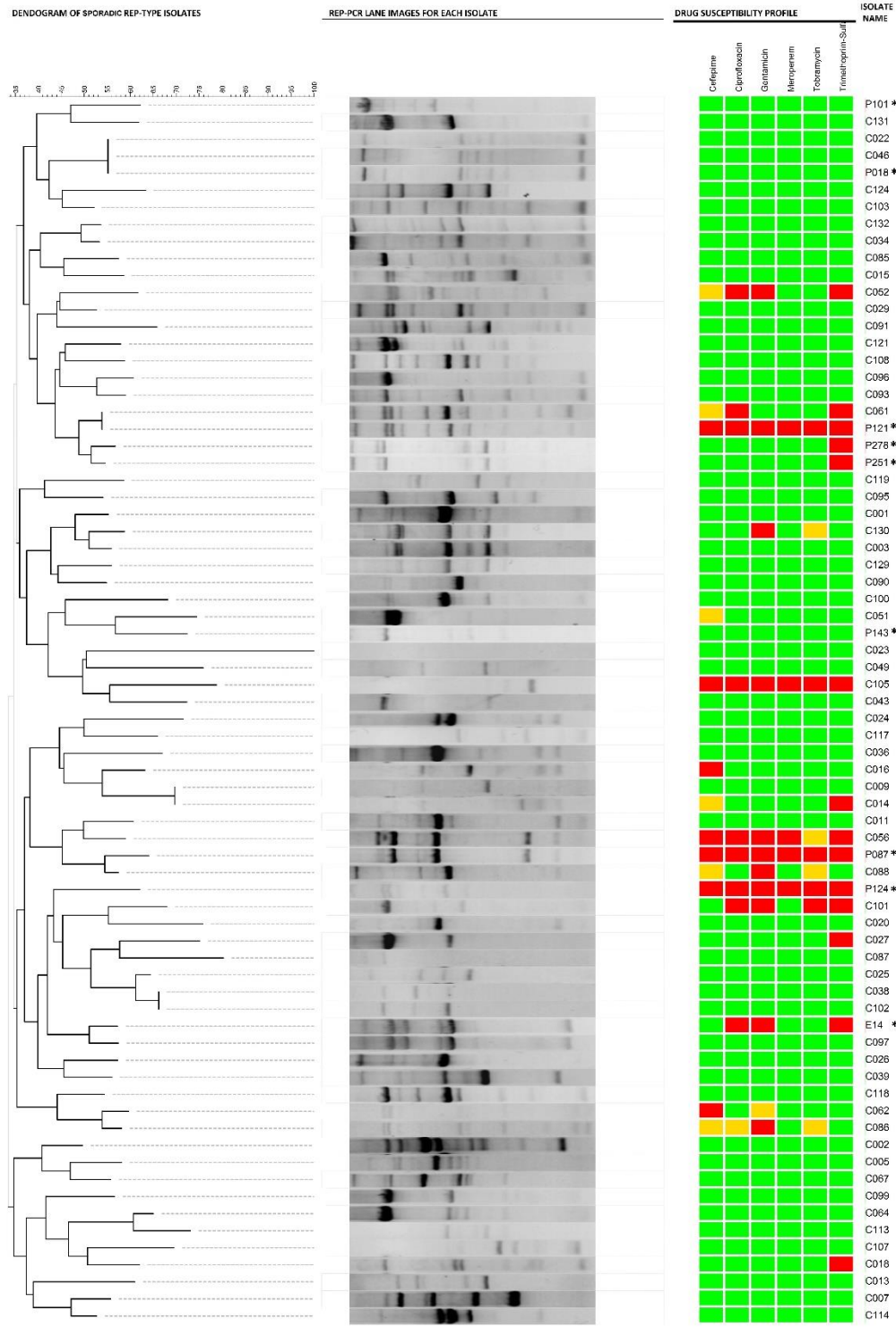
Table 2.3: *Profile of antibiotic resistance, stratified by clinical/environmental status, of 145 dominant (n=73) and sporadic (n=72) A. baumannii rep-types collected from a University Hospital between Aug 2012 and Jan 2014.*

Frequency of Antibiotic Resistance						
	Clinical			Environmental		
Antibiotic	Dominant* n (%)	Sporadic* n (%)	Total n (%)	Dominant† n (%)	Sporadic† n (%)	Total n (%)
Total	**52 (100)**	**63 (100)**	**115 (100)**	**21 (100)**	**9 (100)**	**30 (100)**
Fluoroquinolone						
Ciprofloxacin	50 (96)	4 (6)	54 (47)	21 (100)	4 (44)	25
Cephalosporin						
Cefepime	31 (60)	4 (6)	35 (30)	19 (90)	3 (33)	22
Aminoglycoside						
Gentamicin	32 (62)	7 (11)	39 (34)	14 (67)	4 (44)	18
Tobramycin	11 (21)	2 (3)	13 (11)	12 (57)	3 (33)	15
Carbapenem						
Meropenem	29 (56)	2 (3)	31 (27)	19 (90)	3 (33)	22
MDR positive	33 (63)	3 (5)	36 (31)	14 (67)	3 (33)	17

Multidrug resistance was defined as being resistant to the following three drug classes (20): cephalosporins, fluroquinolones, and aminoglycosides or resistant to two and intermediate to one. Column percentages are shown.
* Paired t-test comparison of clinical dominant and sporadic rep-types, p-value=0.01.
† Paired t-test comparison of environmental dominant and sporadic rep-types, p-value=0.001
CI, Confidence Interval

Figure 2.4: Percent Multidrug Resistant (MDR), Box plots of biofilm OD_{600} *and Survival Curves with standard error bars, hazard ratio (HR) and p-values of* A. baumannii *isolates collected between Aug 2012 and Jan 2014, comparing (A) 115 clinical and 30 environmental isolates (B) 73 dominant and 72 sporadic rep-type isolates and (C) clinical and environmental isolates stratified by rep-type. Multidrug resistance was defined as being resistant to the following three drug classes (20): cephalosporins, fluoroquinolones, and aminoglycosides or resistant to two and intermediate to one.*

A. Clinical vs Environmental
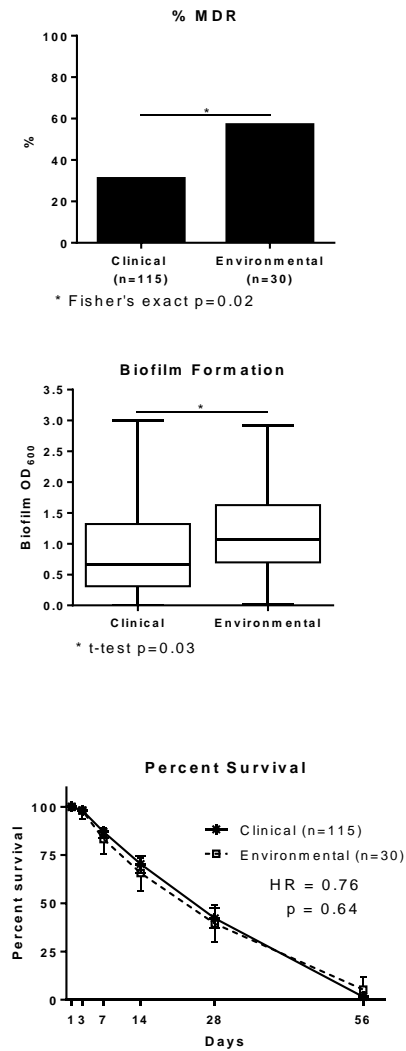
B. Dominant vs Sporadic
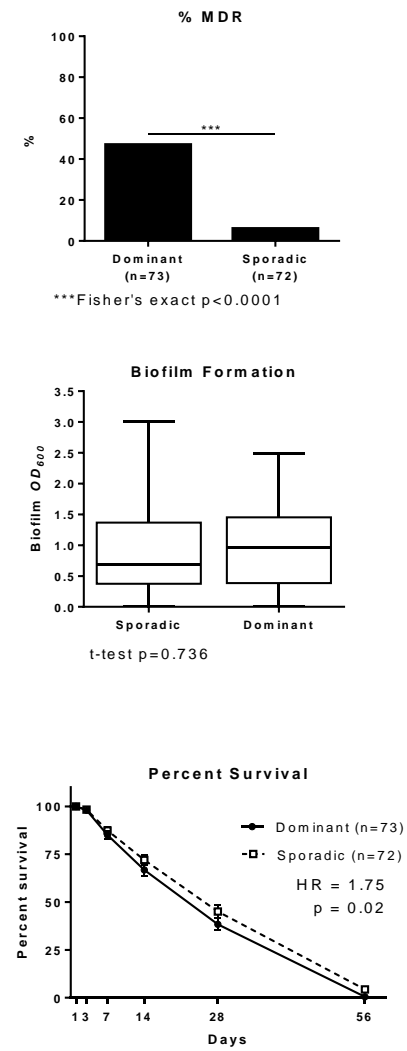
C. Clinical vs Environmental Stratified by Rep-Type
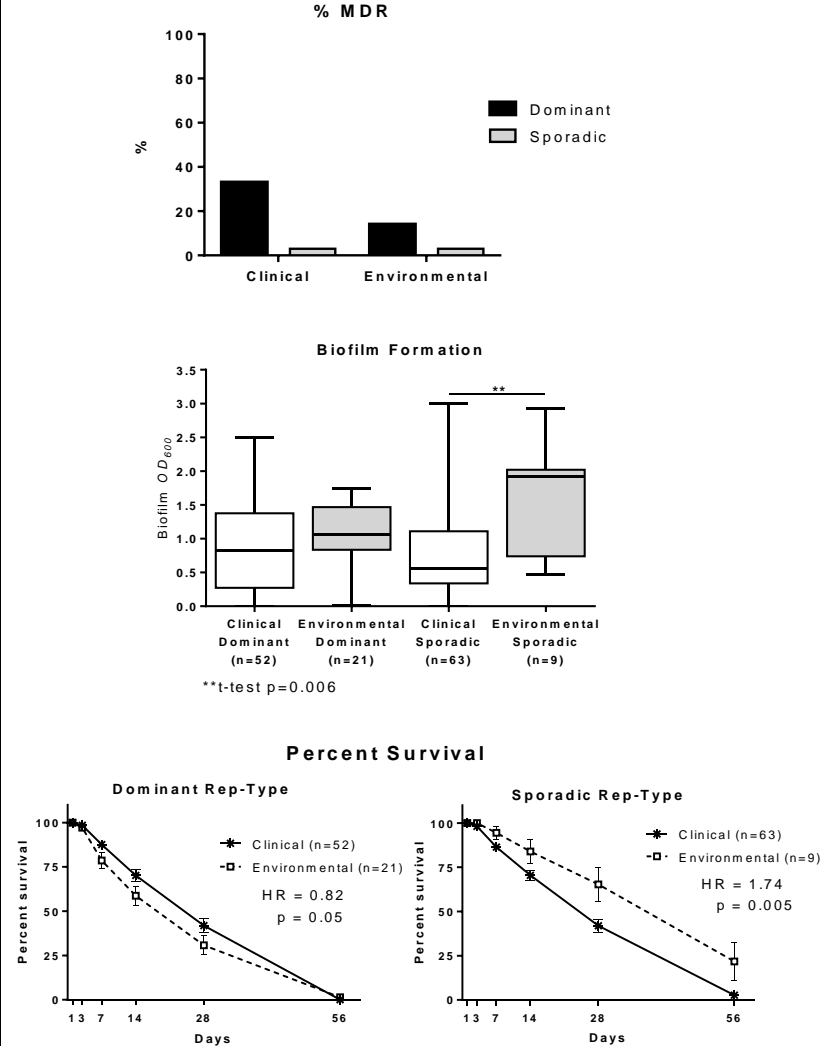
Figure 2.5: Likelihood of survival of 115 clinical and 30 environmental isolates of A. baumannii determined using a Cox proportional hazards model, accounting for rep-type, clinical/environmental status, biofilm formation capability and MDR phenotype. Clinical comparison reference group: MDR-, Low BF, clinical isolates. Environmental comparison reference group: MDR-, Low BF, environmental isolates. MDR-, multidrug negative phenotype; MDR+, multidrug positive phenotype; BF, Biofilm.
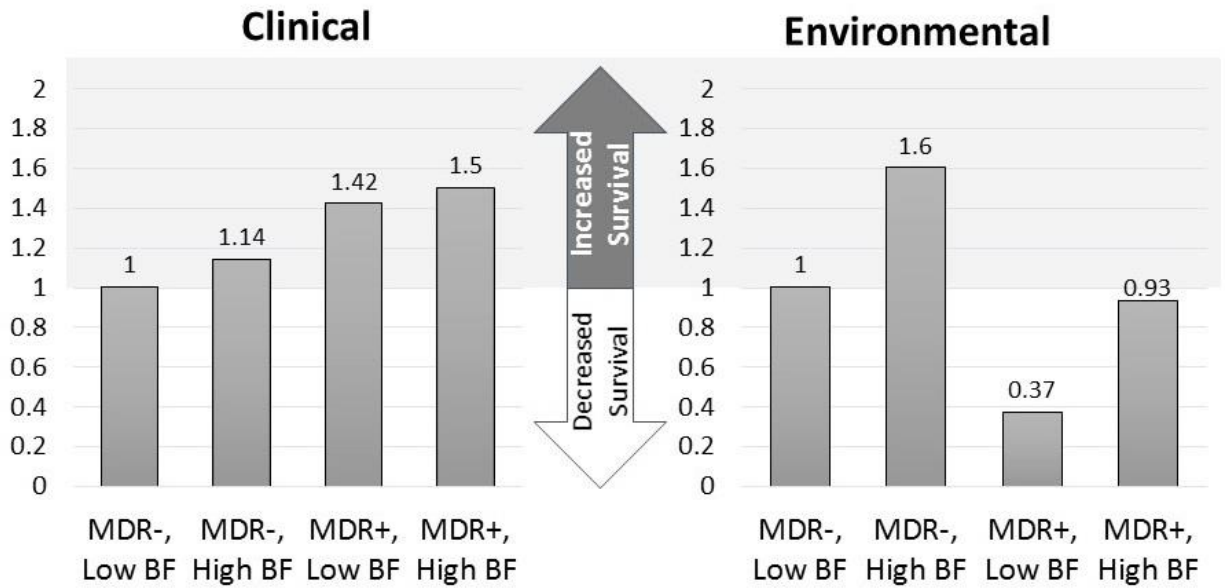
2.4.0 DISCUSSION

Biofilms increase desiccation tolerance (23), (24), (7) and may confer antibiotic resistance (25). We described and compared the prevalence and interactions among biofilm formation, antibiotic resistance and desiccation tolerance in a collection of 115 clinical and 30 environmental *A. baumannii* isolates. Our results suggest a fitness trade-off for the MDR positive phenotype in *A. baumannii* that is dependent upon environmental conditions; the MDR positive <u>environmental</u> isolates had significantly *decreased* survival whereas the MDR positive <u>clinical</u> isolates had significantly *increased* survival. In addition, while the high biofilm phenotype was important for both clinical and environmental isolates to tolerate desiccation, it was critically important for the environmental isolates. We also identified a highly antibiotic resistant, dominant strain with a distinct rep-PCR banding pattern that was endemic in this hospital among clinical and environmental isolates.

Among clinical isolates, the MDR phenotype confers desiccation tolerance and the high biofilm phenotype works synergistically to improve tolerance. Our finding that the MDR positive phenotype among clinical isolates increased desiccation tolerance is consistent with previous studies demonstrating concordance between antibiotic resistances with increased desiccation tolerance among clinical strains. Boll, et al. demonstrated that resistance to cationic antimicrobial peptide drugs also increases *A. baumannii* tolerance to desiccation by fortifying the fatty acid lipid content of the lipid A in the outer membrane via the production of hepta-acylated lipid A (13). Further, Gayoso et al. found that some proteins such as AmpC and Oxa51 that are associated with antibiotic resistance and increased tolerance to detergents like sodium dodecyl sulfate were overexpressed in *A. baumannii* clinical strain AbH12O-A2 when subjected to desiccation-stress (12). We defined MDR as resistance to cephalosporins, fluoroquinolones, and

34

aminoglycosides, or resistant to two and intermediate to one (20). Studies using other definitions might have slightly different outcomes, but our study provides evidence that clinical isolates with the MDR positive phenotype can have increased tolerance to desiccation.

Among environmental isolates, the MDR phenotype carries a fitness cost of decreased desiccation tolerance, and the high biofilm phenotype buffers this cost. Previous studies have demonstrated a genetic fitness cost for the MDR phenotype in bacteria and the potential cost of antibiotic resistance for clinical strains in vivo is well documented (15), (26). However, to our knowledge, no other studies have evaluated the fitness cost of drug resistance in environmental strains. We provide evidence of variation in desiccation tolerance between clinical and environmental isolates of the same phenotypes suggesting a different set of fitness-costs under different environmental conditions. A possible explanation for this may be the effects of epistasis. Epistatic outcomes can be influenced by a number of factors, including the genotype in which the mutation occurs, growth environment and the level of stress or other selective pressures imposed upon the cell (26). For example, rifampicin resistance can be beneficial or deleterious for the microorganism, depending upon the environmental conditions (27), (28), (29). However, we cannot rule out that environmental sampling selected for more desiccant tolerant strains.

The high biofilm forming phenotype provided increased tolerance to desiccation for both clinical and environmental isolates, but was critical for environmental isolate survival. Biofilm formation is suspected of being one of the key pathogenic features of *A. baumannii,* particularly with device-related infections (30), (31). We show a trend of increased survival for high biofilm forming clinical isolates with additional tolerance when coupled with the MDR positive phenotype. By contrast, biofilm formation had a significant impact on desiccation

tolerance for environmental isolates, which likely comes at a cost of reduced drug resistance and may be driven by condition-dependent survival responses. Biofilm genes may vary in expression in response to environmental conditions. Longo et al. report different pili-like structures mediating adhesion among clinical isolates of *A. baumannii*, resulting in wide variability in the ability for different strains to adhere biotic or abiotic surfaces, suggesting that the genes involved in biofilm development on abiotic surfaces are not correlated with those for biofilm development on biological surfaces (25). This may offer some clues to help explain why we observed variation in the effect of high biofilm formation on desiccation tolerance between environmental and clinical isolates. For example, the clinical isolates in this study that were catheter-associated could have a different expression of biofilm in vitro compared to non-catheter-associated isolates. Unfortunately, we did not have access to this information and therefore were only able to consider biofilm in terms of an isolate's ability to form biofilm. Further studies are needed to identify if the variation observed between clinical and environmental isolates resulted from different expressions of the same set of genes.

The sporadic rep-types were more likely to be susceptible to antibiotics and tolerated desiccation better than the multidrug resistant, endemic, dominant rep-types. Half of our collection of 145 isolates shared a common rep-PCR banding pattern; isolates of the dominant rep-type were 19.9 times more likely to be MDR positive than sporadic-type isolates (Figures 2.4). Luo et al. also report a higher level of antibiotic resistance among 169 endemic strains compared to 121 sporadic strains collected at a large hospital system (16). This is not to minimize the clinical significance of sporadic isolates which can cause significant disease among compromised patients, and with their increased desiccation tolerance have a higher probability of environmental spread.

In summary, we demonstrate that the MDR positive phenotype imposes a fitness cost on *A. baumannii* environmental isolates by significantly decreasing desiccation tolerance, even in the presence of the high biofilm phenotype. By contrast the MDR positive phenotype does not affect desiccation tolerance among clinical isolates, and the high biofilm phenotype increases desiccation tolerance. In the absence of the MDR phenotype, biofilm formation improved desiccation tolerance in both clinical and environmental isolates but the impact on survival was significantly greater for environmental isolates. Our research increases current understanding of the association of the MDR phenotype with persistence, and demonstrates that the association is mediated by environmental conditions.

2.5.0 ACKNOWLEDGMENTS

2.6.0 REFERENCES

1. Sunenshine RH, Wright MO, Maragakis LL, Harris AD, Song X, Hebden J, et al. Multidrug-resistant Acinetobacter infection mortality rate and length of hospitalization. Emerg Infect Dis 2007;13(1):97-103.

2. Weber DJ, Rutala WA, Miller MB, Huslage K, Sickbert-Bennett E. Role of hospital surfaces in the transmission of emerging health care-associated pathogens: norovirus, Clostridium difficile, and Acinetobacter species. Am J Infect Control 2010;38(5 Suppl 1):S25-33.

3. Tacconelli E, Cataldo MA, De Pascale G, Manno D, Spanu T, Cambieri A, et al. Prediction models to identify hospitalized patients at risk of being colonized or infected with multidrug-resistant Acinetobacter baumannii calcoaceticus complex. J Antimicrobial Chemother 2008;62(5):1130-7.

4. Lin MF, Lan CY. Antimicrobial resistance in Acinetobacter baumannii: From bench to bedside. World J Clin Cases 2014;2(12):787-814.

5. Wendt C, Dietze B, Dietz E, Ruden H. Survival of Acinetobacter baumannii on dry surfaces. J Clin Microbiol 1997;35(6):1394-7.

6. Villegas MV, Hartstein AI. Acinetobacter outbreaks, 1977-2000. Infect Control Hosp Epidemiol 2003;24(4):284-95.

7. Tomaras AP, Dorsey CW, Edelmann RE, Actis LA. Attachment to and biofilm formation on abiotic surfaces by Acinetobacter baumannii: involvement of a novel chaperone-usher pili assembly system. Microbiology 2003;149(Pt 12):3473-84.

8. McQueary CN, Actis LA. Acinetobacter baumannii biofilms: variations among strains and correlations with other cell properties. J Microbiol 2011;49(2):243-50.

9. Lewis K. Persister cells. Annual Review of Microbiol 2010;64:357-72.

10. Lee HW, Koh YM, Kim J, Lee JC, Lee YC, Seol SY, et al. Capacity of multidrug-resistant clinical isolates of Acinetobacter baumannii to form biofilm and adhere to epithelial cell surfaces. Clin Microbiol Infect 2008;14(1):49-54.

11. Roberts ME, Stewart PS. Modelling protection from antimicrobial agents in biofilms through the formation of persister cells. Microbiology 2005;151(Pt 1):75-80.

12. Gayoso CM, Mateos J, Mendez JA, Fernandez-Puente P, Rumbo C, Tomas M, et al. Molecular mechanisms involved in the response to desiccation stress and persistence in Acinetobacter baumannii. J Proteome Research 2014;13(2):460-76.

13.   Boll JM, Tucker AT, Klein DR, Beltran AM, Brodbelt JS, Davies BW, et al. Reinforcing Lipid A Acylation on the Cell Surface of Acinetobacter baumannii Promotes Cationic Antimicrobial Peptide Resistance and Desiccation Survival. MBio 2015;6(3).

14.   Moffatt JH, Harper M, Harrison P, Hale JD, Vinogradov E, Seemann T, et al. Colistin resistance in Acinetobacter baumannii is mediated by complete loss of lipopolysaccharide production. Antimicrob Agents Chemother 2010;54(12):4971-7.

15.   Vogwill T, MacLean RC. The genetic basis of the fitness costs of antimicrobial resistance: a meta-analysis approach. Evol Appl 2015;8(3):284-95.

16.   Luo TL, Rickard AH, Srinivasan U, Kaye KS, Foxman B. Association of blaOXA-23 and bap with the persistence of Acinetobacter baumannii within a major healthcare system. Front Microbiol 2015;6:182.

17.   Vila J, Marcos MA, Jimenez de Anta MT. A comparative study of different PCR-based DNA fingerprinting techniques for typing of the Acinetobacter calcoaceticus-A. baumannii complex. J Med Microbiol 1996;44(6):482-9.

18.   Snelling AM, Gerner-Smidt P, Hawkey PM, Heritage J, Parnell P, Porter C, et al. Validation of use of whole-cell repetitive extragenic palindromic sequence-based PCR (REP-PCR) for typing strains belonging to the Acinetobacter calcoaceticus-Acinetobacter baumannii complex and application of the method to the investigation of a hospital outbreak. J Clin Microbiol 1996;34(5):1193-202.

19.   Saitou N, Nei M. The neighbor-joining method: a new method for reconstructing phylogenetic trees. Molec Biol and Evolution 1987;4(4):406-25.

20.   Manchanda V, Sanchaita S, Singh N. Multidrug resistant acinetobacter. J Global Infect Dis 2010;2(3):291-304.

21.   Badave GK, Kulkarni D. Biofilm Producing Multidrug Resistant Acinetobacter baumannii: An Emerging Challenge. J Clin Diagn Res 2015;9(1):DC08-10.

22.   Christensen GD, Simpson WA, Younger JJ, Baddour LM, Barrett FF, Melton DM, et al. Adherence of coagulase-negative staphylococci to plastic tissue culture plates: a quantitative model for the adherence of staphylococci to medical devices. J Clin Microbiol 1985;22(6):996-1006.

23.   Espinal P, Marti S, Vila J. Effect of biofilm formation on the survival of Acinetobacter baumannii on dry surfaces. J Hosp Infect 2012;80(1):56-60.

24.   de Breij A, Dijkshoorn L, Lagendijk E, van der Meer J, Koster A, Bloemberg G, et al. Do biofilm formation and interactions with human cells explain the clinical success of Acinetobacter baumannii? PLoS One 2010;5(5):e10732.

25.   Longo F, Vuotto C, Donelli G. Biofilm formation in Acinetobacter baumannii. The New Microbiologica 2014;37(2):119-27.

26.   Melnyk AH, Wong A, Kassen R. The fitness costs of antibiotic resistance mutations. Evolutionary Applications 2015;8(3):273-83.

27.   Rodriguez-Verdugo A, Gaut BS, Tenaillon O. Evolution of Escherichia coli rifampicin resistance in an antibiotic-free environment during thermal stress. BMC Evolutionary Biol 2013;13:50.

28.   Qi Q, Preston GM, MacLean RC. Linking system-wide impacts of RNA polymerase mutations to the fitness cost of rifampin resistance in Pseudomonas aeruginosa. MBio 2014;5(6):e01562.

29.   Hall AR, Angst DC, Schiessl KT, Ackermann M. Costs of antibiotic resistance - separating trait effects and selective effects. Evolutionary Applications 2015;8(3):261-72.

30.   Fournier PE, Richet H. The epidemiology and control of Acinetobacter baumannii in health care facilities. Clin Infect Dis 2006;42(5):692-9.

31.   Gordon NC, Wareham DW. Multidrug-resistant Acinetobacter baumannii: mechanisms of virulence and resistance. Intl J Antimicrobial Agents 2010;35(3):219-26.

Environmental Sampling Procedure

Notification of *A. baumannii*
positive patient isolate from UM
Microbiology Lab

3ml brain-heart
infusion broth

Sample processed in
Xi lab

Go to hospital

Swab is placed
back into tube for
transport back to
lab

Swab areas by rotating cotton tip and
wiping (back and forth) 3-4 times

Sample processing

0 hours
- Swab directly onto selective media
- Transfer liquid sample to a sterile 15mm centrifuge tube
- Homogenize for 30 sec
- Incubate at 37°C

2 hours
- Serial dilute & plate onto selective media
- Place back in incubator at 37°C

24 hours
- Serial dilute & plate onto selective media

Isolation of possible Acinetobacter

MALDI Analysis to confirm ID

Distribution of Clinical and Environmental Isolates

Clinical Isolates (n=132)
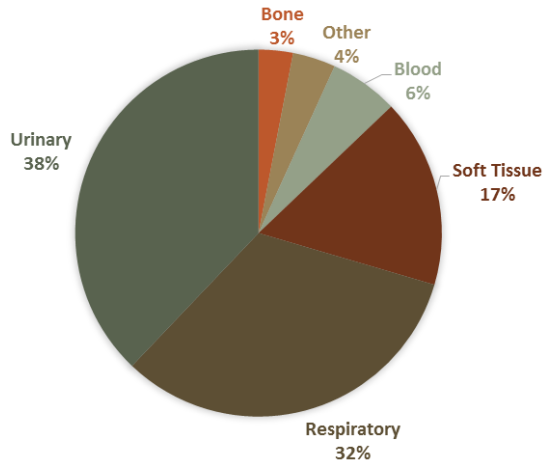
Other: pericar, CSF, drainage, n=132

Environmental Isolates (n=54)
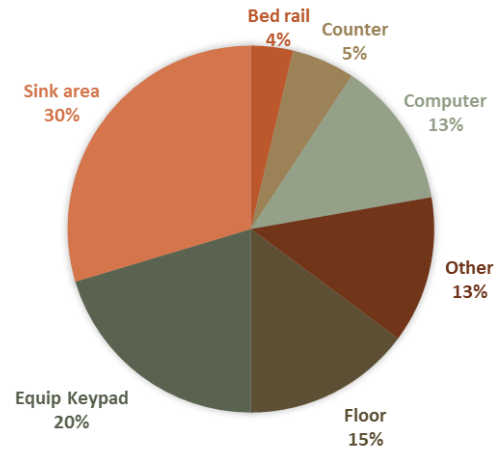
Other: phone, supply cart, light fixture, hall ledge; n=54

A. baumannii dominant clinical strains rate of die-off due to desiccation. Rates were determined

from the mean surviving cells (CFU/cm3/day) during the 56 days of desiccation. Rate of die-off

was calculated using the following equation[2]:

$$rate = -\frac{\ln(1 - risk)}{time}$$

Die-off Rate Due to Dessication

	0-1	1-3	3-7	7-14	14-28	28-56	>56
Die-off Rate	0.431515277	0.134288809	0.019179551	0.006786535	0.00099569	0.000312371	0.001586965
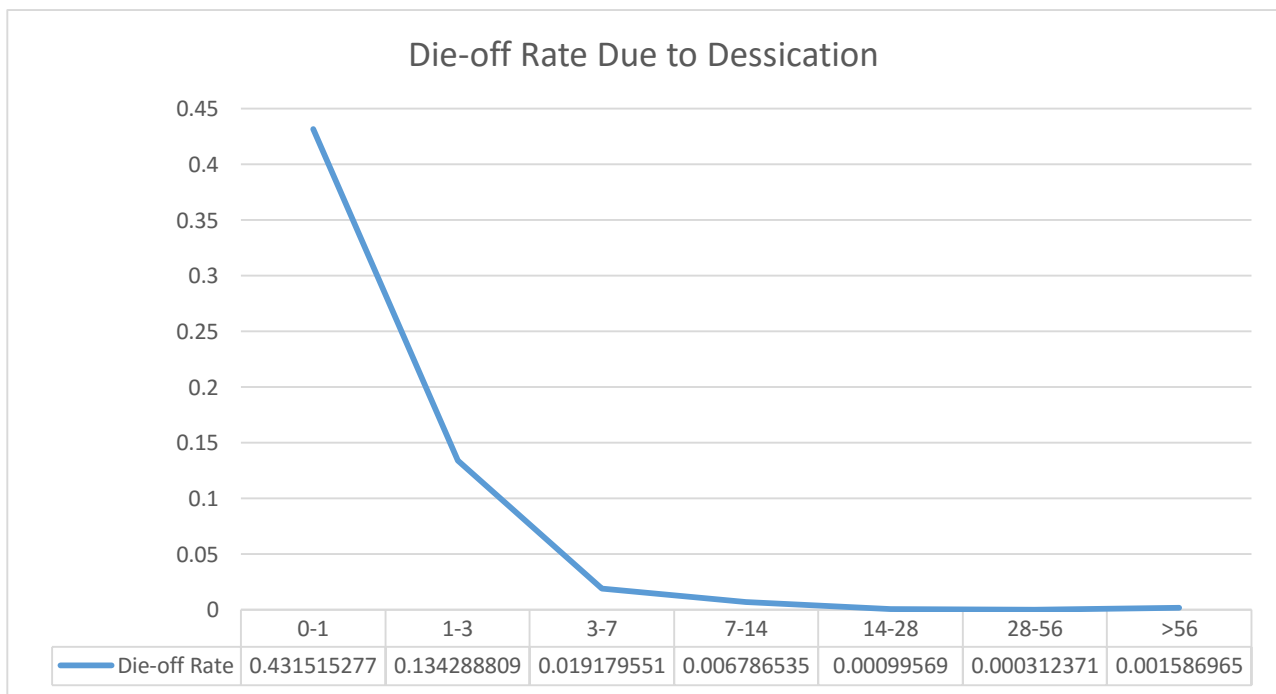
[2] Vynnycky E, White RG. An Introduction to Infectious Disease Modelling. Oxford New York: Oxford Uniersity Press; 2010.

CHAPTER III

Variation in antibiotic susceptibility among planktonic, sessile and detached biofilm cells of *Acinetobacter baumannii*

3.0.0 ABSTRACT

Objectives: *Acinetobacter baumannii* is an increasingly antibiotic resistant pathogen and a known biofilm former. *A. baumannii* also frequently causes device-related infections in hospitals, many of which are due to the formation of biofilms. The biofilm cycle includes attachment to a surface (often a medical device) and development of the extracellular matrix, biofilm maturation and dispersal. When in the biofilm matrix, *A. baumannii* displays increased resistance to antibiotic treatment, but it is unclear if the dispersed biofilm cells lose or retain this antibiotic resistance. Our objective was to compare the antibiotic susceptibilities of *A. baumannii* planktonic cells, biofilm cells, and the detached cells of the biofilm.

Methods: Antibiotic susceptibilities of 5 clinical and 5 environmental *A. baumannii* isolates in the planktonic state, in a biofilm, and as detached biofilm cells were tested against 8 antibiotics from different drug classes.

Results: The mean MICs for biofilm cells were the most and planktonic cells the least, with detached biofilm cells falling in between for gentamicin, colistin, cefotaxime, tetracycline, and the combination drugs ampicillin/sulbactam and trimethoprim/sulfamethoxazole. The mean MIC

for ciprofloxacin was greater for biofilm cells, but the same for planktonic and detached biofilm cells. The mean MIC imipenem was the same for all cell types.

Conclusions: Antibiotic resistance to multiple drug classes is enhanced for *A. baumannii* detached biofilm cells, although somewhat less so than when in the biofilm matrix. The variation in antibiotic sensitivities between planktonic, detached, and sessile biofilm cells calls for greater attention, which can provide insights to more effectively treat biofilm-related infections. For device-related infections, antibiotic therapies targeting the detached biofilm cell population coupled with device removal may offer more effective infection control.

3.1.0 INTRODUCTION [3]

   Acinetobacter baumannii is an opportunistic, gram-negative pathogen that is responsible

for roughly 10% of all nosocomial infections (1). Once infection is established, the risk of

mortality is high: up to 26% for in-hospital patients (2) and up to 43% for intensive care unit

(ICU) patients (3). The clinical persistence of *A. baumannii* is attributed to its increasing

antibiotic resistance, tenacious colonization of medical equipment and device surfaces, and its

ability to form biofilms. Biofilm formation is a recognized mechanism of pathogenesis in

device-related infections (4), (5), (6), resulting in increased treatment costs, and often require

premature device removal in order to eliminate the source of the infection (7). Many of the

infections caused by *A. baumannii* (ranging from urinary tract infections to ventilator-associated

pneumonia) are associated with in-dwelling devices, such as urinary catheters, central lines,

surgical drains, and ventilation equipment (8), (9), which serve as potential sites for biofilm

development (10).

   For gram-negative bacteria like *A. baumannii*, the biofilm life cycle is initiated when

individual planktonic cells encounter a surface, followed by reversible and then irreversible

attachment to that surface, and then biofilm maturation and dispersal. During the maturation

stage, the active biofilm produces sessile cells that take on a variety of physiochemical

characteristics. This results in an assortment of heterogeneous phenotypes within the biofilm

that are distinct from their planktonic counterparts (5), (11), (12). Sessile cells (individually or

as aggregates) can detach from the biofilm and disperse to new locations where they can attach

and generate new biofilms, a significant source for spread of infections (13). If the infection is

---

[3] Information in this chapter has been prepared for submission for future publication with co-authors Jianfeng Wu, PhD, Gayathri Vadlamudi, Duane Newton, PhD, Betsy Foxman, PhD, and Chuanwu Xi, PhD.

device-associated, removal of the device from the patient is frequently necessary to control the infection (14), but the process of device removal often causes microbial detachment from the device and may require additional antibiotic treatment (13).

Antibiotic resistance in biofilms can occur at the community (biofilm) level and at the cellular (planktonic) level (15), and the resistance mechanisms for each are distinctly different. Cellular-level resistance mechanisms are well studied and include hydrolysis, membrane permeability, alteration of targets, drug efflux, and drug inactivation. Cells can acquire these mechanisms via mutations to endogenous genes and lateral gene transfer. Community-level resistance is not well understood; the mechanisms proposed to date include restricted penetration (16), (17), a gradient of reduced metabolically active cells to persister cells (17), an adaptive stress response (18), (17), hypermutability (19) and extracellular DNA cation chelation (16). The acquisition of community-level resistance remains poorly understood, and warrants further investigation.

In vitro antimicrobial susceptibility testing measures the minimum inhibitory concentration (MIC) of antibiotics against a bacterial isolate. The MIC is the lowest concentration of antibiotic needed to inhibit the growth of planktonic bacteria, which exist as single cells in a liquid medium; however, MIC values do not consider biofilm cells. Significantly higher concentrations of antibiotic are needed to inhibit the growth of gram-negative bacteria in a biofilm structure compared to planktonic growth (20), (21). This value is referred to as the minimum biofilm eradication concentration (MBEC), which is the lowest concentration of antibiotic needed to eradicate biofilm (22). MBEC values are typically much higher than current MIC breakpoints for resistance, determined based on planktonic cells (20).

The current assumption is that the detached sessile cells can be treated as equivalent to planktonic cells. However, the biofilm contains a heterogeneous mixture of phenotypes, including variations in antibiotic susceptibility, that are distinct from their planktonic counterparts (5), (11), (12). Further, the heterogeneous genotypic and phenotypic characteristics of detaching sessile cells likely promote their ability to survive in changing environmental conditions (11). To our knowledge, no studies have investigated whether the detached sessile cells revert to the planktonic phenotype or maintain the biofilm phenotype. We hypothesized that the detached cells from biofilms are distinct from their planktonic counterparts and differ in their susceptibility to antibiotics. Therefore, the aim of this study was to test a variety of antibiotics to determine the concentrations needed to eradicate *A. baumannii* biofilms, as well as inhibit the growth of detached and planktonic cells. Understanding differences in antibiotic susceptibility during the life cycle of the biofilm is crucial to developing effective treatment strategies for biofilm-related infections.

3.2.0 MATERIALS AND METHODS

3.2.1 *Bacterial strains and antibiotics*

Five clinical plus five environmental *Acinetobacter baumannii* isolates were randomly chosen from a subset of high-biofilm forming *A. baumannii* isolates collected from the University of Michigan Health System between January 2012 and January 2014 (23). Isolate identification was confirmed using MALDI-TOF mass spectrometry analysis (Bruker Daltonics, Bellerica, MA). For each antibiotic tested, the minimum inhibitory concentration needed to inhibit growth of planktonic and detached cells and the minimum biofilm eradication concentration were determined according to the Clinical and Laboratory Standards Institute (CLSI) standards for *Acinetobacter* species (24). The antibiotics (drug classes) chosen for

testing were ciprofloxacin (fluoroquinolone), gentamicin (aminoglycoside), colistin (lipopeptide), imipenem (carbapenem), cefotaxime (3rd generation cephalosporin), tetracycline (tetracycline), and the combination drugs ampicillin/sulbactam (β-lactam/β-lactam inhibitor) and trimethoprim/sulfamethoxazole (dihydrofolate reductase inhibitor/sulfonamide), based on current treatment options for *A. baumannii* infections (8). All antibiotics were purchased from Thermo Fisher Scientific, Inc. (Waltham, MA).

3.2.2 *Preliminary Preparation of Subcultures and Recovery Medium*

A modified version of the MBECTM High-throughput (HTP) Assay protocol published by Innovotech was used (25). Isolates were prepared from cryogenic stock by streaking onto BBLTM Mueller Hinton II (MHII) agar, (Becton, Dickinson and Co., Sparks, MD) and incubated for 18-24h at 37ºC. A single colony were sub-cultured into MHII broth (Becton, Dickinson and Co., Sparks, MD) and incubated for 15-18h at 37ºC with shaking at 180 rpm, which were then used to create the inoculum for the biofilm MBECTM-HTP plate with peg lid (Innovotech Inc., Edmonton, AB, Canada). The recovery medium was prepared as described in MBECTM High-throughput (HTP) Assay protocol (25).

3.2.3 *Biofilm Growth*

For each isolate, a 30-fold dilution of the above subculture was prepared for a final concentration of approximately 1.0×10^7 CFU/mL. Twenty-two milliliters of this inoculum was added to a sterile MBEC^{TM}-HTP assay trough and covered with the peg lid. The inoculated MBEC plate was placed on a rocking table, set at 1 rock/15s, and biofilm was allowed to develop at room temperature for 48h (26). Starting concentrations were verified by serial dilution of the remaining 8 mL of inoculum to 10^{-6}, spread plated onto MHII agar and incubated overnight at 37ºC for colony enumeration.

3.2.4 Preparation of Challenge Plate with Antibiotics

To a sterile polystyrene 96-well plate, antibiotics from stock solutions were added to wells containing 5× MHII broth for a 1:5 dilution which were then serially diluted across the plate in a 1:2 ratio using 1× MHII broth. No antibiotics were added to wells that served as growth and sterility controls. Stock concentrations and dilution volumes were chosen so that the final concentrations of antibiotics tested would encompass the range of MIC standards for *Acinetobacter* spp., published by the CLSI (24). The stock antibiotic concentrations used and final concentrations of antibiotic in each well of the challenge plate are provided in supplemental materials. Each antibiotic was tested in duplicate for each strain.

3.2.5 Preparation of MIC Plate with Antibiotics and determining MIC of planktonic cells

An initial culture dilution was prepared as a 1:100 dilution of the planktonic bacterial culture from the MBECTM HTP assay plate trough into 1× MHII broth. 5× Culture was prepared as a 1:20 dilution from this initial dilution into 5× MHII broth. 1× Culture was prepared as a 1:10 dilution from the initial culture dilution into 1× MHII broth. The MIC plate was prepared similarly to the challenge plate, but using the inoculated 1× and 5× cultures prepared above rather than sterile broth. The MIC plate was incubated at 37oC with 50 rpm shaking for 24h. A second, identical plate that excludes the bacteria was prepared as a blank. Optical density readings at 600 nm (OD600) of the blank and test plates were measured the next day, which was used to confirm visual observation of bacterial growth and determination of the minimum inhibitory concentration of antibiotic to inhibit growth of planktonic cells (MIC-P).

3.2.6 Exposure of Biofilms to Antibiotic Challenge Plate and determining MIC of detached biofilm cells as a result of antibiotic exposure

After 72h of growth, the peg lid from the MBEC^{TM} HTP assay plate was rinsed in a 96-well microtiter plate containing 1× phosphate buffered saline (PBS) for 1-2 minutes by inserting

the lid over the 96-well plate. The planktonic culture from the biofilm trough was used to prepare the initial culture dilution for MIC plate preparation. Planktonic culture was also serially diluted and spread plated to determine culture concentrations. After rinsing, all pegs corresponding to the growth control wells only of the challenge plate were carefully broken off using sterile pliers, placed into a micro-centrifuge tube containing 1 mL of $1\times$PBS, vortexed for 30s to remove biofilm cells, serial diluted to 10^{-3}, and plate counted to determine concentrations of biofilm cells on the pegs before antibiotic exposure. After rinsing and the removal of the growth control pegs, the biofilms were challenged with antibiotics by inserting the peg lid into the prepared challenge plate, which was then incubated at 37°C. To capture the sessile cells that would detach from the biofilm during the first few hours of antibiotic exposure (i.e. detachment due to environmental conditions (27)), the peg lid was removed after 2 h of antibiotic exposure and an OD_{600} reading was taken of the challenge plate and was observed visually for growth in the wells. The challenge plate was then covered with a semipermeable membrane and further incubated at 37°C for 24h at which time another OD_{600} reading was taken and the wells were again observed visually for growth to determine the minimum inhibitory concentration of antibiotic needed to inhibit growth of cells that detached from biofilm (MIC-D) as a result of antibiotic exposure.

3.2.7 Antibiotic Neutralization and Microbial Recovery and determining minimum biofilm eradication concentratin (MBEC)

After removing the peg lid from the challenge plate, the peg lid was rinsed twice using two 96-well plates containing sterile, $1\times$ PBS buffer, successively for one minute in each plate. Using sterile pliers, each peg was removed from the lid and placed into an individual microcentrifuge tube containing recovery medium to neutralize the antibiotic. Each tube was vortexed for 30 minutes to disrupt biofilm cells from the peg and into the recovery medium. The recovery medium was then pipetted out from each centrifuge tube and placed into its

corresponding well of a Nunc^{TM} 96-well plate, which will be referred to as the recovery plate for the remainder of this paper. The recovery plate was placed in the OD reader for 24h with readings taken every 10 minutes at 600 nm to generate a growth curve, which was used to determine the minimum biofilm eradication concentration (MBEC) for each antibiotic.

3.2.8 Statistical Analysis

Statistical analyses were performed using GraphPad Prism 6 for Windows (Version 6.01, Graph Pad Software, Inc., La Jolla, CA). Statistical significance was assessed using the repeated measures one-way ANOVA and chi-square testing with a significance level of $\alpha \leq 0.05$.

3.3.0 RESULTS

To assess the difference in antibiotic susceptibility between planktonic, detached and biofilm cell populations, the mean inhibitory concentrations for each cell type was compared (Table 3.4). The mean MIC of antibiotic needed to inhibit growth of detached cells (MIC-D) was either higher than or equal to the corresponding mean planktonic (MIC-P) values for all drugs tested. The MIC-D of the detached cells was statistically significantly higher than that of the planktonic cells for colistin (p=0.02), ampicillin/sulbactam (p=0.03), and trimethoprim/sulfamethoxazole (p=0.02) and statistically significantly lower than the minimum biofilm eradication concentration (MBEC) values for all drugs except imipenem and cefotaxime (Table 3.4).

Table 3.4: Mean minimum inhibitory concentrations (MIC) of planktonic and detached cells and mean minimum biofilm eradication concentration values (µg/mL) to selected antibiotics for ten *A. baumannii* strains collected from a large University Hospital.

Antibiotic (MIC breakpoint) [§]	Mean MIC value (µg/mL)			ANOVA[†] p-value	P-values[‡] of MIC Comparison		
	Planktonic Cells*	Detached Cells*	Biofilm Cells*		Planktonic vs Detached	Detached vs Biofilm	Planktonic vs Biofilm
Ciprofloxacin (≥4)	11.5	11.5	16.1	0.040	> 0.999	0.027	0.027
Gentamicin (≥16)	31.2	33.2	64.1	0.005	0.541	0.007	0.007
Colistin (≥4)	2.4	4.6	16.1	<0.0001	0.020	<0.0001	<0.0001
Ampicillin (≥32)	32.0	49.6	128.0	<0.0001	0.029	<0.0001	<0.0001
Sulbactam (≥16)	16.0	24.8	64.0	<0.0001	0.029	<0.0001	<0.0001
Imipenem (≥8)	32.1	32.1	32.1	> 0.999	> 0.999	> 0.999	> 0.999
Cefotaxime (≥64)	87.2	110.4	128.1	0.044	0.099	0.184	0.042
Tetracycline (≥16)	11.6	13.2	64.1	<0.0001	0.343	<0.0001	<0.0001
Trimethoprim (≥4)	3.7	5.9	16.1	<0.0001	0.017	<0.0001	<0.0001
Sufamethoxazole (≥76)	70.3	112.1	304.0	<0.0001	0.017	<0.0001	<0.0001

[§] MIC breakpoint for resistance for *Acinetobacter* spp. were obtained from the Clinical and Laboratory Standards Institute (CLSI), (18).

* n=10 for each drug

[†]Repeated Measures One-Way ANOVA

[‡]Student t-test

The testing of 8 different antibiotics against 10 *A. baumannii* strains resulted in 80 drug/strain combinations for each cell type. For the inhibition of planktonic cell growth (MIC-P), 61% (49/80) of the combinations were resistant to the antibiotic used. For the inhibition of detached cell growth (MIC-D), 76% (61/80) were resistant. All 80 drug/strain combinations were unable to eradicate biofilm growth. We used the Chi-square test for trend to assess the statistical significance between these differences observed in susceptibility/resistance patterns. Comparisons of resistance patterns for MIC-D vs MIC-P (OR=2.031, p=0.04), for MBEC vs MIC-D (OR=4.672, p<0.0001) and for MBEC vs MIC-P (OR=9.49, p<0.0001) showed that the detached cells (MIC-D) were statistically significantly different from both the planktonic (MIC-P) as well as biofilm cells (MBEC). It is noted that since all biofilm cells were resistant in all 80

combinations, we substituted susceptible=1, intermediate=1, resistant=78 to obtain a minimum value of 1 in the susceptible category so that the chi-square test could be applied.

Of the 8 drugs tested, colistin had the greatest % efficacy *in vitro* (10% planktonic and 70% detached cell populations resistant using standard breakpoints) and imipenem had the least (100% resistance for both planktonic and detached cells). The other six antibiotics had intermediate efficacies ranging from 50-90% of the isolates resistant among planktonic and detached cell types.

3.4.0 DISCUSSION

In this study of 5 clinical and 5 environmental isolates of *A. baumannii* collected from a large university hospital, we quantified the minimum biofilm eradication concentration (MBEC) and the minimum inhibitory concentration (MIC) of the corresponding biofilm-associated, planktonic and detached sessile cells for 8 antibiotics from different drug classes (totaling 80 strain-drug combinations). We report two key findings regarding *in vitro* antibiotic susceptibility for the planktonic, detached, and biofilm cells of *A. baumannii:* First, we provide evidence that the cells that appear to have been detached or sloughed from the biofilm have a minimum inhibitory concentration (MIC) that is greater than that for planktonic cells, yet less than that for biofilm cells. This finding is clinically significant because it suggests that therapy should be sufficient to target the detached cell population rather than planktonic cells for the treatment of biofilm-related infections. Second, the MBEC for all the stains grown as a biofilm were well over the MIC breakpoint for resistance.

The detachment (or shedding) of bacteria from biofilms is a well-documented process where cells or aggregates of cells break away from the biofilm and can reattach in a new location

for the continuation of the biofilm life cycle. Hall-Stoodley et al. suggested that the detachment process is not a passive behavior, but a strategy used by cells in the biofilm community, perhaps in response to depleting resources (11). Detachment also may be a response to environmental assaults, such as antibiotic exposure. We confirmed this hypothesis in the following way: when we subjected well-rinsed, peg-adhered biofilms to varying concentrations of antibiotics, we observed growth in the medium-containing wells after 24 hours of incubation; this growth appears to be a result of cells that detached from the biofilm in response to the antibiotic environment. Further, this detached cell population presented MIC values that were statistically significantly greater than that for planktonic cells (p=0.04) and yet statistically significantly less than the MBEC (p<0.0001). This result suggests a characteristically different phenotype expressed by this cell population -- at least with regard to antibiotic susceptibility. Environmental stressors can trigger differentially regulated genes between biofilm cells and their planktonic counterparts (27), (28). Thus, it is conceivable that the detached cells of the biofilm retain at least some sessile cell characteristics resulting in a detached cell population that is phenotypically unique from both sessile cells and planktonic cells. Alternatively, the detached cell population may be a mixture of single cells and cell aggregates where only the cell aggregates maintain the community level resistance resulting in a combined MIC level that is less than that of the biofilm and greater than that of the planktonic only population, which once again might explain the differences in antibiotic susceptibilities observed. This finding is potentially clinically significant and may have implications for therapy.

A. baumannii biofilms were resistant to all antibiotics tested. MIC values needed to inhibit planktonic cell growth were not effective in eradication of the corresponding biofilms for each antibiotic/isolate combination over a period of 24 hours, even at the highest concentrations

of antibiotics. Indeed, out of the 80 drug/strain combinations tested for ability to inhibit cell growth, in approximately 61% (49/80) of the combinations planktonic cells were resistant, compared to 100% of biofilm cells, establishing that significantly greater concentrations of antibiotic are needed to eradicate *A. baumannii* biofilms. This is consistent with previous reports of higher antibiotic concentrations needed to eradicate biofilm compared to planktonic cells of *A. baumannii* (1), (29) as well with a growing number of studies for a variety of pathogens including *Escherichia coli* and *Pseudomonas* (20) nontypeable *Haemophilus influenza* (30), *Staphylococcus aureus* (31) and Group A streptococcus (32).

While *A. baumannii* is generally susceptible to colistin, a polymyxin that acts as a detergent and solubilizes the outer membrane, we identified lineages that display colistin resistance. Never the less, colistin was the most effect antibiotic, where only 40% of the isolate-drug combinations for planktonic and detached cells were resistant. Imipenem, a beta-lactam that affects its antibacterial activities by inhibiting cell wall synthesis, was not able to inhibit growth of planktonic, detached or biofilm cells for any of the ten strains. This is consistent with a study by Song *et al.,* who also reported that imipenem was not effective against *A. baumannii* biofilm at MIC levels (≤4 µg/mL) (29). The *in vitro* activities of the remaining six classes of drugs evaluated were intermediary to those of imipenem and colistin. The resistance patterns we observed are consistent with other reports, suggesting that broader spectrum agents like carbapenems and colistin are required more frequently than previously to treat *A. baumannii* infections (8), (33). The presence of colistin-resistant strains underscores the limits of such alternative antibiotics and urges the need for the development of new therapies against *A. baumannii*.

In conclusion, this study provides evidence suggesting that detached biofilm cells are phenotypically distinct from planktonic cells, retaining at least some of the sessile phenotype. We found that the antibiotic concentration needed to inhibit detached cells of the biofilm is greater than that needed to inhibit planktonic cells, while biofilms require even greater concentrations. This is an important consideration for the use of antibiotic therapy in device-related infections. For example, a more effective approach may be to couple device removal with antibiotic therapies that target the detached cell population. Further research characterizing the full nature of the detached cell population is needed.

3.6.0 REFERENCES

1.   Badave GK, Kulkarni D. Biofilm Producing Multidrug Resistant Acinetobacter baumannii: An Emerging Challenge. J Clin Diagn Res 2015;9(1):DC08-10.

2.   Sunenshine RH, Wright MO, Maragakis LL, Harris AD, Song X, Hebden J, et al. Multidrug-resistant Acinetobacter infection mortality rate and length of hospitalization. Emerg Infect Dis 2007;13(1):97-103.

3.   Weber DJ, Rutala WA, Miller MB, Huslage K, Sickbert-Bennett E. Role of hospital surfaces in the transmission of emerging health care-associated pathogens: norovirus, Clostridium difficile, and Acinetobacter species. Am J Infect Control 2010;38(5 Suppl 1):S25-33.

4.   Lee HW, Koh YM, Kim J, Lee JC, Lee YC, Seol SY, et al. Capacity of multidrug-resistant clinical isolates of Acinetobacter baumannii to form biofilm and adhere to epithelial cell surfaces. Clin Microbiol Infect 2008;14(1):49-54.

5.   Longo F, Vuotto C, Donelli G. Biofilm formation in Acinetobacter baumannii. The New Microbiologica 2014;37(2):119-27.

6.   Lewis K. Persister cells. Annual Review of Microbiol 2010;64:357-72.

7.   Mirijello A, Impagnatiello M, Zaccone V, Ventura G, Pompa L, Addolorato G, et al. Catheter-related bloodstream infections by opportunistic pathogens in immunocompromised hosts. European review for medical and pharmacological sciences 2015;19(13):2440-5.

8.   Manchanda V, Sanchaita S, Singh N. Multidrug resistant acinetobacter. J Global Infect Dis 2010;2(3):291-304.

9.   Patel SJ, Oliveira AP, Zhou JJ, Alba L, Furuya EY, Weisenberg SA, et al. Risk factors and outcomes of infections caused by extremely drug-resistant gram-negative bacilli in patients hospitalized in intensive care units. Am J Infect Control 2014;42(6):626-31.

10.   Cohen R, Shimoni Z, Ghara R, Ram R, Ben-Ami R. Effect of a ventilator-focused intervention on the rate of Acinetobacter baumannii infection among ventilated patients. Am J Infect Control 2014;42(9):996-1001.

11.   Hall-Stoodley L, Stoodley P. Biofilm formation and dispersal and the transmission of human pathogens. Trends in Microbiol 2005;13(1):7-10.

12.   Fux CA, Costerton JW, Stewart PS, Stoodley P. Survival strategies of infectious biofilms. Trends in Microbiol 2005;13(1):34-40.

13.   Stewart PS. Biophysics of biofilm infection. Pathogens and Disease 2014;70(3):212-8.

14.   Dohnt K, Sauer M, Muller M, Atallah K, Weidemann M, Gronemeyer P, et al. An in vitro urinary tract catheter system to investigate biofilm development in catheter-associated urinary tract infections. J Microbiological Methods 2011;87(3):302-8.

15.   Penesyan A, Gillings M, Paulsen IT. Antibiotic discovery: combatting bacterial resistance in cells and in biofilm communities. Molecules 2015;20(4):5286-98.

16.   Mulcahy H, Charron-Mazenod L, Lewenza S. Extracellular DNA chelates cations and induces antibiotic resistance in Pseudomonas aeruginosa biofilms. PLoS pathogens 2008;4(11):e1000213.

17.   Stewart PS. Mechanisms of antibiotic resistance in bacterial biofilms. Intl J Med Microbiol 2002;292(2):107-13.

18.   Mah TF, O'Toole GA. Mechanisms of biofilm resistance to antimicrobial agents. Trends in Microbiol 2001;9(1):34-9.

19.   Hoiby N, Bjarnsholt T, Givskov M, Molin S, Ciofu O. Antibiotic resistance of bacterial biofilms. Intl J Antimicrobial Agents 2010;35(4):322-32.

20.   Sepandj F, Ceri H, Gibb A, Read R, Olson M. Minimum inhibitory concentration (MIC) versus minimum biofilm eliminating concentration (MBEC) in evaluation of antibiotic sensitivity of gram-negative bacilli causing peritonitis. Peritoneal Dialysis Intl 2004;24(1):65-7.

21.   Feng X, Sambanthamoorthy K, Palys T, Paranavitana C. The human antimicrobial peptide LL-37 and its fragments possess both antimicrobial and antibiofilm activities against multidrug-resistant Acinetobacter baumannii. Peptides 2013;49:131-7.

22.   Ceri H, Olson M, Morck D, Storey D, Read R, Buret A, et al. The MBEC Assay System: multiple equivalent biofilms for antibiotic and biocide susceptibility testing. Methods in enzymology 2001;337:377-85.

23.   Greene C, Vadlamudi G, Newton D, B. F, Xi C. The impact of biofilm formation and multidrug resistance on environmental survival of clinical and environmental isolates of Acinetobacter baumannii. Am J Infect Control Submitted, Sept. 5, 2015.

24.   CLSI. Performance Standards for Antimicrobial Susceptibility Testing; Twenty-Second Informational Supplement. CLSI document M100-S22. Wayne, PA: Clinical and Laboratory Standards Institute; 2012 January 2012.

25.   Wroblewska MM, Sawicka-Grzelak A, Marchel H, Luczak M, Sivan A. Biofilm production by clinical strains of Acinetobacter baumannii isolated from patients hospitalized in two tertiary care hospitals. FEMS Immunol and Med Microbiol 2008;53(1):140-4.

26.   Kaplan JB. Biofilm dispersal: mechanisms, clinical implications, and potential therapeutic uses. J Dental Research 2010;89(3):205-18.

27.   Sauer K, Camper AK. Characterization of phenotypic changes in Pseudomonas putida in response to surface-associated growth. J Bacteriology 2001;183(22):6579-89.

28.   Rumbo-Feal S, Gomez MJ, Gayoso C, Alvarez-Fraga L, Cabral MP, Aransay AM, et al. Whole transcriptome analysis of Acinetobacter baumannii assessed by RNA-sequencing reveals different mRNA expression profiles in biofilm compared to planktonic cells. PLoS One 2013;8(8):e72968.

29.	Song JY, Cheong HJ, Noh JY, Kim WJ. In vitro Comparison of Anti-Biofilm Effects against Carbapenem-Resistant Acinetobacter baumannii: Imipenem, Colistin, Tigecycline, Rifampicin and Combinations. Infect and Chemother 2015;47(1):27-32.

30.	Takei S, Hotomi M, Yamanaka N. Minimal biofilm eradication concentration of antimicrobial agents against nontypeable Haemophilus influenzae isolated from middle ear fluids of intractable acute otitis media. J Infect and Chemother 2013;19(3):504-9.

31.	Girard LP, Ceri H, Gibb AP, Olson M, Sepandj F. MIC versus MBEC to determine the antibiotic sensitivity of Staphylococcus aureus in peritoneal dialysis peritonitis. Peritoneal Dialysis Intl 2010;30(6):652-6.

32.	Conley J, Olson ME, Cook LS, Ceri H, Phan V, Davies HD. Biofilm formation by group a streptococci: is there a relationship with treatment failure? J Clin Microbiol 2003;41(9):4043-8.

33.	Moffatt JH, Harper M, Harrison P, Hale JD, Vinogradov E, Seemann T, et al. Colistin resistance in Acinetobacter baumannii is mediated by complete loss of lipopolysaccharide production. Antimicrob Agents Chemother 2010;54(12):4971-7.

APPENDIX 3-D

Clinical and Laboratory Standards Institute (CLSI).

MIC Standards for *Acinetobacter* spp.

S, Antibiotic susceptible; I, Intermediate susceptibility; R, Antibiotic resistant.

Group	Antimicrobial Agent	MIC Interpretive Criteria (µg/mL)		
		S	I	R
Penicillins	Piperacillin	≤16	32-64	≥128
	Mezlocillin	≤16	32-64	≥128
	Ticarcillin	≤16	32-64	≥128
β-lactam/ β-lactam Inhibitor Combinations	Ampicillin-Sulbactam	≤8/4	16/8	≥32/16
	Piperacillin-tazobactam	≤16/4	32/4 – 64/4	≥128/4
	Ticarcillin-clavulanate	≤16/2	32/2 – 64/2	≥128/2
Cephems	Ceftazidime	≤8	16	≥32
	Cefepime	≤8	16	≥32
	Cefotaxime	≤8	16-32	≥64
	Ceftriaxone	≤8	16-32	≥64
Carbapenems	Doripenem	≤2	4	≥8
	Imipenem	≤2	4	≥8
	Meropenem	≤2	4	≥8
Lipopeptides	Polymyxin B	≤2	–	≥4
	Colistin	≤2	–	≥4
Aminoglycosides	Gentamicin	≤4	8	≥16
	Tobramycin	≤4	8	≥16
	Amikacin	≤16	32	≥64
	Netilmicin	≤8	16	≥32
Tetracyclines	Tetracycline	≤4	8	≥16
	Doxycycline	≤4	8	≥16
	Minocycline	≤4	8	≥16
Fluoroquinolones	Ciprofloxacin	≤1	2	≥4
	Levofloxacin	≤2	4	≥8
	Gatifloxacin	≤2	4	≥8
Folate Pathway Inhibitors	Trimethoprim-sulfamethoxazole	≤2/38	–	≥4/76

Method: Growth of biofilm on the peg lid of the HTP assay plate.
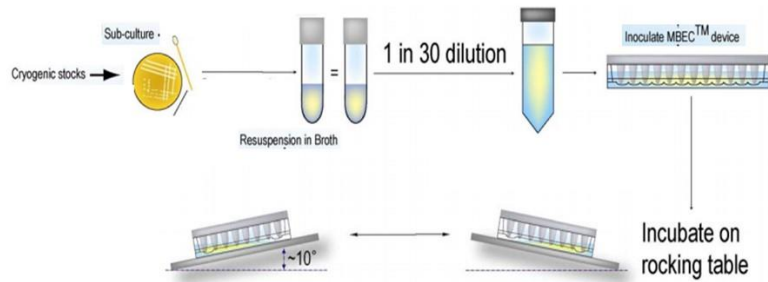
Growth of biofilm on pegs of HTP assay plate. The peg plate can then be inserted into 96-well plates containing antibiotic diluctions, neutralizing media, etc.
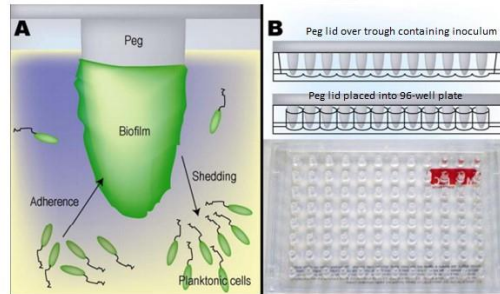
Method: Antibiotic Challenge Plate Set-Up.

Setup of 96-well antibiotic challenge plate for each strain, showing final concentrations of antibiotic in μg/mL Column 1 = sterility controls. Column 2 = growth controls. Columns 3-7, antibiotic challenges. Columns 8-12, duplicate antibiotic challenges.

Drug	Stock Conc.	1	2	3	4	5	6	7	8	9	10	11	12
Ciprofloxacin	80			16	8	4	2	1	16	8	4	2	1
Gentamicin	320			64	32	16	8	4	64	32	16	8	4
Colistin	80			16	8	4	2	1	16	8	4	2	1
Ampicillin Sulbactam	640 320			128 64	64 32	32 16	16 8	8 4	128 64	64 32	32 16	16 8	8 4
Imipenem	160			32	16	8	4	2	32	16	8	4	2
Cefotaxime	640			128	64	32	16	8	128	64	32	16	8
Tetracycline	320			64	32	16	8	4	64	32	16	8	4
Trimethoprim/ Sulfamethoxazole	80/ 1520			16 304	8 152	4 76	2 38	1 19	16 304	8 152	4 76	2 38	1 19

Method: An illustration of biofilm exposure to antibiotic dilutions.
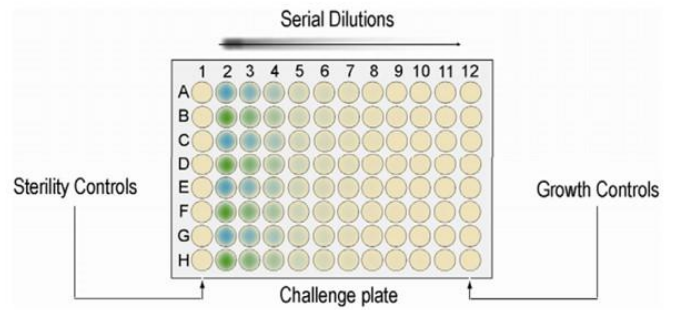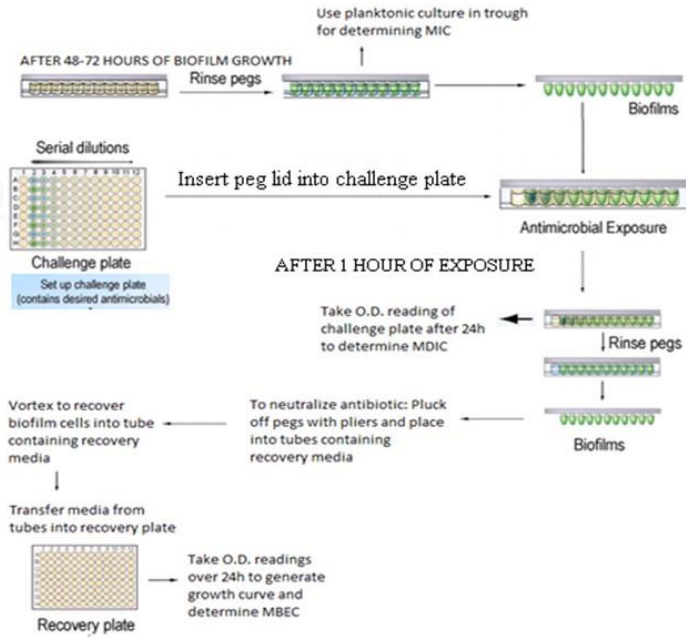
CHAPTER IV

Evaluation of the Ability of *Acinetobacter baumannii* to Form Biofilms on Six Different Biomedical Associated Surfaces

4.0.0 ABSTRACT

Objective: *Acinetobacter baumannii* is a gram-negative, antibiotic resistant, opportunistic pathogen that is a known biofilm former and frequently causes device-related infections in hospitals. A critical step in the biofilm development process is the ability to adhere to a surface. In addition to bacterial adhesion mechanisms, the physio-chemical properties of the substrata effect the colonization of microbes to that surface. Research comparing *A. baumannii* biofilms on different surfaces is lacking. The objective of this study was to compare the ability of *A. baumannii* to form biofilm on six different material types commonly found in the hospital environment: glass, ceramic, stainless steel, rubber, polycarbonate plastic and polypropylene plastic.

Methods: Biofilms were developed on six different material coupons using a CDC biofilm reactor. Biofilms were visualized and quantified using fluorescent staining and imaging by confocal laser scanning microscope and by direct viable cell counts.

Results: Mean biomass values for biofilms grown on glass, rubber, porcelain, polypropylene, stainless steel and polycarbonate were 0.04, 0.26, 0.62, 1.00, 2.08 and 2.70 $\mu m^3/\mu m^2$ respectively. Polycarbonate developed statistically more biofilm mass than glass, rubber,

porcelain and polypropylene. Direct viable cell counts data are in agreement with the microscopic observation.

Conclusion: Polycarbonate was the best surface for the formation of biofilm by *A. baumannii* ATCC17978 followed by stainless steel. Glass was least favorable for biofilm formation. Alternatives to polycarbonate in the producing of medical and dental devices need to be identified.

4.1.0 Introduction

    A. baumannii can persist and transmit in the hospital environment, contributing to nosocomial outbreaks and causing serious disease in the critically ill. Many of the infections caused by *A. baumannii* (ranging from urinary tract infections to ventilator-associated pneumonia) are associated with indwelling devices (1), (2) due to the formation of biofilm on these surfaces. The biofilms of *A. baumannii* are found on the surfaces of many medical devices including urinary catheters, central lines, surgical drains, ventilation equipment, dental water lines, and cleaning equipment as well as on a variety of other surfaces in the hospital environment (2, 3, 4).

    Biofilms are a dynamic, heterogeneous community of microorganisms within a complex matrix of extrapolymeric substance that undergo structural and genetic adaptations, have integrated metabolic activities, and produce sessile phenotypes markedly different from their planktonic counterparts (5, 6, 7). A critical step for biofilm formation is the pathogen's ability to adhere to a surface. *A. baumannii* mediate attachment via pili, encoded by the *csu*A/BABCDE chaperone-usher pilus assembly operon (8) and there is some evidence suggesting that the *bla*$_{PER-1}$ gene also enhances substrate adhesion (9). In terms of surface chemistry, the physio-chemical properties of the surface also play a role in in the colonization of microbes to that surface. Electrostatic forces, Lifshitz-van der Waals forces, and hydrophobic/hydrophilic forces positively or negatively influence microbial adhesion to a surface (10). Increased surface roughness can increase the hydrophobicity of the surface by effecting the surface contact angle (11). For example, *Staphylococcus epidermidis* has greater adhesion to hydrophobic surfaces compared to hydrophilic surfaces (12).

A variety of material types are used in medical equipment and in the hospital setting. Polycarbonate, a sturdy, low-cost plastic that can undergo autoclave sterilization is found in a variety of medical devices including urinary catheters, gastrointestinal tubes, and cardiopulmonary bypass circuits, blood oxygenators and flood filters used in the bypass circuit (13). Mesh prosthetics are often composed of polypropylene (14) and ceramic is commonly used in many implants and dental crowns (15), (16). Stainless steel makes up the majority of surgical equipment and rubber has a number of uses, particularly rubber seals, such as that used in disposable plastic syringes (17). Cells of *A. baumannii* can persist on most of these inanimate surfaces (18) but *A. baumannii* biofilms only have been demonstrated on a limited number of substrata such as glass (19) and plastic surfaces (8). The aim of this study was to compare the ability of *A. baumannii* to form biofilm on six different material types: glass, ceramic, stainless steel, rubber, polycarbonate plastic and polypropylene plastic. Understanding the propensity for biofilm formation on various surfaces provides critical information to different parties for selecting low biofilm materials, which is essential for minimizing the risk of biofilm-associated infections.

4.2.0   METHODS

4.2.1   Bacterial strain and culture conditions

Acinetobacter baumannii ATCC 17978 (American Type Culture Collection, Manassas, VA) was used for all biofilm tests. A single colony on Mueller Hinton II (MHII) agar plate was sub-cultured into MHII broth (Becton, Dickinson and Co., Sparks, MD) and incubated for 15-18h at 37ºC, which was then used to create the inoculum for biofilm development.

4.2.2 Preparation of material coupons

All material coupons were round discs that are one centimeter in diameter and approximately 3 millimeters thick. The following non-porous material coupons were used to grow *A. baumannii* biofilms: medical grade stainless steel (RD128-304), AHW BUNA-N Rubber (RD128-BUNA), porcelain (RD128-PL), polycarbonate plastic (RD128-PC), polypropylene plastic (RD128-PP) and borosilicate glass (RD128-GL) (all material coupons from BioSurface Technologies, MO). Before use, all material coupons were washed with soap and water, followed by a 70% ethanol bath, and then autoclaved for sterilization.

4.2.3 Biofilm development

A CDC biofilm reactor (Biosurface Technologies, Bozeman, MT) was used for biofilm growth. The CDC biofilm reactor and its coupon holders were autoclaved before use. Material coupons were mounted on the coupon holders and the reactor was supplemented with 10% LB medium by a peristaltic pump with a continuous flow rate of 100 mL/h. Overnight cultures of *A. baumannii* ATCC 17978 (grown under shaking conditions at 37 °C) were diluted by 1:100 and inoculated into the glass vessel of the CDC reactor aseptically. The liquid growth medium was circulated through the vessel and a magnetic stir bar rotated by a magnetic stir plate generated a shear force. The CDC biofilm reactor was placed on a bench and biofilms were grown at room temperature. After four days of growth, the coupons were aseptically removed for biofilm imaging and viable bacteria plate counting. All experiments were conducted in triplicate.

4.2.4 Bacterial count determination

Biofilms on the coupons were recovered by homogenizing the coupon in 3 mL of 1× phosphate buffered saline (PBS, 10 mM, pH7.2) solution for 1 min using Omni-Tip™ disposable rotor stator generator probes (OMNI International, Kennesaw, GA). Samples were then serial

diluted to 10^{-3}, spread plated onto MHII agar and incubated overnight at 37°C for colony enumeration.

4.2.5 Microscope Analysis

One from each kind of coupon was used for fluorescent staining and imaging by confocal laser scanning microscope (CLSM). Coupons with adhered biofilm were stained with LIVE/DEAD BacLight Bacterial Viability kit (L7012, Invitrogen, Carlsbad, CA) according to kit instructions. Fluorescent images were acquired with an inverted CLSM (Olympus 1X71, Center Valley, PA) equipped with Fluorescence Illumination System (X-Cite 120, EXFO) and filters for SYTO-9 (excitation = 488 nm/emission = 520 nm) and Propidium Iodide (excitation = 535 nm/emission = 617 nm) fluorescence. Images were obtained using an oil immersion 60×objective lens, and for each location, images were scanned at 1μm intervals. After acquiring images, a 3-D image was re-constructed by using Imaris® Bitplane core scientific software. Five different surface areas of each material coupon were randomly chosen for imaging in order to better represent biofilms. Biofilm biomass was calculated based on microscopic images by using Comstat 2 (20), (21).

The surface of the rubber took up the live/dead stain causing challenges in distinguishing the biomass from the background. Therefore, data on the biomass and live/dead ratio obtained for rubber using microscopy was presented just for a reference. However, the viable cell count data is reliable to determine biofilm biomass developed on the rubber.

4.2.6 Statistical Analysis

Statistical analyses were performed using GraphPad Prism 6 for Windows (Version 6.01, Graph Pad Software, Inc., La Jolla, CA). Statistical significance was assessed using one-way ANOVA with multiple comparisons using t-test and a significance level of $\alpha \leq 0.05$.

4.3.0   RESULTS

In order to determine the effect of surface materials, *A. baumannii* biofilms were developed on disc coupons of glass, rubber, porcelain, polypropylene, stainless steel and polycarbonate in a CDC reactor for 4 days. Biofilm biomass along with the viable count of cells recovered from the biofilms was determined for each material type. Mean biomass values for biofilms grown on glass, rubber, porcelain, polypropylene, stainless steel and polycarbonate were 0.04, 0.26, 0.62, 1.00, 2.08 and 2.70 $\mu m^3/\mu m^2$ respectively (Figure 4.9). Polycarbonate developed statistically more biofilm mass than glass, rubber, porcelain and polypropylene. Stainless steel developed statistically more biofilm mass than glass, rubber and porcelain. The mean CFU/mL for each surface type is presented in Figure 4.10 and corroborate the mean biomass values determined using the confocal microscope. The biofilms growing on polycarbonate had a statistically significantly higher CFU/mL compared to all other surface types. The mean CFU/mL values for the biofilms grown on glass, rubber, porcelain, polypropylene, stainless steel and polycarbonate were 4.05 x 10^6, 8.20 x 10^6, 1.02 x 10^7, 1.41 x 10^7, 2.00 x 10^7 and 8.32 x 10^7 respectively.

The ratio of live to dead cells was quantified for each material type to verify biomass estimations derived via fluorescent microscopy. The mean values are presented in Figure 4.11. Mean live/dead ratios of the biofilms grown were 3.97, 1.51, 3.47, 6.26, 7.42 and 4.23 for glass, rubber, porcelain, polypropylene, stainless steel and polycarbonate respectively. Stainless steel had statistically significantly higher ratio of live to dead cells compared to all other surface types except for polypropylene. Rubber had the lowest ratio and was statistically lower than all other material types.

Biofilm imaging using the confocal microscope was performed for each material type and

select images are shown in Figure 4.12. The difficulty in discerning biofilm mass from the

rubber surface background can be seen in Figure 4.12B.

Figure 4.6: Biomass of A. baumannii ATCC17978 biofilms grown on selected material types with corresponding microscopic images.
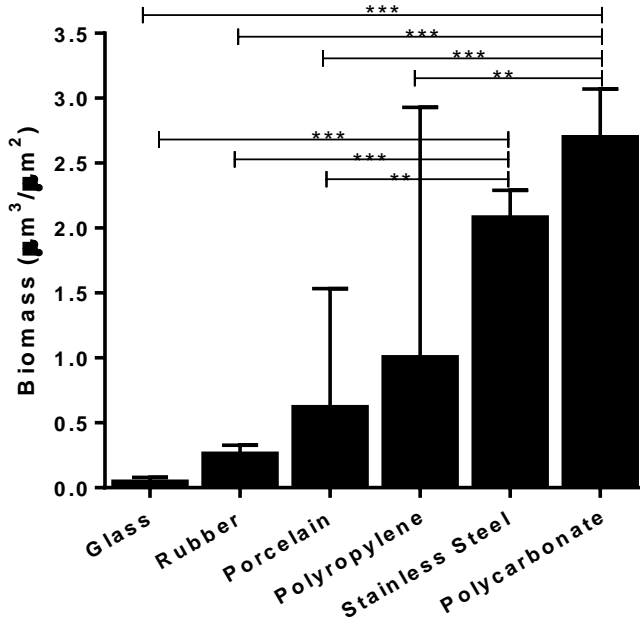
One-Way ANOVA p-0.008
**p=0.02; ***p≤0.009

Figure 4.7: Viable A. baumannii ATCC17978 cells on selected material types.

n=5
One-Way Anova p=0.004; ***p≤0.001
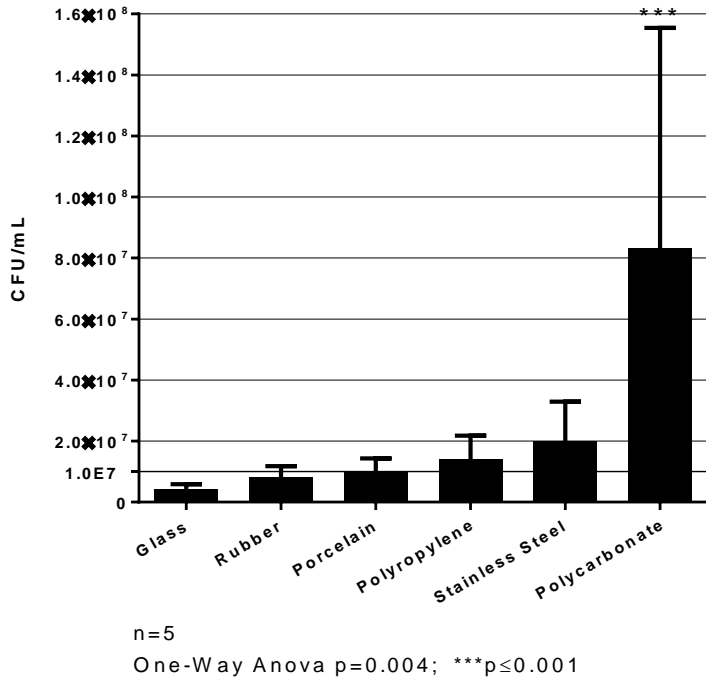
Figure 4.8: Live/Dead ratio of A. baumannii ATCC17978 biofilms grown on selected material types.

One-Way ANOVA p=0.0002
*p=0.01, **p≤0.001
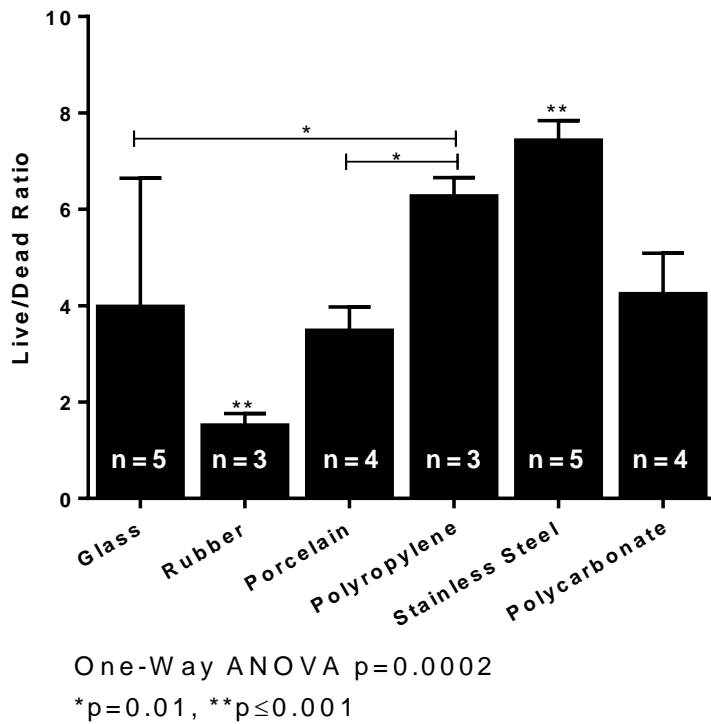
Figure 4.9: Top: Images of A. baumannii ATCC17978 biofilm cells stained with live/dead stain and visualized using the confocal microscopy on glass (A), rubber (B), porcelain (C), polypropylene (D), stainless steel (E), and polycarbonate (F). Bottom: Top and side views of Glass, Ceramic, Stainless Steel and Polycarbonate.
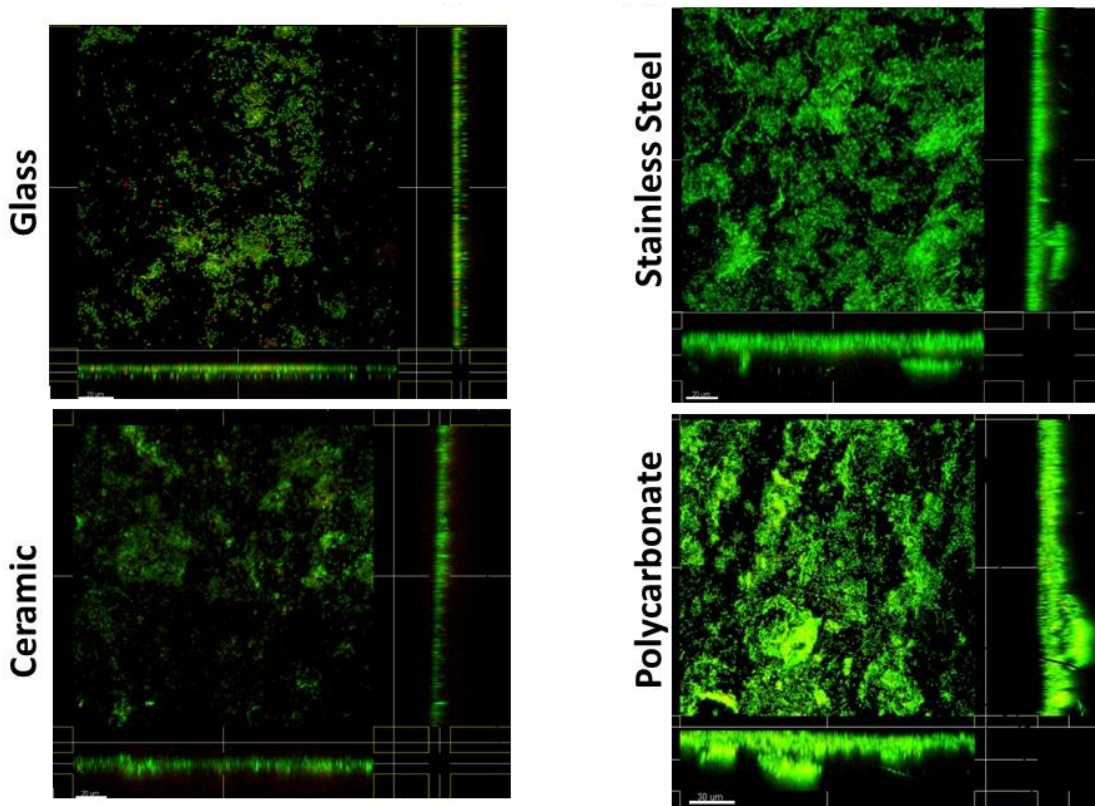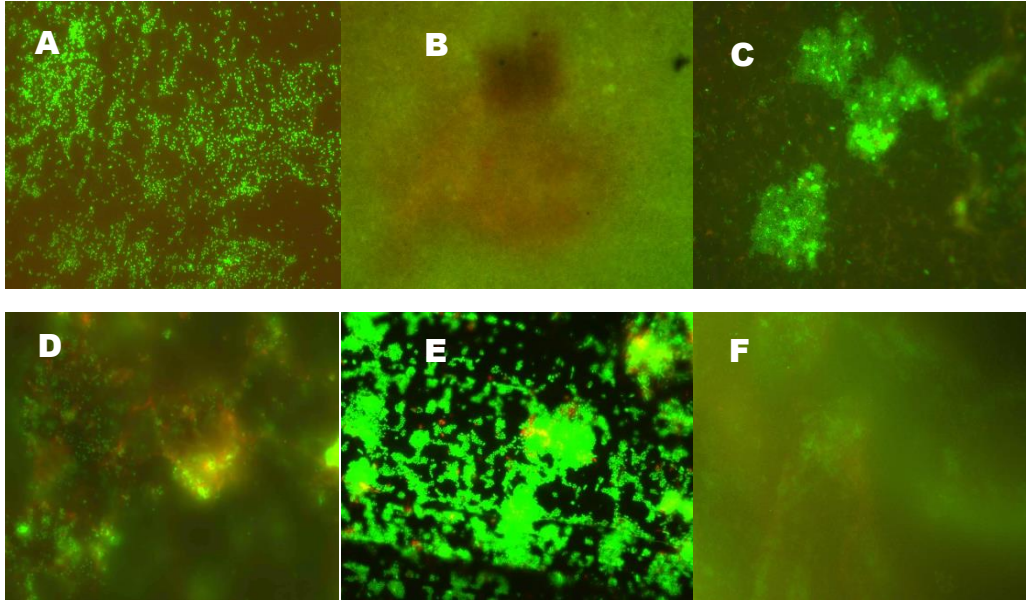
4.4.0 DISCUSSION

The material substratum is an essential factor that contributes to the ability of a pathogen to adhere to and form biofilm on a surface (22), (23). Aside from cellular properties and pathogen adhesion mechanisms, variations in surface roughness, hydrophobicity and chemical structure can impede or promote a pathogens ability to attach and populate on that surface. We evaluated the ability of *A. baumannii* ATCC17978 to form biofilms on six different surfaces: glass, rubber, porcelain, polypropylene, stainless steel and polycarbonate.

In this study, the surface with the highest level of biofilm mass was polycarbonate, a hydrophobic type of plastic. Our finding of high biofilm formation on polycarbonate is consistent with the finding of Brandao et al. who demonstrated that polycarbonate composite orthodontic brackets sustained the highest level of bacterial adhesion in the buccal cavity compared to metal and ceramic brackets (23). To our knowledge, there are no published studies comparing biofilm formation of *A. baumannii* on polycarbonate with other material types. In contrast to polycarbonate, *A. baumannii* cells did not adhere well to glass, which is typically hydrophilic, and weakly formed small aggregates of biofilm. We found no statistically significant difference in biofilm mass on glass compared to ceramic and polypropylene, although higher biofilm mass was formed on these surfaces, which could also be visually seen. This is consistent with several other studies showing that biofilm formation by *A. baumannii* was less favorable on glass compared to plastic such as polystyrene, polypropylene and Teflon plastics (8), (24).

We found that stainless steel had statistically significantly more biofilm mass compared to porcelain and glass. We used a brushed stainless steel, which has a striated surface structure. While the high surface energy of stainless results in a more hydrophilic surface, the roughness of

75

the surface contributes to a more hydrophobic surface. The surface groves also increase the surface area and enhance microbial colonization. This may also account for the high live/dead ratio seen for stainless steel as cells adhere within the grooves, forming a strong base, onto which live cells attach and subsist. A qualitative comparison of microscan images with studies by Nan et al. who compared the biofilms of *Staphylococcus aureus* on stainless steel with copper treated stainless steel (25) and by Fernandez-Delgado et al. who evaluated the biofilms of *P. mirabilis* on stainless steel (22), reveals similarity in biofilm development with regard to this metal.

A limitation of this study is that we evaluated the biofilm formation of a single, clonal species of *A. baumannii*. However, biofilms are known to exist as mixed species in nature and the combination of bacteria present dictate (or affect) bacterial attachment and the formation of (26). Therefore, the level of biofilm we observed may be over or underestimated from what might occur in the natural environment. This study grew biofilms under dynamic (versus static) conditions. Dynamic conditions result in less biofilm formation when compared to static conditions (8). Therefore, our measures of biofilm mass do not represent biofilm that would form in the open environment lacking shearing stress. Of note, the hydrophobicity parameters of each substratum were not determined prior to use in this study, so we cannot definitively correlate differences in biofilm development on the basis of surface hydrophobicity.

We demonstrate that there are differences in biofilm formation by *A. baumannii* ATCC17978 across different surfaces. Specifically, we found that polycarbonate was the best surface for the formation of biofilm by *A. baumannii* ATCC17978 followed by stainless steel and that glass was least favorable for biofilm formation. Alternatives to polycarbonate in the producing of medical and dental devices need to be identified. The differences in biofilm formation across different material types may be due to variations in surface roughness and

76

porosity, ionic charge, and hydrophobicity and the extent to which the material surface influences attachment and biofilm formation warrant further investigation. The results of this study suggest that polycarbonate should be avoided in the manufacture of invasive devices.

4.5.0 ACKNOWLEDGEMENTS

4.6.0 REFERENCES

1.   Manchanda V, Sanchaita S, Singh N. Multidrug resistant acinetobacter. J Global Infect Dis 2010;2(3):291-304.

2.   Patel SJ, Oliveira AP, Zhou JJ, Alba L, Furuya EY, Weisenberg SA, et al. Risk factors and outcomes of infections caused by extremely drug-resistant gram-negative bacilli in patients hospitalized in intensive care units. Am J Infect Control 2014;42(6):626-31.

3.   Donlan RM, Costerton JW. Biofilms: survival mechanisms of clinically relevant microorganisms. Clin Microbiol Reviews 2002;15(2):167-93.

4.   Cohen R, Shimoni Z, Ghara R, Ram R, Ben-Ami R. Effect of a ventilator-focused intervention on the rate of Acinetobacter baumannii infection among ventilated patients. Am J Infect Control 2014;42(9):996-1001.

5.   Sutherland IW. The biofilm matrix--an immobilized but dynamic microbial environment. Trends in Microbiol 2001;9(5):222-7.

6.   Hall-Stoodley L, Stoodley P. Biofilm formation and dispersal and the transmission of human pathogens. Trends in Microbiol 2005;13(1):7-10.

7.   Stoodley P, Sauer K, Davies DG, Costerton JW. Biofilms as complex differentiated communities. Annual Review of Microbiol 2002;56:187-209.

8.   Tomaras AP, Dorsey CW, Edelmann RE, Actis LA. Attachment to and biofilm formation on abiotic surfaces by Acinetobacter baumannii: involvement of a novel chaperone-usher pili assembly system. Microbiology 2003;149(Pt 12):3473-84.

9.   Lee HW, Koh YM, Kim J, Lee JC, Lee YC, Seol SY, et al. Capacity of multidrug-resistant clinical isolates of Acinetobacter baumannii to form biofilm and adhere to epithelial cell surfaces. Clin Microbiol Infect 2008;14(1):49-54.

10.   Bos R, van der Mei HC, Busscher HJ. Physico-chemistry of initial microbial adhesive interactions--its mechanisms and methods for study. FEMS Microbiol Rev 1999;23(2):179-230.

11.   Patankar NA. Transition between superhydrophobic states on rough surfaces. Langmuir 2004;20(17):7097-102.

12.   Cerca N, Pier GB, Vilanova M, Oliveira R, Azeredo J. Quantitative analysis of adhesion and biofilm formation on hydrophilic and hydrophobic surfaces of clinical isolates of Staphylococcus epidermidis. Research in Microbiol 2005;156(4):506-14.

13.   Duty SM, Mendonca K, Hauser R, Calafat AM, Ye X, Meeker JD, et al. Potential sources of bisphenol A in the neonatal intensive care unit. Pediatrics 2013;131(3):483-9.

14.   Byrd JF, Agee N, Nguyen PH, Heath JJ, Lau KN, McKillop IH, et al. Evaluation of composite mesh for ventral hernia repair. JSLS 2011;15(3):298-304.

15.   Ren L, Zhang Y. Sliding contact fracture of dental ceramics: Principles and validation. Acta Biomaterialia 2014;10(7):3243-53.

16.   Schroder D, Bornstein L, Bostrom MP, Nestor BJ, Padgett DE, Westrich GH. Ceramic-on-ceramic total hip arthroplasty: incidence of instability and noise. Clinical Orthopaedics and Related Research 2011;469(2):437-42.

17.   Hamilton G. Contamination of contrast agent by MBT in rubber seals. Canadian Med Assoc J 1987;136(10):1020-1.

18.   Wendt C, Dietze B, Dietz E, Ruden H. Survival of Acinetobacter baumannii on dry surfaces. J Clin Microbiol 1997;35(6):1394-7.

19.   Vidal R, Dominguez M, Urrutia H, Bello H, Gonzalez G, Garcia A, et al. Biofilm formation by Acinetobacter baumannii. Microbios 1996;86(346):49-58.

20.   Heydorn A, Nielsen AT, Hentzer M, Sternberg C, Givskov M, Ersboll BK, et al. Quantification of biofilm structures by the novel computer program COMSTAT. Microbiology 2000;146 (Pt 10):2395-407.

21.   Vorregaard M. Comstat2 - a modern 3D image analysis environment for biofilms, in Informatics and Mathematical Modelling. Kogens Lyngby, Denmark: Technical University of Denmark; 2008.

22.   Fernandez-Delgado M, Duque Z, Rojas H, Suarez P, Contreras M, Garcia-Amado MA, et al. Environmental scanning electron microscopy analysis of biofilms grown on chitin and stainless steel. Annals of Microbiol 2015;65(3):1401-1409.

23.   Brandao GA, Pereira AC, Brandao AM, de Almeida HA, Motta RR. Does the bracket composition material influence initial biofilm formation? Indian J Dental Research 2015;26(2):148-51.

24.   McQueary CN, Actis LA. Acinetobacter baumannii biofilms: variations among strains and correlations with other cell properties. J Microbiol 2011;49(2):243-50.

25.   Nan L, Yang K, Ren G. Anti-biofilm formation of a novel stainless steel against Staphylococcus aureus. Materials Science and Engineering 2015;51:356-61.

26.   McEldowney S, Fletcher M. Adhesion of bacteria from mixed cell suspension to solid surfaces. Archives of Microbiol 1987;148(1):57-62.

CHAPTER V

Fomite-Fingerpad Transfer Efficiency (pick-up and deposit) of *Acinetobacter baumannii* With and Without a Latex Glove

5.0.0 ABSTRACT

Background: *Acinetobacter baumannii* is a significant healthcare-associated pathogen as it is easily transmitted via fomites, extremely difficult to eradicate from the environment, and highly drug resistant. Understanding the environmentally mediated transmission dynamics of *A. baumannii* is critical for more effective infection control. However, transfer efficiency of pathogen pick-up and deposit remains poorly understood. Our study estimates the transfer efficiency of *A. baumannii* with and without latex glove use from the fingerpad to a fomite and from a fomite to the fingerpad.

Methods: Fomite-fingerpad transfer efficiencies were determined for six materials (glass, stainless steel, porcelain, polypropylene, polycarbonate, and rubber).

Results: For *A. baumannii*, the fomite-to-fingerpad transfer efficiency was 24.1% and the fingerpad-to-fomite transfer efficiency was 5.6%. When latex gloves were worn, the fomite-to-fingerpad transfer efficiency was reduced by 55.9% (to 10.6%) and the fingerpad-to-fomite transfer efficiency was reduced by 47.1% (to 3.0%). The average transfer efficiency between two skin surfaces was 32.5%.

Conclusions: The fomite-to-fingerpad transfer efficiency of *A. baumannii* was statistically significantly higher than the fingerpad-to-fomite transfer efficiency, regardless of glove use. There was no significant difference in transfer efficiency by material type, except for rubber, which resulted in marginally higher transfer efficiencies. Our results underscore the importance of frequently changing gloves during patient care as well as frequent hand washing/hand hygiene during bare-handed care for the reduction of pathogen transmission.

5.1.0 INTRODUCTION [4]

Acinetobacter baumannii transmission within hospitals is a significant problem (1), (2). This gram negative, frequently multi-drug resistant bacterium produces a variety of healthcare-associated infections including pneumonia, bacteremia, wound infections and urinary tract infections, primarily among those who are already very ill, making it particularly a problem within intensive care units (3). Effective control is challenging as *A. baumannii* can survive long periods of desiccation, persisting in the environment for 1-4 months (4), (5), (6) and typical disinfection practices are often inadequate (7), (8). Therefore, understanding the environmentally mediated transmission dynamics of *A. baumannii* is critical for identifying a more targeted approach to effective infection control. Previous studies have determined the pick-up transfer efficiencies (fomite-to-fingerpad/hand) for a variety of gram-positive and gram negative bacteria (9), (10), but to our knowledge, transfer efficiencies in the direction of fingerpad/hand-to-fomite have not been previously reported. Since these studies have already shown that transfer efficiency is dependent on organism and material type, we have chosen six nonporous surface materials that are commonly found in the hospital environment to evaluate the variation in transfer efficiencies.

Most fate and transport mathematical models assume the same transfer efficiency value for calculating both the fomite-to-fingerpad rate of pathogens and the fingerpad-to-fomite rate of pathogens (11), (12), (13). This assumption may be appropriate when the two contacting surfaces are composed of the same material of similar physical characteristics (i.e. dry skin-skin contact). However, when the two contacting surfaces are not composed of the same material (i.e.

---

contact between the skin and an environmental surface), this assumption may not hold. Moreover, transfer efficiencies of *A. baumannii* have never been quantified. Thus, the first aim of this study is to compare the transfer efficiencies of *A. baumannii* in two directions; fomite-to-fingerpad and fingerpad-to-fomite, with and without the use of latex gloves. For comparative purposes, we also determined the transfer efficiency of *A. baumannii* between two skin surfaces: fingerpad-to-fingerpad. Specific pathogen transmission parameters, such as pathogen transfer efficiencies in both directions of transfer, are needed to fill current knowledge gaps of environmental infection transmission systems. These data will enable more robust use of quantitative microbial risk assessment (QMRA) models for exposure assessment and evaluation of pathogen fate and transmission in the hospital environment.

5.2.0 METHODS

Ten volunteer subjects participated. The study protocol was reviewed and approved by the University of Michigan IRB (HUM00075484).

5.2.1 Preparation of initial inoculum

All transfer experiments were performed using *Acinetobacter baumannii* ATCC 17978 (American Type Culture Collection, Manassas, VA). The initial inoculum was prepared fresh for each experiment by transferring a frozen aliquot of the ATCC17978 into 2.5 mL of BBL^{TM} Mueller Hinton II (MHII) broth (Becton, Dickinson and Co., Sparks, MD), and incubating at 37°C for 18±2 h on a rotating shaker table (150-180 rpm). The culture was streaked onto BBL^{TM} MHII agar (Becton, Dickinson and Co., Sparks, MD) and grown at 37°C. An isolated colony was transferred to MHII broth and incubated at 37°C with shaking at 150-180 rpm for 15-18

hours. From this, a starting culture with an OD600 of 0.200 ± 0.01, which approximates 10^8 CFU/mL, was used (Synergy™ HT Multi-Mode Microplate Reader, BioTek® Instruments, Inc.).

5.2.2 *Preparation of fomite material coupons*

All material coupons were round discs that are one cm in diameter and approximately 3 mm thick. The following non-porous material coupons were used to determine *A. baumannii* transfer efficiencies: medical grade stainless steel (RD128-304), AHW BUNA-N Rubber (RD128-BUNA), porcelain (RD128-PL), polycarbonate plastic (RD128-PC), polypropylene plastic (RD128-PP) and borosilicate glass (RD128-GL) (all material coupons from BioSurface Technologies, MO). Before and after each use, all material coupons were washed with soap and water, followed by a 70% ethanol bath, and then autoclaved for sterilization (13).

5.2.3 *Method for determining the direct recovery rate of bacteria*

The direct recovery rate was determined to estimate the total amount of bacteria that can theoretically be recovered from each surface after drying. The direct recovery rate was used to help validate study results by demonstrating that differences seen between the fomite-to-finger and fingerpad-to-fomite transfer efficiencies were not due to possible biases in recovery methods from the various surface types. For this determination, a transfer of bacteria between the two surfaces was not performed. In triplicate, each material used in these experiments (the six material coupons, the glove fingertips and fingerpads of a hand) were prepared as described for each material type, inoculated with 20 μL (or 1.4×10^9 CFUs) of *A. baumannii* and allowed to dry. Once dry (with no transfer event), the bacteria was recovered exactly as described below for that surface type and the percent CFUs recovered was calculated by ($CFU_{Recovered}/CFU_{Applied}$) X 100.

5.2.4   Preparation of Volunteer hands

Before and after each transfer event, volunteer hands were prepared using the following control wash procedure regardless of glove use (10): Hands were squirted with 70% ethanol for 10 sec, the alcohol was rubbed thoroughly over hands (concentrating on the finger tips) for 15 sec and then rinsed with tap water for 15 sec. Hands were then scrubbed for 1 min with 2ml of Huntington brand Medi-Scrub® liquid soap containing the active ingredient 0.6% Chloroxylenol (Ecolab Inc., MN) and warm water. Hands were rinsed in warm water for 15s and air dried until thoroughly dry.

5.2.5   Recovering bacteria from the fingerpad

Immediately following each transfer event, bacteria on the finger was recovered using a sterile, individually wrapped, CultureSwab[TM] (Becton, Dickinson and Co., Sparks, MD) swab, moistened in 3 mL of 1X PBS buffer. Excess buffer was first pressed out of the swab by pressing the tip of the swab against the inside of the tube. The fingerpad was swabbed in both a forward-back motion and a side-to-side motion while rotating the tip of the swab (10). The swab was then returned to the 1X PBS buffer and homogenized in the buffer using Omni-Tip™ disposable rotor stator generator probes (OMNI International, Kennesaw, GA) for 45 sec to remove all cells from the swab. Samples were then serial diluted to 10^{-3}, spread plated onto MHII agar and incubated overnight at 37°C for colony enumeration. All samples were kept on ice during sampling. This swab method was used in order to avoid an additional step of bacterial transfer, for example, from fingerpad to the inside wall of the centrifuge tube containing the PBS buffer.

5.2.6   Recovering bacteria from fomite coupons and latex gloves

Bacteria on the coupons and gloves were recovered by vortexing the sample in a sterile, 50 mL conical centrifuge tube (Falcon^{TM}, Corning Life Sciences DL) containing 6 mL of 1X PBS buffer for 1 min. Samples were then serial diluted to 10^{-3}, spread plated onto MHII agar and incubated overnight at 37°C for colony enumeration. All samples were kept on ice during processing.

5.2.7   Simulation of fingerpad-to-fomite transfer event by the fingerpad (n=10)

A cleaned, randomly chosen fingerpad was inoculated with 20 μL of *A. baumannii* ATCC 17978 and allowed to air-dry for 10-15 min in a laminar hood. Once dry, the inoculated fingerpad was placed onto a coupon, applying an average constant pressure of 25 kPa (range of 16-38 kPa) for 30 sec (14). This was performed using a top-loading balance (XP-1500, Denver Instrument Co.) to monitor the amount of pressure applied in grams/cm^2. After the transfer event was complete, the coupon was placed in a centrifuge tube containing 1X PBS buffer and the finger was swabbed (Figure 5.13A). All samples were stored on ice.

5.2.8   Simulation of fingerpad-to-fomite transfer event by the latex glove (n=10)

Powder-free, single use, latex exam gloves (19-058-801C, Fisher Scientific, Pittsburgh, PA) were placed on a clean hand (cleaned as described above). The fingerpads of the glove were cleaned with 70% ethanol, inoculated with 20 μL of *A. baumannii* ATCC 17978 and allowed to air-dry in a laminar hood. Once dry, the inoculated area of the latex fingerpad was placed onto a coupon and the transfer event was performed in the same manner as for determining the fingerpad-to-fomite transfer efficiency described above (Figure 5.13A). After the transfer event was complete, the top 1.5 inches of the glove fingertip was aseptically snipped from the finger

and immediately placed into a centrifuge tube containing 1X PBS buffer. The coupon was

placed in a separate centrifuge tube containing 1X PBS buffer.

5.2.9   Simulation of fomite-to-fingerpad transfer event by the fingerpad (n=10)

Sterile coupons were inoculated with 20 μL of *A. baumannii* ATCC 17978 and allowed

to air-dry for 15-20 min in a laminar hood. Once dry, a cleaned fingerpad was placed onto the

contaminated coupon, applying an average constant pressure of 25 kPa (range of 16-38 kPa) for

30 sec, using the same top-loading balance as described above. After the transfer event was

complete, the coupon was placed in a centrifuge tube containing 1X PBS buffer and the finger

was swabbed (Figure 5.13B).

5.2.10   Simulation of fomite-to-fingerpad transfer event by the latex glove (n=10)

This was performed in the same manner as for the pick-up transfer efficiency by the

fingerpad except that the cleaned hand was wearing a latex glove (Figure 5.13B). After the

transfer event was complete, the top 1.5 inches of the glove finger was aseptically snipped from

the finger and immediately placed into a centrifuge tube containing 1X PBS buffer.

Figure 5.10: Schematic show of procedures for simulating deposit (A) and pick-up (B) transfer event.
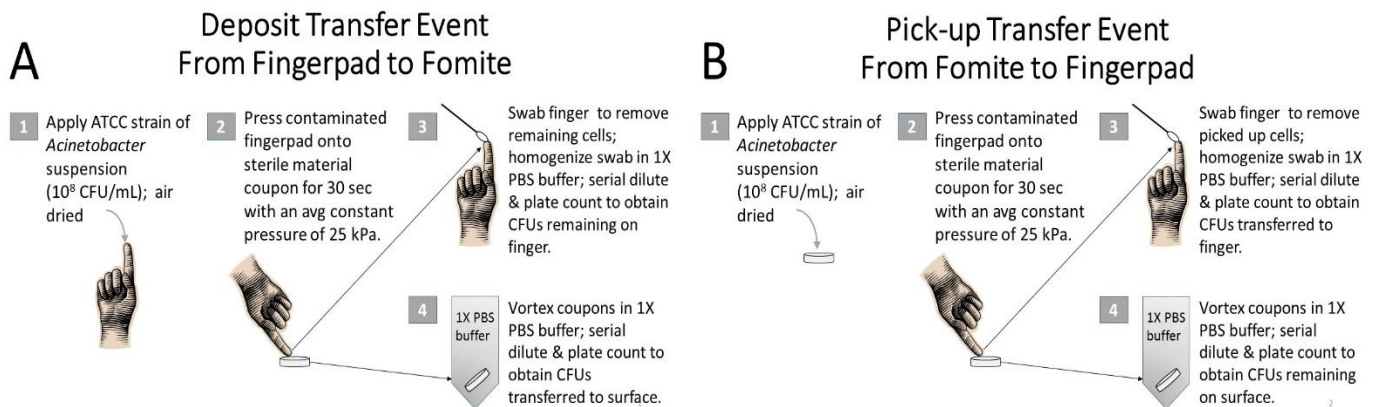
5.2.11   Simulation of fingerpad-fingerpad (skin-skin) transfer event (n=6)

A cleaned fingerpad was inoculated with 20 µL of *A. baumannii* ATCC 17978 and allowed to air-dry for 10-15 min in a laminar hood. Once dry, the inoculated fingerpad (the donor finger) was pressed up against a clean recipient finger with pressure similar to that of a hand-shake for 1 min. This was performed with three fingers at a time (the fore, middle and ring fingers) to achieve consistency in applied pressure between transfer events. Both the donor and recipient fingers were swabbed and samples were stored on ice.

5.2.12   Statistical analysis

Mean colony counts recovered from the material coupons, fingerpads and gloves were determined and used to calculate percent transfer efficiency. Colony forming units recovered (CFU_R) were determined for both surfaces involved in each transfer event. CFU_R was used to calculate the percent transfer efficiency for each direction in the transfer event where: **CFU_R =** (Avg CFUs counted/volume of sample plated) X (sample volume) X (dilution factor).

Percent Transfer efficiency(14) **= [CFU_{RR}/(CFU_{RR} + CFU_{RD})] x 100**

       CFU_{RR} = CFUs recovered from the recipient surface

       CFU_{RD} = CFUs recovered count from the donor surface

All statistical analysis was performed using GraphPad Prism 6 for Windows (Version 6.01, Graph Pad Software, Inc., La Jolla, CA). Statistical significance was assessed using the paired and unpaired t tests (as appropriate), the Holm-Šídák test and one-way ANOVA with a significance level of $\alpha \leq 0.05$. To account for the possible errors in initial inoculum and differences in our ability to measure bacteria from each surface, a multivariate logistic regression analysis was conducted, which included the theoretical recovery and variation in initial

concentration. Regression analysis was performed using R: A language and environment for statistical computing (R Foundation for Statistical Computing, Vienna, Austria).

5.3.0 RESULTS

Table 5.4 shows the bi-directional transfer efficiency results generated by the fingerpad and the latex glove, and transfer efficiencies by material type for both directions of transfer. Four samples were removed from the analysis due to documented sampling or processing errors in the lab. We found that the fomite-to-fingerpad transfer efficiency was statistically significantly higher than the fingerpad-to-fomite deposit transfer efficiency for all material types, regardless of glove use, with the exception of rubber when gloves were worn (unpaired t-test p-value=0.37), (Table 5.4). The fomite-to-fingerpad transfer efficiencies did not depend on material type, regardless of glove use (fingerpad and latex glove one-way ANOVA p-values =0.08 and 0.26, respectively), (Table 5.4). The fingerpad-to-fomite transfer efficiencies by the bare fingerpad also did not depend on material type but when gloves were worn, we found a statistically significant difference in the fingerpad-to-fomite transfers by material type (one-way ANOVA, p=0.30 and p=0.01, respectively), (Table 5.4). A pairwise comparison of the latex glove fingerpad-to-fomite transfer efficiencies singles out the transfer efficiency to rubber as statistically significantly higher than glass, stainless steel, porcelain, polypropylene and polycarbonate (p=0.002, 0.002, 0.003, 0.005 and 0.02 respectively).

Table 5.5: *Average percent transfer efficiency (TE) by material type for transfers occurring by the fingerpad only as well as for transfers with the use of latex gloves. For each transfer event, the average percent TE with standard deviations and the minimum/maximum TE per fomite material type tested are presented along with the t-test p-value results for comparisons of the fomite-to-fingerpad vs. the fingerpad-to-fomite transfer efficiencies for six material types. For each material type (in both directions of transfer), n=10 except where noted with "*".*

| Fomite Material Type | Average Percent Transfer Efficiency (TE) by Material Type | | | | | | | | | | | | | | Fingerpad vs. Latex Gloves | |
| | Fingerpad | | | | | | | Latex Gloves | | | | | | | | |
	Fomite-to-Fingerpad % TE	± SD	Min-Max	Fingerpad-to-Fomite % TE	± SD	Min-Max	t-test p-value (a)	Fomite-to-Fingerpad % TE	± SD	Min-Max	Fingerpad-to-Fomite % TE	± SD	Min-Max	t-test p-value (b)	Fomite-to-Fingerpad (c)	Fingerpad-to-Fomite (d)
Glass	**22.00**	13.51	4.50-44.00	**5.40**	2.49	2.53-10.46	0.0013	**11.73**	14.48	0.0-45.09	**0.82***	1.58	0.0-4.87	0.039	<0.0001	<0.0001
Stainless Steel	**21.11**	11.44	6.98-37.66	**5.59**	4.55	0.67-16.70	0.0009	**5.39**	4.67	0.0-11.76	**0.71**	0.61	0.0-1.84	0.006	0.001	<0.0001
Porcelain	**27.43**	15.46	10.4-53.72	**4.80**	5.27	0.40-4.80	0.0004	**6.07**	4.34	0.25-12.28	**1.18**	2.04	0.0-6.54	0.005	<0.0001	0.009
Poly-propylene	**21.37**	13.30	3.70-43.75	**4.21**	3.99	0.34-12.63	0.0010	**11.02**	12.80	0.0-36.67	**1.62***	2.61	0.0-7.63	0.045	0.063	0.030
Poly-carbonate	**17.26**	10.30	4.82-39.91	**3.80**	3.64	0.23-12.28	0.0011	**13.56**	13.73	0.0-39.15	**3.45**	6.11	0.0-16.84	0.047	0.347	0.139
Rubber	**35.53**	19.24	5.88-69.47	**10.26***	13.28	0.0-34.47	0.0043	**16.02**	13.06	0.21-38.44	**10.40***	14.17	0.02-36.81	0.371	0.023	0.592
1 way ANOVA p-value	**0.0816**			**0.3021**				**0.2556**			**0.0143†**					

[a] t-test p value from comparing the pick-up vs deposit percent transfer efficiencies generated by the fingerpad for each material type

[b] t-test p value from comparing the pick-up vs deposit percent transfer efficiencies generated by the latex glove for each material type.

[c] t-test p value from comparing fingerpad pick-up vs. glove pick-up percent transfer efficiencies for each material type

[d] t-test p value from comparing fingerpad deposit vs. glove deposit percent transfer efficiencies for each material type

† Latex glove deposit transfer efficiency for rubber is statistically higher than glass, stainless steel and porcelain (Turkey's multiple comparisons test p value = 0.03, 0.02, and 0.03 respectively).

* n=9

The overall mean transfer efficiencies generated with and without latex glove use, skin-skin transfer efficiencies, and associated statistical significances are shown in Table 5.5. Regardless of glove use, we found a statistically significant difference between the overall mean bi-directional percent transfer efficiencies both with and without latex glove use (p-value<0.0001). The percent transfer efficiency between the skin of two fingerpads was 32.5%. Using the Holm-Sidak's multiple comparisons test, the transfer efficiency between two skin surfaces was statistically higher than the overall fomite-to-fingerpad transfer efficiency by latex glove (p<0.0001) but not statistically different than the overall fomite-to-fingerpad transfer efficiency by fingerpad (p=0.06). Skin-skin transfer efficiency was statistically higher than the fingerpad-to-fomite transfer efficiency regardless of glove use (p<0.0001 for both latex glove and fingerpad transfers), (Table 5.5).

Table 5.6: The overall mean percent transfer efficiencies (TE), standard deviations, minimum/maximum TE, and p-value results for overall mean transfer efficieny comparisons (assumes no difference across fomite material types).

	Direction of Transfer	n	Overall Mean % TE	± SD	Min-Max	Comparing % TE by direction†	Comparisons with Skin-skin‡
Fingerpad	*Fomite-to-Fingerpad*	60	24.12 (a)	14.81	3.70-69.47	p<0.0001	p = 0.0651
	Fingerpad-to-Fomite	59	5.60 (b)	6.46	0.0-34.47		p < 0.0001
Latex Glove	*Fomite-to-Fingerpad*	60	10.63 (a)	11.52	0.0 – 45.09	p<0.0001	p < 0.0001
	Fingerpad-to-Fomite	57	2.96 (b)	6.94	0.0 – 36.81		p < 0.0001
Skin-Skin	Fingerpad-to-Fingerpad	6	32.53	12.07	17.32 – 43.26		

†Unpaired t-test p-values from comparing the fomite-to-fingerpad vs fingerpad-to-fomite overall mean percent transfer efficiencies for the fingerpad and for latex glove.

‡Holm-Šídák test p-values from comparing the mean skin-skin percent transfer efficiency with each of the overall mean fomite-to-fingerpad and fingerpad-to-fomite percent transfer efficiencies generated with and without glove use.

(a) Unpaired t-test of fingerpad vs glove overall mean fomite-to-fingerpad transfer efficiencies: p-value <0.0001.

(b) Unpaired t-test of fingerpad vs glove overall mean fingerpad-to-fomite transfer efficiencies: p-value = 0.036.

In order to evaluate the influence of measurement error from different surface types, we measured the direct recovery rate of bacteria from each of the surface types used in our primary experiments when no transfer event occurs (Table 5.6). We used a one-way ANOVA to assess the differences between the means. We found an overall difference between the means of the CFUs recovered (one-way ANOVA $p<0.001$) and that the latex glove was significantly higher than the other material types ($p<0.01$ for all comparisons).

Table 5.7: Estimates of direct recovery rates from each of the material types used including latex gloves and the fingerpad. The CFUs of bacteria applied to each material type = 1.42 x 109 CFUs.

Direct Recovery Rates				
Material Type	**(n)**	**Mean CFUs Recovered**	Min-Max	% Recovery
Glass	3	2.43×10^5	1.72×10^5 - 3.02×10^5	0.017
Stainless Steel	3	1.50×10^5	4.98×10^4 - 2.03×10^5	0.011
Porcelain	3	1.47×10^5	1.35×10^5 - 1.72×10^5	0.010
Polypropylene	3	1.24×10^5	1.08×10^5 - 1.38×10^5	0.009
Polycarbonate	2	1.17×10^5	8.46×10^4 - 1.50×10^5	0.008
Rubber	3	1.72×10^5	1.31×10^5 - 2.29×10^5	0.012
Fingerpad	3	1.33×10^5	1.15×10^5 - 1.60×10^5	0.009
Latex Glove	3	6.46×10^5	3.60×10^5 - 9.18×10^5	0.046

The results of the regression analysis showed that (1) for both glove-fomite and fingerpad-fomite transfers, there remained a significant difference between fomite-to-fingerpad and fingerpad-to-fomite transfer efficiencies ($p<0.0001$ in both cases), even when accounting for theoretical recovery and variation in initial concentration, (2) for fingerpad-fomite transfers, material type did not affect transfer efficiency, (3) for glove-fomite transfers, rubber had a significant effect on transfer efficiency in both the fomite-to-fingerpad direction ($p=0.03$) and in the fingerpad-to-fomite direction ($p=0.02$) and (4) no interaction between the initial concentration and material type.

5.4.0 DISCUSSION

In this transfer efficiency study, conducted using 10 volunteer subjects, we had three key findings: First, the fomite-to-fingerpad transfer efficiency of *A. baumannii* was significantly higher than the fingerpad-to-fomite transfer efficiency, regardless of glove use. Second, compared to no glove use, the *A. baumannii* fomite-to-fingerpad transfer efficiency was reduced by 56% and the fingerpad-to-fomite transfer efficiency was reduced by 47% when latex gloves are worn. Lastly, the fomite-to-fingerpad and fingerpad-to-fomite transfer efficiency varied by fomite material type, but these variations were largely not statistically significant. Only rubber showed potential for having a significant influence on transfer efficiency.

We found no studies directly estimating transfer efficiencies of *A. baumannii*. In addition, we found no studies that directly compare fomite-to fingerpad to fingerpad-to-fomite transfer efficiencies. Lopez et al. (2013) compare only the average fomite-to-fingerpad transfer efficiencies of *E. coli*, *S. aureus* and *B. thuringiensis* between porous and nonporous surfaces

under conditions of high and low relative humidity (10). By contrast, our experiments were performed at approximately 72°F (22°C) with a relative humidity level of approximately 40% throughout the study and we compared fomite material types that were all nonporous. Given the differences in study design, methods and microorganisms tested, our data and theirs can only be compared qualitatively.

We compared the fomite-to-fingerpad transfer efficiency with the fingerpad-to-fomite transfer efficiency using bacteria. Under the assumption that recovery from different surfaces is equally effective, our study demonstrates that the fomite-to-fingerpad transfer efficiency is not equal to the fingerpad-to-fomite transfer efficiency when the two contact surfaces involved are not identical (i.e. fomite-skin transfers or fomite-glove transfers). We found the overall fomite-to-fingerpad transfer efficiency (24.1%) by the fingerpad was 4.0 times greater than the overall fingerpad-to-fomite transfer efficiency (5.6%) by the fingerpad ($p<0.0001$). Further, when we stratify by material type, the fomite-to-fingerpad transfer efficiency by the fingerpad was significantly higher than the fingerpad-to-fomite transfer efficiency by the fingerpad for each material type. These are novel findings that are significant for understanding the transmission dynamics of infectious diseases since most fate and transport mathematical models assume that the transfer efficiency value for calculating both the fomite-to-fingerpad rate and the fingerpad-to-fomite rate of pathogens is the same value (11), (12), (13). Our study demonstrates that for *A. baumannii*, when the two contacting surfaces are of unlike material, this assumption of symmetrical transfer does not hold.

This study is again novel in that we evaluated the impact of using latex gloves on fomite-to-fingerpad and fingerpad-to-fomite transfer efficiencies. Similar to the transfer efficiencies by the fingerpad, the overall fomite-to-fingerpad transfer efficiency (10.6%) by the latex glove was

also greater (3.6 times greater) than the overall fingerpad-to-fomite transfer efficiency (3.0%), (p<0.0001). Further, we show a significant reduction in bacterial transfer efficiency with the use of latex gloves; reducing the fomite-to-fingerpad transfer efficiency by 55.9% and the fingerpad-to-fomite transfer efficiency by 47.1% with latex glove use. Standard precautions established by the CDC (15) the use of gloves for the purpose of reducing pathogen transmission. Our study provides quantifiable evidence demonstrating that frequent glove changes during patient care are critical to ensure the greatest reduction in pathogen transmission. Further, we show that -- although significantly reduced -- there is still a transfer of pathogens between surfaces and the latex glove, underscoring the importance of frequent hand hygiene/glove changes by healthcare workers and hospital staff alike for the reduction of pathogen transmission. Stratifying by material type, the fomite-to-fingerpad transfer efficiency by the latex glove was statistically significantly higher than the fingerpad-to-fomite transfer efficiency by the latex glove for each material type except for rubber. Interestingly, when gloves were worn, the fomite-to-fingerpad and fingerpad-to-fomite transfer efficiencies for rubber were not statistically different (P=0.38). Since latex gloves are composed of natural rubber lattices, it would make sense that the fomite-to-fingerpad transfer efficiency equals the fingerpad-to-fomite transfer efficiency between these two similar material types, adding support our hypothesis that the fomite-to-fingerpad and fingerpad-to-fomite transfer efficiencies are not equivalent when the two surfaces involved are not identical. This study demonstrates that the use of latex gloves significantly reduces both the fomite-to-fingerpad and fingerpad-to-fomite transfer efficiencies compared to no glove use, but certainly does not eliminate it. Recognizing that nitrile gloves are a preferred alternative for those with allergies to latex, this study could be repeated to compare the reduction of transfer efficiencies by nitrile gloves with that of latex gloves. Never the less, these findings are

significant in quantifying the importance of glove use by all persons who encounter patient areas and urges frequent glove changes, particularly during patient care.

We evaluated the transfer efficiencies across six nonporous surface types both with and without latex glove use. The results of this study suggest that, although there was variation in transfer efficiency by material types, there was no statistical difference by fomite material type with the possible exception of rubber. As for glass, porcelain, stainless steel, polypropylene and polycarbonate, we found no statistical difference in the fomite-to-fingerpad transfer efficiency between these material types or in the fingerpad-to-fomite transfer efficiency values between these material types, regardless of glove use. This may be due to a loss of statistical power by stratification as we move from approximately n=60 overall to approximately n=10 per material type. The tendency for rubber to have higher transfer efficiencies regardless of glove use is a trend that warrants further investigation.

We also quantified the skin-skin transfer efficiency of *A. baumannii* between the skin of two fingerpads. We determined that the percent transfer efficiency from skin to skin was 33%. This is consistent with the results published by Rusin et al. who report a 34% hand to lip transfer efficiency for *Serratia rubidea* and 41% for *Micrococcus luteus* (9). We compared the skin-skin transfer efficiency to that by the fingerpad and found that the transfer efficiency from the skin to the skin is 1.35 times greater than from the fomite to the skin and 5.8 times greater than from the skin to the fomite. Clearly, the highest transfer rates occur from skin to skin, further stressing the importance for hand cleaning and glove use during direct patient care.

There may be sources of error that could confound our measurements. Of particular interest is the possibility of differing errors and biases in both our initial inoculation of the

fomite/glove/skin and our measurement of the bacteria on each surface. This issue is also of concern in previous studies of transfer efficiencies but has not been addressed in the existing literature. To evaluate the influence of measurement error from different surface types, we measured CFUs that could be directly recovered from each of the surface types used in our primary experiments when no transfer event occurs (Table 5.6). Latex glove had a higher mean direct CFU recovery (0.05%) compared to all other material surface types (0.01%) including the fingerpad ($p<0.001$) suggesting a possible bias in our fomite-to-fingerpad and fingerpad-to-fomite comparison for gloves. However, the significant differences by direction are also seen for fingerpad-fomite transfers where the direct CFU recoveries for these surfaces are the same. Thus, recovery fractions do not appear to explain the differences we measure by direction indicating that, while measurement biases exist, they are not sufficient enough to explain the differences we measure by direction. Finally, we validated our results further using a multivariate logistic regression analysis that included both the variation in the initial inoculum and the maximum theoretical recovery for all surfaces which confirmed the same significant results as reported in Table 5.4. Collectively, these results suggest that the differences in transfer efficiencies seem likely to persist in the face of potential biases.

In summary, the results of this transfer efficiency investigation show that the fomite-to-fingerpad transfer efficiency of *A. baumannii* was significantly higher than the fingerpad-to-fomite transfer efficiency, regardless of glove use and suggest the importance of using appropriate fomite-to-fingerpad and fingerpad-to-fomite transfer efficiencies in the mathematical modeling of bacterial transmission. In addition, we show that bacterial transfer efficiencies are significantly reduced, but not eliminated, by glove use, stressing the important role of glove use with frequent changes during patient care for the reduction of the transfer of pathogens. We

recommend that the standard precautions set by the CDC for glove use should also apply to hospital personnel who are in contact with patient environments and that glove changes should always occur immediately after direct physical contact with the patient if possible. Lastly, our results suggest that the variations between nonporous fomite material types do not significantly affect transfer efficiency in either direction. Of the six material types tested, only rubber showed trends of having an influence on the transfer efficiency of *A. baumannii* in either direction. Further investigation into the interactions between rubber and microbial attachment and the effect of rubber on the transfer efficiency of pathogens is needed. Results from our study will help improve the accuracy of mathematical estimation of environmental mediated infectious disease transmission and serve to strengthen current guidelines for control of hospital-acquired infections.

5.6.0 REFERENCES

1.   Magill SS, Edwards JR, Bamberg W, Beldavs ZG, Dumyati G, Kainer MA, et al. Multistate point-prevalence survey of health care-associated infections. N Engl J Med 2014;370(13):1198-208.

2.   CDC. Antibiotic Resistance Threats in the United States, 2013. In. Atlanta: U.S. Department of Health and Human Services; 2013. p. 59-60.

3.   McConnell MJ, Actis L, Pachon J. Acinetobacter baumannii: human infections, factors contributing to pathogenesis and animal models. FEMS Microbiol Rev 2013;37(2):130-55.

4.   Wendt C, Dietze B, Dietz E, Ruden H. Survival of Acinetobacter baumannii on dry surfaces. J Clin Microbiol 1997;35(6):1394-7.

5.   Jawad A, Seifert H, Snelling AM, Heritage J, Hawkey PM. Survival of Acinetobacter baumannii on dry surfaces: comparison of outbreak and sporadic isolates. J Clin Microbiol 1998;36(7):1938-41.

6.   Rebmann T, Rosenbaum PA. Preventing the transmission of multidrug-resistant Acinetobacter baumannii: an executive summary of the Association for Professionals in infection control and epidemiology's elimination guide. Am J Infect Control 2011;39(5):439-41.

7.   Markogiannakis A, Fildisis G, Tsiplakou S, Ikonomidis A, Koutsoukou A, Pournaras S, et al. Cross-transmission of multidrug-resistant Acinetobacter baumannii clonal strains causing episodes of sepsis in a trauma intensive care unit. Infect Control Hosp Epidemiol 2008;29(5):410-7.

8.   Morgan DJ, Liang SY, Smith CL, Johnson JK, Harris AD, Furuno JP, et al. Frequent multidrug-resistant Acinetobacter baumannii contamination of gloves, gowns, and hands of healthcare workers. Infect Control Hosp Epidemiol 2010;31(7):716-21.

9.   Rusin P, Maxwell S, Gerba C. Comparative surface-to-hand and fingertip-to-mouth transfer efficiency of gram-positive bacteria, gram-negative bacteria, and phage. J Appl Microbiol 2002;93(4):585-92.

10.   Lopez GU, Gerba CP, Tamimi AH, Kitajima M, Maxwell SL, Rose JB. Transfer efficiency of bacteria and viruses from porous and nonporous fomites to fingers under different relative humidity conditions. Appl Environ Microbiol 2013;79(18):5728-34.

11.   Li S, Eisenberg JN, Spicknall IH, Koopman JS. Dynamics and control of infections transmitted from person to person through the environment. Am J Epidemiol 2009;170(2):257-65.

12.   Plipat N, Spicknall IH, Koopman JS, Eisenberg JN. The dynamics of methicillin-resistant Staphylococcus aureus exposure in a hospital model and the potential for environmental intervention. BMC Infect Dis 2013;13:595.

13.   Zhao J, Eisenberg JE, Spicknall IH, Li S, Koopman JS. Model analysis of fomite mediated influenza transmission. PLoS One 2012;7(12):e51984.

14.   Julian TR, Leckie JO, Boehm AB. Virus transfer between fingerpads and fomites. J Appl Microbiol 2010;109(6):1868-74.

15.   Siegel JD, Rhinehart E, Jackson M, Chiarello L. 2007 Guideline for Isolation Precautions: Preventing Transmission of Infectious Agents in Health Care Settings. Am J Infect Control 2007;35(10 Suppl 2):S65-164.

Chapter VI

Evaluation of the Effect of Asymmetrical Transfer Efficiencies On the Risk of *Acinetobacter baumannii* Transport Between Patients in the Hospital Environment

6.1.0 BACKGROUND

Healthcare-associated infections (HAIs) are a major concern worldwide with an estimated 722,000 healthcare-associated infections reported in the United States in 2011 (1). Among the pathogens of serious concern for spread in hospitals are multidrug-resistant *Acinetobacter baumannii,* which is responsible for approximately 12,000 HAI each year in the United States alone according to the CDC. *A. baumannii* is most commonly associated with HAIs, particularly in the intensive care units, producing a variety of infections including pneumonia, bacteremia, wound infections and urinary tract infections (2). The environment (3), (4) and the healthcare worker (5), (6) play a significant role in the transmission of this microorganism in hospitals. *A. baumannii* can survive long periods of desiccation, persisting in the environment for 1-4 months (3), (7), (8), and typical disinfection practices are often inadequate for effective infection control (4), (9). Therefore, understanding the environmentally mediated transmission dynamics of *A. baumannii* is critical for identifying a more targeted approach to effective infection control.

Li, et al. was one of the first groups to develop an Environmental Infection Transmission System (EITS) model to specifically include the fomite in the environmental transmission

process (10). Others, such as Plipat, et al. have expanded on this model by incorporating healthcare worker mediated transmission dynamics (11). A common simplifying assumption in fate and transport mathematical models is that the transfer of bacteria between the fingerpad and fomite surface during a touching event is symmetrical. This assumption uses the same transfer efficiency value for calculating both the pick-up rate and the deposit rate of pathogens. This assumption may be appropriate when the two contacting surfaces are composed of the same material (i.e. skin-to-skin contact). However, we recently reported that the transfer efficiency of *A. baumannii* from the fomite to the fingerpad is statistically significantly greater than that from the fingerpad to the fomite (12). Therefore, the simplifying assumption of symmetry may result in erroneous modeling estimates of environmentally mediated transmission. In addition to demonstrating the asymmetrical transfer of bacteria between two unlike contacting surfaces, we also previously demonstrated that there was no statistical difference in transfer efficiencies of *A. baumannii* across fomite material types (12), regardless of the direction of transfer. Thus, it is appropriate to assume the same pickup and deposit transfer efficiency across all fomite material types. It remains unclear if a realistic relaxation of the simplifying assumption of symmetry in pathogen transfer efficiencies changes the risks of transport between patients and rooms.

6.2.0 HYPOTHESIS AND AIMS

To address the effect of asymmetrical bacterial transfer efficiencies on the environmentally mediated transport between patients and rooms, we constructed an *A. baumannii* fate and transport model that simulates the touching interactions between non-porous environmental surfaces, the healthcare worker (HCW) and patients using either symmetrical or asymmetrical transfer efficiencies. This mathematical model aims to evaluate the differences in pathogen dissemination by comparing a model that assumes bacterial transfer symmetry with one

that employs the asymmetrical transfer efficiencies as measured by Greene et al. The rationale

for this hypothesis is based on evidence that the fomite-to-fingerpad (pick-up) and skin-skin

transfer efficiencies are statistically significantly higher than the fingerpad-to-fomite (deposit)

transfer efficiencies, regardless of glove use (12). In an asymmetrical system, the higher transfer

rate can cause a flow from a lower concentration to a higher concentration in the direction that

has the higher transfer efficiency. Due to the high pick-up transfer efficiency, higher

concentrations of bacteria may remain on the hands of the HCW compared to the fomites for

subsequent transfer to the uncolonized patient via direct contact. Alternatively, in a scenario

involving glove use during direct patient care or a high rate of environmental touching by the

HCW relative to touching the patient, there would be a reduction in the transfer of bacteria

between the HCW and patient. Under this scenario, asymmetrical transfer may result in

increased transfer from the fomites.

6.3.0 METHODS

A deterministic, linear, fate and transport model was developed using Berkeley

Madonna® Version 8.3.18 software (program code is provided in Appendix 6-H). This model is

based off of the EITS model developed by Li et al., (10) and the exposure assessment model

developed by Plipat et al. (11). This model treats the healthcare worker (HCW) and the hospital

environment as vectors for the transmission of *Acinetobacter baumannii* between two patients in

separate hospital rooms - one who is colonized and one who is uncolonized. In this model,

transfer efficiencies are parameterized in order to simulate both symmetrical and asymmetrical

transfer events. It describes the contact-mediated process between the healthcare worker (HCW)

and the environment in transporting microorganisms between patients and it evaluates the

robustness of realistically relaxing the simplifying assumption of symmetry in bacterial transfer by touch.

6.3.1 Model Description

This fate and transport model describes the transport and fate of *A. baumannii* between two patients via the healthcare worker (HCW) and the environment. This model is designed to isolate pathogen transport via the environment in which the HCW is the only vector. Thus, airborne transmission and environmental transport by visiting family members, general hospital staff and the movement of patients between their room and other hospital areas for procedural purposes is not considered here.

The model consists of four main areas; the HCW, the non-porous surfaces in the hospital environment, the colonized patient and the uncolonized patient. These areas are divided into 5 compartments: (1) the colonized patient's skin (hands plus skin) (Pc), (2) the non-porous, environmental surfaces in colonized patient's room (Ec), (3) the healthcare worker's hands (HCW), (4) the uncolonized patient's hands (Pu), and (5) the non-porous, environmental surfaces in uncolonized patient's room (Eu), (Table 6.8, Figure 6.14).

Figure 6.11: Schematic of fate and transport mathematical model.
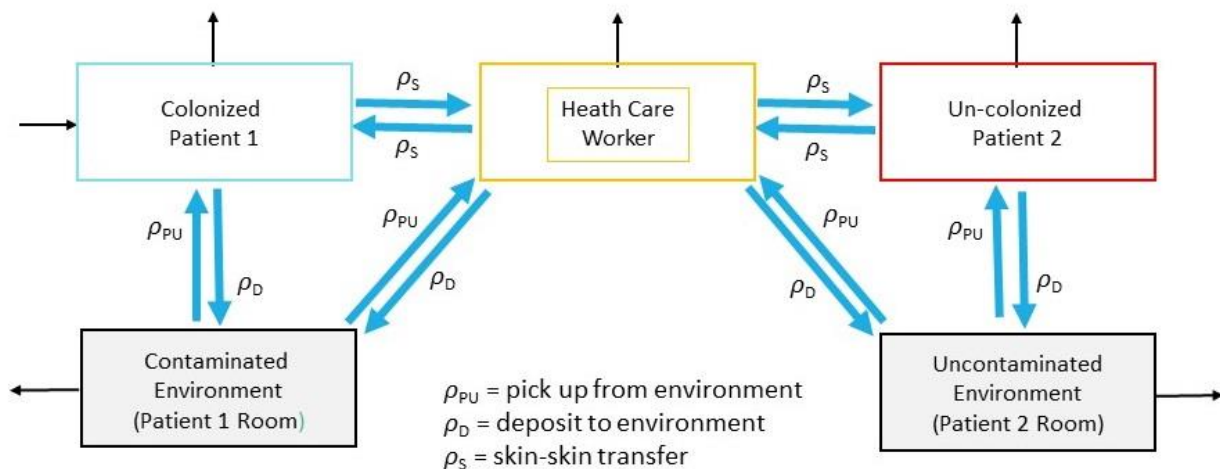
6.3.2 *Model Compartments*

Patients

The model includes one patient who is colonized with *A. baumannii* and one who is uncolonized (Table 6.8). The two patients are in separate hospital rooms and remain in their respective rooms; movement of patients for services to other areas of the hospital is not considered. Patients are described by the concentration of *A. baumannii* (cfu/cm^2) on their hands and skin. The initial value for the concentration of *A. baumannii* on the skin and hands of the colonized patients (Pc) was set at 26 cfu/cm^2 and was determined by setting all the flows involving the following compartments to equilibrium: Pc, HCW and Ec. The colonized patient's skin (skin plus hands) is the only source of contamination. Upon admission, the colonized and uncolonized patients are admitted into initially uncontaminated hospital rooms. The colonized patient contaminates their room environment (1) by shedding squamous skin cells that instantaneously settle on the surrounding surfaces and (2) by touching the surrounding surfaces with their contaminated hands. Because there is little evidence of colonization of the nares by *A. baumannii*, transfer or self-inoculation via nose touching is not considered here. In addition to touching the environment, the colonized patient can also undergo touching events with the HCW. Once the initially uncolonized patient is contaminated, the previously uncolonized patient sheds *A. baumannii* from their skin and can undergo touching events with the environment and HCW. *A. baumannii* may naturally die off from the skin of both patients. Because this model only considers the total accumulation of microorganisms on the uncolonized patient and the flows by which the contamination came, the colonized and uncolonized patients are not separated out into separate compartments of hands and skin. In addition, inherent to this

model form is the intrinsic assumption of instantaneous equilibrium of pathogen concentration across the skin and hands of both patients.

Healthcare Worker

The HCW is described by the concentration of *A. baumannii* on their hands only (Table 6.8). The HCW is assumed initially uncolonized and it is assumed that once colonized, the concentration of pathogens is instantaneously equally distributed on the hands. The HCW works an 8-hour shift and only one HCW is available to the two patients during that shift, caring for both patients. For each hour worked, the first 20 minutes are spent in the colonized patient's room where touching events with the patient and environment can occur followed by a second 20-minute visit to the uncolonized patient's room where the same touching events also occur. The HCW washes their hands after each patient visit. The remaining 20 minutes of each hour are spent at the nurse's station where touching events are not considered. *A. baumannii* may naturally die off from the skin of the HCW.

Environment

The environment is divided into two compartments: the non-porous surfaces in the colonized patient's room (Ec) and the non-porous surfaces in the uncolonized patient's room (Eu), (Table 6.8). For both patient rooms, only the non-porous environmental surfaces are considered and are described by *A. baumannii* concentration levels. Once on the environmental surface, some of these pathogens will naturally die off. While *A. baumannii* can survive in the environment for extended periods of time (ranging from several weeks to 4 months (7), (13), (14) it is assumed that all remaining cells are available for pick-up and transport by the HCW or by the patient. At the end of each 24-hour period, both rooms undergo a daily cleaning (disinfection).

Either patient can contaminate the surfaces in their respective rooms in one of two ways: (1) the shedding of their squamous skin cells colonized with *A. baumannii* onto the surrounding environmental surfaces (which is assumed to instantly settle) and (2) by touching environmental surfaces with their hands. The environment of either patient's room can become contaminated by the HCW via touching events between the HCW and the non-porous surfaces once the initial contaminating touching event in the colonized patient's room has occurred. The disinfection (cleaning) of patient rooms occurs every 24 hours.

Table 6.8: The Five compartments of a Fate and Transport Mathematical Model of *A. baumannii* with Descriptions and Model Events for each Compartment.

Symbol	Initial Value (CFU/cm²)	Compartment Description	Events
Pc	26*	Colonized patient's exposed skin and hands.	Shedding Touching surfaces Natural die off
Pu	0	Uncolonized patient's exposed skin and hands	Shedding Touching surfaces Natural die off
HCW	0	Exposed hands of HCW	Visiting patient's room Touching surfaces Touching the patient Natural die off Hand hygiene
Ec	0	Non-porous environmental surfaces in the colonized patient's room	Natural die off Surface decontamination (once every 24 hrs)
Eu	0	Non-porous environmental surfaces in the uncolonized patient's room	Natural die off Surface decontamination (once every 24 hrs)

*The initial value for the concentration of *A. baumannii* on the skin and hands of the colonized patients (Pc) was set at 26 cfu/cm² and was determined by setting all the flows involving Pc, HCW and Ec to equilibrium.

6.3.3   Model Assumptions

The model assumptions are as follows:

1. The *A. baumannii* is assumed to be of one clonal strain that instantaneously and homogenously mixes on surfaces, skin, and hands.

2. The initial source of *A. baumannii* is from one colonized patient who can transmit the microorganism to the environment by touching with the hands or by shedding from the skin and to the HCW via touching.

3. *A. baumannii* replenishes itself on the skin and hands of the colonized patient only, and this occurs at the same rate at which it is shed off into the environment.

4. *A. baumannii* on the skin of the uncolonized patient and HCW is assumed not to replenish itself.

5. The *A. baumannii* that is dispersed via the shedding of skin cells is assumed to instantly settle onto surfaces.

6. The HCW, a vector in the transmission process, is assumed initially uncolonized and is assumed not to shed.

7. The HCW is assumed to spend exactly 20 minutes per patient room visit.

8. The HCW is assumed to wash their hands at the end of each patient visit and only at this time.

9. All environmental surfaces are assumed non-porous.

10. The transmission probability from a person to the environment is assumed the same for all persons and for all non-porous surface types.

6.3.4 Model Parameters & Initial Values

Model parameter values with descriptions are shown below in Table 6.9. Pathogen levels are quantified in cfu/cm^2. The transfer efficiency of this pathogen is assumed the same across all fomite material types, regardless of the direction of transfer (12).

Table 6.9: List of Model Parameters with Values and Descriptions.

Symbol	Values	Description	Reference
Attenuation and Die-off Rates			
α	0.1	Fraction of shed squamous cells with viable bacteria	(15)
μ_E	0.00533	Attenuation rate from (non-porous) environmental surfaces (min^{-1})	(14)
μ_S	0.00353	Die-off rate from human skin and tissue (min^{-1})	(16)
Touching Rates			
τ_{PE}	0.134	Touching rate of patient hands with non-porous environment (min^{-1})	(11)
τ_{WE}	0.400	Touching rate of HCW with non-porous environment during each 20 min visit with patient (min^{-1})	(11)
τ_{WP}	0.400	Touching rate of HCW with each patient during 20min visit (min^{-1})	(11)
Transfer Efficiencies			
ρ_{PU}	0.2412	Fraction transferred from fomite to skin/hands (pick-up)	(12)
ρ_D	0.056	Fraction transferred from the skin/hands to fomite (deposit)	(12)
ρ_S	0.3253	Fraction transferred from a person's hand/sin to another's hand/skin (symmetrical)	(12)
Surface Areas			
A_T	1	Contact surface area of fingertip (cm^2)	
A_{PL}	150	Contact surface area of palm (cm^2)	
A_H	300	Hand surface Area (cm^2)	
A_E	2000	Total exposed surface area for all non-porous surfaces (cm^2)	(11)
A_P	2000	Total exposed skin area for patients (cm^2)	(11)
A_W	300	Total exposed skin area for HCW (cm^2)	
Decontamination Functions			
λ_D	0.75	Daily surface decontamination efficiency	(17)
λ_H	0.96	Hand hygiene efficiency	(18), (19)
λ_C	0.50	% compliance with precautionary methods (i.e. handwashing)	(20)

6.3.5 Exposure Pathways

Exposure pathways to the uncolonized patient are limited to a contact-mediated process. When the hand touches the environmental surface, a fraction of the microorganisms will transfer to the hand. If the hand or skin is already colonized, then there will be an exchange of microorganisms between the hand and the surface. The fraction transferred between the hand and the fomite will vary depending on the transfer rates between the two surfaces (hand, surface) involved and the direction of the transfer (moving from a higher concentration to a lower concentration). Therefore, each touching event with the environment by either the HCW or the patient may incur either a pick-up (hand contamination) or a transfer (surface contamination) of microorganisms. Transfer rates are calculated using the transfer efficiency parameter (ρ). Model assumptions, parameters, transfer events and equations are presented below.

6.3.6 Model Events

We studied the effect of asymmetrical transfer efficiencies given large (2000 cm^2) and small (200 cm^2) exposed environmental surface areas on which touching events can occur, and in a system with reduced direct transmission by the HCW. For touching events involving the skin, we follow the Plipat model (11) and assume that the total exposed skin areas of the patient is 2000 cm^2 each but assume that the total exposed skin area of the HCW is the hands only or 300 cm^2. Both the colonized and uncolonized patient lose *A. baumannii* by natural die-off, by touching surfaces, shedding squamous skin cells and by direct contact with the HCW. Only the colonized patient gains bacteria by bacterial replenishment on the skin. Both patients can gain bacteria by touching events with the HCW and the non-porous surfaces in their environment. The shedding rate is set equal to the gain back due to the natural replenishing (growth) rate. Concentrations on the HCW are diminished due to hand hygiene occurring after each 20-minute

patient visit. The environment is cleaned every 24 hours. The model determines the

concentration of *A. baumannii* in cfu/cm^2. Initial concentrations on the colonized patient were

set at 26 cfu/ cm^2, which was determined to be the equilibrium state concentration for the

following variables: the colonized patient, their environment and the HCW. The model uses

Euler's Method and runs with discrete fixed time steps. The time-step was set such that further

reductions in the time-step did not produce meaningful difference in model. The model time unit

is in minutes and the time step used in the numerical solution of this differential equation model

is in 0.01 minutes. It starts at the beginning of a HCW's 8 hour shift and simulates seven days.

In the following sections, we describe in greater detail the model events, and assumptions

inherent to this model.

Shedding

In the model, the first shedding event by the colonized patient onto environmental

surfaces initiates the movement of microorganisms. Approximately 10^7 particles are dispersed

from the healthy skin per day, and 10% of these squamous skin cells contain viable bacteria (15).

The concentration of shed pathogen (cfu/cm2) is determined by the product of the shedding rate

(α) and the concentration of pathogen on the contaminated patient, or α*Pc, where the baseline

shedding rate is set to 0.1 (15).

Hand hygiene and Surface Decontamination

The washing of hands by the HCW (hand hygiene) is assumed to occur after each room

visit. The percent compliance with infection control methods/procedures is included as a

parameter and is set at 50% (20). When the event is executed, a fraction of pathogen according

to the hand-hygiene efficacy times the decontamination compliance rate is removed from the

nurse's hand. At baseline, this is set to 0.96*0.50 (18), (19), (20). Surface decontamination

events are set to occur once every 24 hours. The surface decontamination efficacy, such that a fraction of the pathogen is removed from the surface area at each cleaning, is set at 75% (17).

Natural die-off of A. baumannii

The levels of *A. baumannii* on environmental surfaces and on the skin of patients and the HCW decreases continuously at fixed die-off rates. *A. baumannii* die-off rates from environmental surfaces were quantified via the desiccation tolerance experiments described in Chapter 2. In these experiments, the risk of death was determined for 6 time points over 56 days (day 1, 3, 7, 14, 28 and day 56). The rate of death (CFU/day) was calculated using the formula (21):

$$rate = -\frac{\ln(1-risk)}{time}$$

Although the starting concentration of pathogen was calculated in these experiments, the initial die-off at "time zero" was not determined. Therefore, to account for the initial die-off of bacteria that would occur *before* the start of the experiment, the death rate is adjusted by approximately 10%. Die off-rates from the skin and non-porous surfaces are presented in Table 6.9.

Touching

This model assumes that the pathogen is of one clonal strain, is homogeneously mixed and is evenly distributed on all surfaces. Touching events can occur as follows:

a) Colonized patient's fingertip with the non-porous environmental surfaces

b) Uncolonized patient's fingertip with the non-porous environmental surfaces

c) HCW's hands with the non-porous environmental surfaces

d) HCW's hands with the colonized patient's exposed skin/hands

e) HCW's hands with the uncolonized patient's exposed skin/hands

The exchange of pathogens between two surfaces depends upon the concentrations of pathogen on each surface as well as the surface areas involved in the contact process. The flow of pathogen is always bidirectional and the net flow is calculated for each time step. The direction of transfer (net flow) depends upon if the transfer efficiency is a symmetric or asymmetric system. In a symmetrical transfer efficiency system, the flow of pathogens will always move from an area with higher concentrations to the area of lower concentrations. In an asymmetrical system, the higher transfer rate can cause a flow from a lower concentration to a higher concentration in the direction that has the higher transfer efficiency. The amount of transfer is dependent upon the transfer efficiency and the surface areas involved. This analysis evaluates how the dynamics of the system are effected using asymmetrical transfer efficiencies compared to using symmetrical transfer efficiencies. For each touching event, the *A. baumannii* at risk for transfer is proportional to the surface area and the proportion that is transferred and is dependent on the fraction transferred. The bidirectional calculation of the concentration of pathogen transferred is shown in Table 6.10, which uses the following formula for each direction:

$$\boldsymbol{Transferred\ Concentration} = \frac{conc.of\ A.b.(CFU)}{sq.area\ surface\ (cm2)} \times \frac{contact\ area\ (cm2)}{Total\ exposed\ surf\ area\ (cm2)} \times$$

$$transfer\ efficiency\ \times touch\ rate$$

As shown in the equation above, the fate and transport of *A. baumannii* is a contact-mediated process, which can be quantified if the pathogen concentrations on each surface and the

areas of the surfaces involved are known. The risk for transfer of pathogen in any touching event is the ratio of the concentration of pathogen on the contact surface to the total exposed area. For example, the risk of contaminating the environment via a touching event between the colonized patient hands and their room environment is influenced by the proportion of *A. baumannii* that contacts the surface (i.e. the palm contact surface area (cm^2)) divided by the total exposed skin and hand surface area (cm^2) of the patient or (A_{PL}/A_P).

Flows

The flow of the pathogen to be transferred in either direction is determined by the fraction effectively transferred, or the transfer efficiency (ρ). This is not necessarily a symmetrical event. For example, the fraction transferred from a non-porous surface to the palm of the hand per cm^2 may be greater than or less than the fraction effectively transferred from the palm to the non-porous surface per cm^2. Thus, the direction of the flow is dependent upon the concentration of the microorganism present on each surface as well as the fraction that is effectively transferred (ρ) between the two surfaces. Greene et al. found that the touching event between two unlike surface types is an asymmetrical event and report overall mean fomite-to-fingerpad (ρ_{PU}), fingerpad-to-fomite (ρ_D) and skin-skin transfer efficiencies (ρ_S) for *A. baumannii* (12) which are used in this study. Since the flow is bi-directional, the net effect (net transfer of microorganisms) will depend on the fraction transferred, the surface concentrations and the surface areas involved. In asymmetrical transfer, the flow of pathogens may go in the direction of higher transfer efficiency even if pathogen concentrations are higher in the opposite direction. Using the available data regarding non-porous surfaces on *A. baumannii,* the asymmetrical transfer efficiencies are ρ_{PU}=0.2412 (pick-up), ρ_D=0.056 (deposit) and ρ_S=0.3253 (skin-skin) as shown in Table 6.9. Furthermore, the total exposed surface areas for the HCW is the hands only

or 300 cm^2. Like the Plipat model, the total exposed surface areas for the environmental surface and patient are assumed to be the same and are set to 2000 cm^2 (Table 6.9). The area of contact varies depending on the nature of the touching event. For example, touches by the patient to the environment occur with the fingertip of the patient, a ratio of 1cm^2/2000cm^2 and touches by the HCW to the environment occur with the palm of the hand, which is a ratio of 150cm^2/2000cm^2. An example of the bidirectional flows of *A. baumannii* during a touching event between the colonized patient and the colonized patient's room is shown in Table 6.10. Net transfer may result in hand or surface contamination depending on the difference in the two flows and on the transfer efficiency.

Table 6.10: Description of the contact mediation process with an example of pathogen flows between the colonized patient and the nonporous surface.

	Colonized patient's hand	Colonized patient's Environment
Contact surface area	A_T	A_T
Total surface area	A_H	A_E
Pick-up Transfer Efficiency	ρ_{PU}	ρ_{PU}
Deposit Transfer Efficiency	ρ_D	ρ_D
Pathogen concentration per total surface area	Pc	Ec
Touching Rate with Environment	τ_{PE}	τ_{PE}
Flow of pathogen transferred from colonized patient's hand to nonporous surface	$Pc(A_T/A_H) * \rho_D * \tau_{PE}$	
Flow of pathogen transferred from nonporous surface to colonized patient's hand	$Ec(A_T/A_E) * \rho_{PU} * \tau_{PE}$	

6.3.7   Equilibrium

The initial concentration of *A. baumannii* on the skin and hands of the colonized patient is set at 26 cfu/ cm^2. This concentration is maintained at equilibrium by the gain and loss of *A. baumannii* over time. The gain is a result of natural microbial growth rate times the total available skin area on the colonized patient. This gain replenishes the loss of natural die-off and loss due to shedding into the environment. The shedding rate is assumed to be the same as the replenishing rate.

6.3.8   Differential Equations

The change of concentration of microorganisms in each compartment, or the flows into and out of a compartment, is governed by the transfer efficiencies, the fraction of exposed areas and touching rates. In addition, the concentrations are influenced by the natural die-off rates as well as disinfection and hand washing procedures. Each flow can be expressed as a differential equation that allows for the expression of change over time.

Individual Flows

The individual flows for each compartment are provided below where HCW=Healthcare worker, Pc=Colonized Patient, Pu=Uncolonized Patient, Ec=Environment of Colonized Patient, and Eu=Environment of Uncolonized Patient:

Individual Flows – Colonized Patient (Pc)

From Ec to Pc	$+ Ec \left(\dfrac{A_T}{A_E}\right) \rho_{PU} \tau_{PE}$
From HCW to Pc	$+ HCW \left(\dfrac{A_H}{A_W}\right) \rho_S \tau_{wp} \, f(t)$
From Pc to Ec	$- Pc \left(\dfrac{A_T}{A_H}\right) \rho_d \tau_{PE}$
From Pc to HCW	$- Pc \left(\dfrac{A_H}{A_P}\right) \rho_S \tau_{wp} \, f(t)$
Die-off of pathogen from skin of Pc	$- Pc(\mu_S)$
Pathogen Shed from skin of Pc onto Ec	$- Pc(\alpha)$
Replenishment of pathogen on the skin	$+ \alpha(A_P)$

Individual Flows – Environment of Colonized Patient (Ec)

From Ec to Pc	$- Ec \left(\dfrac{A_T}{A_E}\right) \rho_{PU} \tau_{PE}$
From Pc to Ec	$+ Pc \left(\dfrac{A_T}{A_H}\right) \rho_D \tau_{PE}$
From Ec to HCW	$- Ec \left(\dfrac{A_{PL}}{A_E}\right) \rho_{PU} \tau_{WE} \, f(t)$
From HCW to Ec	$+ HCW \left(\dfrac{A_{PL}}{A_W}\right) \rho_D \tau_{WE} f(t)$
Pathogen removed from Ec due to daily cleaning	$- Ec(\lambda_d) h(t)$
Die-off of pathogen from environmental surfaces	$- Ec(\mu_E)$
Pathogen Shed from skin of Pc onto Ec	$+ Pc(\alpha)$

Individual Flows – Uncolonized Patient (Pu)

From Eu to Pu	$+\,Eu\left(\dfrac{A_T}{A_E}\right)\rho_{PU}\tau_{PE}$
From HCW to Pu	$+HCW\left(\dfrac{A_H}{A_W}\right)\rho_s\tau_{WP}g(t)$
From Pu to Eu	$-Pu\left(\dfrac{A_T}{A_H}\right)\rho_D\tau_{PE}$
From Pu to HCW	$-Pu\left(\dfrac{A_H}{A_P}\right)\rho_S\tau_{WP}g(t)$
Die-off of pathogen from skin of Pu	$-\,Pu(\mu_S)$
Pathogen Shed from skin of Pu onto Eu	$-Pu(\alpha)$

Individual Flows – Environment of Uncolonized Patient (Eu)

From Eu to Pu	$-Eu\left(\dfrac{A_T}{A_E}\right)\rho_{PU}\tau_{PE}$
From Pu to Eu	$+Pu\left(\dfrac{A_T}{A_H}\right)\rho_D\tau_{PE}$
From Eu to HCW	$-Eu\dfrac{A_{PL}}{A_E}\rho_{PU}\tau_{wE}\,g(t)$
From HCW to Eu	$+HCW\dfrac{A_{PL}}{A_W}\rho_D\tau_{WE}g(t)$
Pathogen removed from Eu due to daily cleaning	$-Eu\lambda_d h(t)$
Die-off of pathogen from environmental surfaces	$-\,Eu(\mu_S)$
Pathogen Shed from skin of Pu onto Eu	$+Pu(\alpha)$

Individual Flows – Healthcare worker (HCW)

From Pc to HCW	$+ Pc \left(\dfrac{A_H}{A_P} \right) \rho_S \tau_{WP} \, f(t)$
From Pu to HCW	$+ Pu \left(\dfrac{A_H}{A_P} \right) \rho_S \tau_{WP} \, g(t)$
From HCW to Pu	$- HCW \left(\dfrac{A_H}{A_W} \right) \rho_S \tau_{WP} \, g(t)$
From HCW to Pc	$- HCW \left(\dfrac{A_H}{A_W} \right) \rho_S \tau_{WP} \, f(t)$
From Ec to HCW	$+ Ec \left(\dfrac{A_{PL}}{A_E} \right) \rho_{PU} \tau_{WE} \, f(t)$
From Eu to HCW	$+ Eu \left(\dfrac{A_{PL}}{A_E} \right) \rho_{PU} \tau_{WE} \, g(t)$
From HCW to Ec	$- HCW \left(\dfrac{A_{PL}}{A_W} \right) \rho_D \tau_{WE} \, f(t)$
From HCW to Eu	$- HCW \left(\dfrac{A_{PL}}{A_W} \right) \rho_D \tau_{WE} \, g(t)$
Pathogen removed from HCW due to hand hygiene after visiting first patient	$- HCW \left(\dfrac{A_H}{A_W} \right) (\lambda_H)(\lambda_C) \, x(t)$
Pathogen removed from HCW due to hand hygiene after visiting the second patient	$- HCW \left(\dfrac{A_H}{A_W} \right) (\lambda_H)(\lambda_C) \, y(t)$
Removal of HCW at the end of each 8 hour shift	$- HCW \, s(t)$
Die-off of pathogen from skin of HCW	$- HCW \, (\mu_S)$

Sum of Flows

The sums of the flows for each compartment of the model are as follows:

The colonized patient (Pc)

The initial value of the colonized patient's skin is assigned the equilibrium value of 26 cfu/cm^2. The change of *A. baumannii* on the skin/hands of the colonized patient (Pc) over time is given by:

$$\frac{dPc}{dt} = Ec\left(\frac{A_T}{A_E}\right)\rho_{PU}\tau_{PE} + HCW\left(\frac{A_H}{A_W}\right)\rho_S\tau_{wp}\, f(t) - Pc\left(\frac{A_T}{A_H}\right)\rho_d\tau_{PE} - Pc\left(\frac{A_H}{A_P}\right)\rho_S\tau_{wp}\, f(t) - Pc(\mu_S)$$

$$- Pc(\alpha) + \alpha(A_P)$$

$$f(t) = \begin{cases} 1, & t \in [n-1, n - \frac{2}{3}) \\ 0, & t \in \left[n - \frac{2}{3}, n\right) \end{cases}$$

Where n is a positive real number.

The symbol $f(t)$ represents the amount of time that the HCW spends in the colonized patient's room such that during the first 20 minutes of the hour, $f(t)=1$ and for all other times, $f(t)=0$.

The non-porous surfaces in the colonized patient's room (Ec)

The initial value of *A. baumannii* on the environmental surface of the colonized patient's room is set to zero. The change of *A. baumannii* on the environmental surfaces of the colonized patient's room (Ec) is given by:

$$\frac{dEc}{dt} = -Ec\left(\frac{A_T}{A_E}\right)\rho_{PU}\tau_{PE} + Pc\left(\frac{A_T}{A_H}\right)\rho_D\tau_{PE} - Ec\left(\frac{A_{PL}}{A_E}\right)\rho_{PU}\tau_{WE}\, f(t) + HCW\left(\frac{A_{PL}}{A_W}\right)\rho_D\tau_{WE}f(t)$$

$$- Ec(\lambda_d)h(t) - Ec(\mu_E) + Pc(\alpha)$$

$$h(t) = \begin{cases} 1, & t = n*24 \\ 0, & otherwise \end{cases}$$

Where n is a positive real number.

The symbol $h(t)$ is a time indicator function that represents the decontamination of the room every 24 hours.

The uncolonized patient (Pu)

    The initial concentration of pathogen on the uncolonized patient is set to zero and remains zero until the first visit by the HCW. The change of *A. baumannii* on the skin and hands of the uncolonized patient (Pu) over time is given by:

$$\frac{dPu}{dt} = Eu\left(\frac{A_T}{A_E}\right)\rho_{PU}\tau_{PE} + HCW\left(\frac{A_H}{A_W}\right)\rho_s\tau_{WP}g(t) - Pu\left(\frac{A_T}{A_H}\right)\rho_D\tau_{PE} - Pu\left(\frac{A_H}{A_P}\right)\rho_s\tau_{WP}g(t) - Pu(\mu_S)$$
$$- Pu(\alpha)$$

$$g(t) = \begin{cases} 1, & t \in \left(n - \frac{2}{3}, n - \frac{1}{3}\right) \\ 0, & t \in \left(n - 1, n - \frac{2}{3}\right) or \left(n - \frac{1}{3}, n\right) \end{cases}$$

Where n is a positive real number. The symbol $g(t)$ functions like that of $f(t)$ where it represents the time spent by the HCW with the uncolonized patient.

The non-porous surfaces in the colonized patient's room (Eu)

    The initial concentration of pathogen in the uncolonized patient's room is set to zero. The change in *A. baumannii* concentrations in the uncolonized patient's room over time is expressed by the following differential equation:

$$\frac{dEu}{dt} = -Eu\left(\frac{A_T}{A_E}\right)\rho_{PU}\tau_{PE} + Pu\left(\frac{A_T}{A_H}\right)\rho_D\tau_{PE} - Eu\frac{A_{PL}}{A_E}\rho_{PU}\tau_{wE}\,g(t) + HCW\frac{A_{PL}}{A_W}\rho_D\tau_{WE}g(t)$$
$$- Eu\lambda_d h(t) - Eu(\mu_S) + Pu(\alpha)$$

The HCW

The initial concentration of *A. baumannii* on the HCW hands is set to zero. The change

in concentration of this pathogen over time is expressed by the following differential equation:

$$\frac{dHCW}{dt} = Pc\left(\frac{A_H}{A_P}\right)\rho_S\tau_{WP}\,f(t) + Pu\left(\frac{A_H}{A_P}\right)\rho_S\tau_{WP}\,g(t) - HCW\left(\frac{A_H}{A_W}\right)\rho_S\tau_{WP}\,g(t)$$

$$- HCW\left(\frac{A_H}{A_W}\right)\rho_S\tau_{WP}\,f(t) + Ec\left(\frac{A_{PL}}{A_E}\right)\rho_{PU}\tau_{WE}\,f(t) + Eu\left(\frac{A_{PL}}{A_E}\right)\rho_{PU}\tau_{WE}\,g(t)$$

$$- HCW\left(\frac{A_{PL}}{A_W}\right)\rho_D\tau_{WE}\,f(t) - HCW\left(\frac{A_{PL}}{A_W}\right)\rho_D\tau_{WE}\,g(t)$$

$$- HCW\left(\frac{A_H}{A_W}\right)(\lambda_H)(\lambda_C)\,x(t) - HCW\left(\frac{A_H}{A_W}\right)(\lambda_H)(\lambda_C)\,y(t) - HCW\,s(t)$$

$$- HCW(\mu_S)$$

$$x(t) = \begin{cases} 1, & t = n - 2/3 \\ 0, & otherwise \end{cases}$$

$$y(t) = \begin{cases} 1, & t = n - \dfrac{1}{3} \\ 0, & otherwise \end{cases}$$

$$s(t) = \begin{cases} 1, & t = n - 8 \\ 0, & otherwise \end{cases}$$

Where n is a positive real number.

The nurse is expected to wash their hands after each patient visit. The time-indicator

functions for hand hygiene are as follows: *x(t)* represents the hand hygiene event after visiting

the colonized patient where $x(t)=1$ for 1st 20 min of each hour and $x(t)=0$ for all other times; *y(t)*

the hand hygiene event after visiting the uncolonized patient where $y(t) =1$ when 20 min $\geq$ time

≤ 40 min of each hour and $y(t)=0$ for all other times; *s(t)* represents the removal of the HCW at

the end of each 8 hour shift.

6.4.0 RESULTS

6.4.1 *Model Analysis*

This model compares three different methods of defining transfer efficiencies for a touching event between the skin and an environmental surface (Table 6.11): asymmetrical transfer efficiency (ATE), symmetrical transfer efficiency (STE) and the mean bi-directional transfer efficiency (MTE). **The asymmetrical transfer efficiency (ATE)** uses a measured, fomite to skin (pick-up) and a measured, skin-to-fomite (deposit) transfer efficiency value of *A. baumannii* for the calculation of pickup and deposit transfer rates of a touching event with the environment. **The symmetrical transfer efficiency (STE**) applies only one measured transfer efficiency value, the fomite-to-skin (pick-up) transfer efficiency, to calculate both the pick-up and the deposit transfer rates of a touching event with the environment. This commonly used method represents the calculations that would result from assuming symmetry as a result of only measuring the fomite-to-skin transfer efficiency. The **mean bi-directional transfer efficiency (MTE)** applies only one value, the geometric mean of the measured pick-up and measured deposit transfer efficiencies (calculated by $\sqrt{0.2412 * 0.056}$), to calculate the pick-up and deposit transfer rates of a touching event with the environment. Thus, the MTE is symmetrical but without the measurement error inherent to the STE system. Because it uses a transfer efficiency value derived from the ATE measured values, the total amount of pathogen transferred in each touching event with the environment remains the same as that for the ATE.

Table 6.11: Transfer symmetry methods compared in this analysis

Abbreviation	Description	Fomite-to-Skin	Skin-to-Fomite
ATE	**Asymmetrical transfer efficiencies** derived from the bi-directional measurement of transfer of *A. baumannii* between the skin and surfaces.	0.2412	0.056
STE	**Symmetrical transfer efficiency** uses an assumed skin-to-fomite transfer efficiency value that is equal to the measured, fomite-to-skin transfer efficiency value.	0.2412	0.2412
MTE	**Mean, bi-directional transfer efficiency** applies the geometric mean of the measured, asymmetrical transfer efficiencies to both directions of transfer.	0.1162	0.1162

The asymmetrical transfer efficiency values used in this model are the bi-directionally measured transfer efficiencies for skin-fomite touching events involving *A. baumannii* - which is considered to be more realistic than the simplifying assumption of symmetrical transfer. Therefore, our baseline model uses the ATE system and all output using the other transfer efficiency systems (STE and MTE) are compared to the ATE system model. We first describe contamination levels of *A. baumannii* (cfu/cm^2) in the environment, on the healthcare worker (HCW), on the patients and the movement of pathogens between these compartments using the ATE system in a model involving a large environment of 2000 cm^2. Next, the effects of using asymmetrical transfer efficiencies (ATE) on the dynamics of this system are directly compared to systems using symmetrical (STE) and the mean bi-directional (MTE) transfer efficiencies. Then, the size of the environment is reduced10 fold and again the three transfer systems are directly compared. Lastly, we minimize the role of the HCW by applying gloves to the HCW during direct patient care, reducing the skin-skin transfer efficiency from 0.3253 to 0.1063

during HCW-patient touches (only), for a final direct comparison of these three systems. The end measures for all comparisons are the total contamination levels in the uncolonized patient's room (Eu), on the uncolonized patient (Pu) and on the HCW.

6.4.2   *Explanation of the movement of pathogens in a system*

We describe the movement of pathogens in a system that uses asymmetric transfer efficiencies (ATE) in a relatively large environmental area of 2000 cm^2. There are seven main events that occur in each 24 hour period: (1) In the first 20 minutes, the HCW visits the colonized patient's (Pc) room where touching events occur between the Pc and their environment (Ec), the HCW and Ec, and between the HCW and Pc. (2) Upon leaving the Ec, the HCW washes their hands. (3) In the second 20 minutes, the HCW visits the uncolonized patient (Pu) in their room (Eu) where the same touching events can occur. (4) Upon leaving Eu, the HCW again washes their hands. (5) In the last 20 minutes of the hour, the HCW is at the nurses' station. During this time-period, each patient only has contact with their own environments and there are no interactions between the HCW and either patient. (6) Every 8 hours, the HCW is replaced with a new, uncolonized HCW. (7) At the 24th hour, the environment undergoes cleaning.

From 0 min to 20 min: In the first 20 min of every hour, the initially uncolonized HCW is visiting the colonized patient (Pc) in their room (Ec). As shown in Figure 6.15, during the first 1/3 hour, the concentration of *A. baumannii* decreases sharply on Pc and increases proportionately on the HCW. The skin-skin transfer rate is symmetrical and the flow of pathogens travels from high to low concentration areas. Thus, we see a transfer of pathogens from the colonized patient to the uncolonized HCW. While concentrations on the HCW are significantly increasing, concentrations on Ec are also increasing, but at a much slower rate

(Figure 6.16). The increase of contamination on the Ec over time is very gradual due to the low

skin-to-fomite (deposit) transfer efficiency (ρ_D=0.0.056) of *A. baumannii* in the ATE system

compared to the significantly higher skin-skin transfer efficiency (ρ_S=0.3253).

Figure 6.12: Concentration of A. baumannii on the Colonized patient (green) and on the Healthcare Worker (red line) from time 0 to time 4 hours (asymmetrical transfer efficiencies, Environment area = 2000 cm^2).
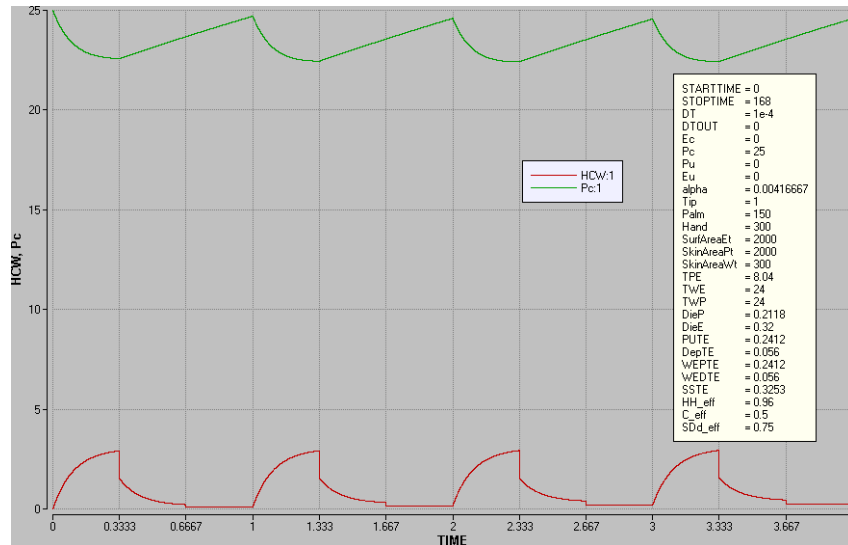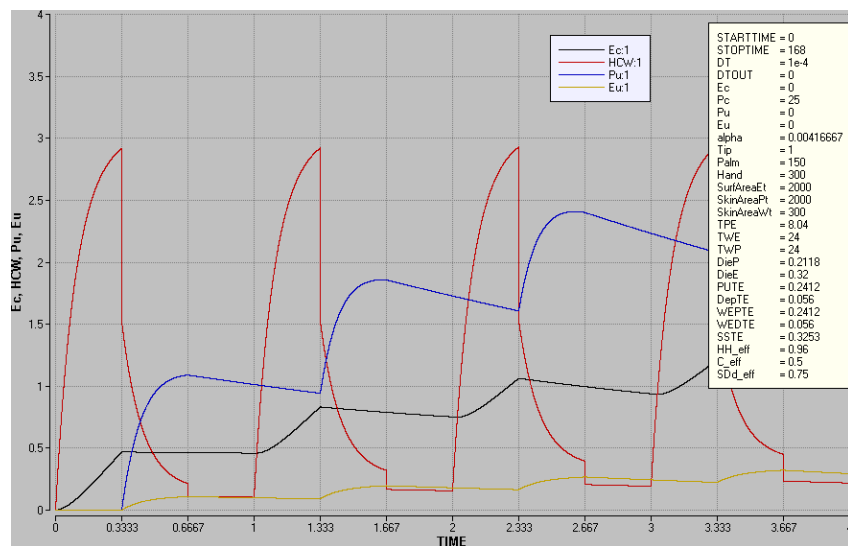

Figure 6.13: Concentration of A. baumannii on the colonized patient environment, Ec (black), the HCW (Red), the uncolonized patient, Pu (blue), on the uncolonized patient environment, Eu (yellow line) from time 0 to time 4 hours (asymmetrical transfer efficiencies; Environment area = 2000 cm^2).

At every 20 minutes and 40 minutes of each hour: After the 20-minute visit with Pc, and after the next 20-minute visit with Pu, the HCW washes their hands. These events are characterized by a sharp decrease in pathogen concentrations on the HCW after the first 1/3 and 2/3 of every hour (Figure 6.15-6.16). The sharp decrease is proportional to the cleaning efficacy of hand washing times the compliance efficacy of the HCW. Thus, each handwashing only removes a proportion of the contamination from the HCW.

From 20 minutes to 40 minutes within each hour: During the second 20-minute period of each hour, the HCW visits the uncolonized patient (Pu) in their room (Eu), which is also initially uncolonized. Pu and Eu become contaminated during the first visit with the HCW (Figure 6.16). During this time, concentrations on Pu increase sharply; concentrations on Eu increase more slowly as the concentrations decrease sharply on the HCW. This is influenced by the higher transfer rate for skin-skin transfer during touches with the patient compared to the deposit rate from skin to fomite during touches with the environment. The flow of pathogens moves from the more contaminated HCW to the lower concentrations found on Pu and Eu. Meanwhile, pathogen concentrations continue to increase almost linearly on Pc, despite the fact that the HCW is no longer in Ec (Figure 6.15). This is because the skin contamination on Pc continues to replenish itself. Additionally, Pc continues to touch the environment, effectively "cleaning" the environment with their hands because the fomite to skin transfer efficiency is 4.31 times greater than the skin to fomite transfer efficiency. Consequently, concentrations on Ec decrease during this time while that on Eu is increasing.

From 40 minutes to 60 minutes within each hour: During the last 20-minute period of every hour, the HCW is at the nurse's station, away from both of the patients. Therefore, there is no increase or decrease of pathogen levels on the HCW during this time. As in the second 20-

127

minute period of the hour, despite the absence of the HCW, pathogen concentrations continue to *increase* almost linearly on Pc. This occurs because the skin contamination on Pc continues to replenish itself and Pc continues to touch the environment, where each touch is effectively "cleaning" the surface due to the high pickup transfer efficiency relative to the deposit transfer efficiency. Thus, concentrations on Ec gradually decrease during this time. Concentrations on Pu *decline* during this 3rd period, despite the fact that Pu is also touching their environment with a high pickup transfer efficiency because (1) they are shedding to the environment and (2) in contrast to the colonized patient, the pathogen does not replenish itself on Pu. Concentrations on Pu sharply rise at the start of the next visit by the HCW (Figure 6.15-6.16).

At every 8th hour: A new, uncolonized HCW enters the system every 8 hours, which zero's out the pathogen concentrations on the HCW. This significant decrease of pathogen levels on the HCW results in very small decreases in pathogen concentrations on Pc and Pu every 8 hours.

At every 24th hour: Every 24 hours, the environments are cleaned with an efficacy of 75%. This is indicated by the sharp decrease in pathogen concentrations on Ec and Eu every 24th hour. This also results in small decreases in concentrations on Pu, Pc and the HCW at the start of each new day.

6.4.3   *Large Environment (2000 cm^2)*

We compared the system dynamics of the model using the ATE method to same model using the STE and the MTE methods, all in a large environment of 2000 cm^2, which approximates the touchable surface area around the patient including the bed rails, equipment and counter space. For all compartments and flows in each model system, the maximum

concentration (cfu/cm^2) of pathogen was calculated. Table 6.12 presents the ATE model

maximum concentrations and the % change from the ATE model by the STE and MTE models.

Table 6.12: Comparing *A. baumannii* concentrations at 72 hours derived from the model using Asymmetrical transfer efficiencies (ATE) with that using symmetrical transfer efficiencies (STE) and the mean bi-directional transfer efficiencies (MTE) within a large environmental area of 2000 cm^2.

		Large Environmental Area *(2000 cm^2)*		
		ATE CFU/cm^2	STE % Change	MTE % Change
5 Main Compartments	EC	1.50	220.28	109.96
	EU	0.49	160.76	95.82
	HCW	3.00	-21.15	-10.67
	PC	24.87	-7.55	-3.80
	PU	3.84	-36.21	-18.75
Flows	EU to PU	0.0005	160.76	-5.66
	PU to EU	0.006	162.77	60.95
	HCW to PU	12.21	-21.13	-10.66
	PU to HCW	4.49	-36.21	-18.69
	HCW to PC	23.40	-21.25	-10.81
	PC to HCW	29.12	-7.55	-3.80
	PC to EC	0.0373	298.18	99.12
	EC to PC	0.0015	220.25	0.73
	HCW to EC	1.05	239.70	84.97
	EC to HCW	0.65	220.28	0.74
	HCW to EU	1.05	239.70	84.96
	EU to HCW	0.21	160.76	-6.03

HCW=Healthcare worker; PC=Colonized Patient; PU=Uncolonized Patient; EC=Environment of Colonized Patient; EU=Environment of Uncolonized Patient

Symmetry overestimates contamination in the large environment. In the ATE method, the fomite-to-finger (ρ_{PU}) and the finger-to-fomite (ρ_D) transfer efficiencies are measured and have their own independent values. For *A. baumannii*, ρ_{PU}=0.2412 and ρ_D=0.056, so the fraction of pathogens deposited to the environment relative to what is picked up in any given touch is small. In contrast, the STE and MTE methods assume that $\rho_D = \rho_{PU}$ which, for *A. baumannii*, is equal to 0.2412 and 0.1162 for the STE and MTE methods respectively. In both methods of symmetry, the rate of deposit to the environment is grossly overestimated, resulting in greater concentrations transferred to the surface with every touch. This has implications for the transfer of microorganisms to the uncolonized patient. For example, contamination levels in the uncontaminated patient's room (Eu) are significantly overestimated in both symmetric models (160.8% and 95.8% for the STE and MLE models respectively). Figure 6.17 shows the contamination levels in Eu of size 2000 cm^2 over time. Compared to the ATE model (yellow line), the STE model (blue line) grossly overestimates contamination levels in the Eu. Although the MTE model (green line) is a better approximation, it still inflates the true levels of contamination in this environment.

Figure 6.14: A. baumannii contamination on the non-porous environmental surfaces of the uncolonized patient's room (Eu) over 72 hours where the surface area = 2000 cm^2. Yellow=ATE, Green=MTE and Blue=STE.
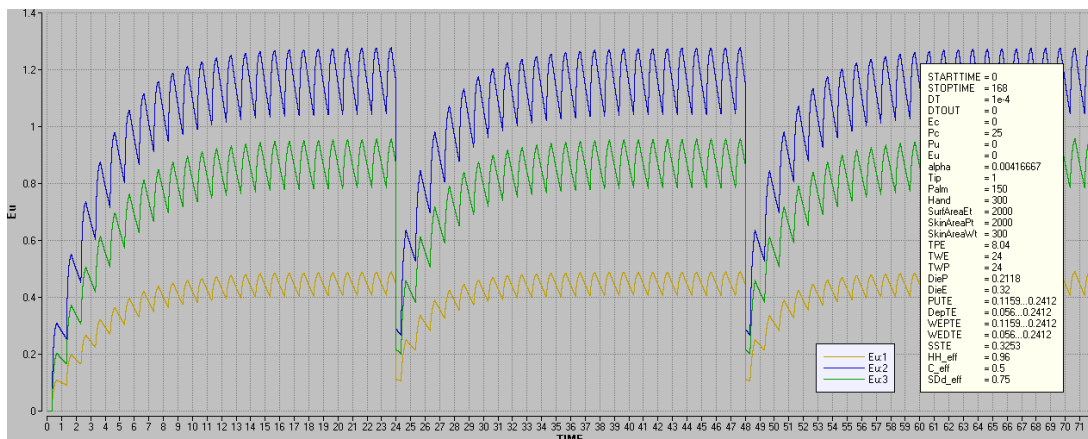
Symmetry underestimates contamination levels on the patients and HCW in a large environment. The STE system underestimates pathogen concentrations on the uncolonized patient (Pu) by approximately 36% (Figure 6.18), the colonized patient (Pc) by almost 8% and on the HCW by about 21%. This is because the deposit transfer efficiency used in the STE system is more than 4 times greater than that used in the ATE system, resulting in a "cleaning" of the skin with every touch by the environment, when pathogen levels are higher on the skin compared to surfaces. The MTE system also underestimates these pathogen contamination levels on the patient and HCW in the large environment; contamination is underestimated on the Pu by almost 19%, the Pc by almost 4% and on the HCW by almost 11%. In the MTE system, not only is the fraction of pathogens picked up from the environment by the patient much lower than that for the ATE system, the deposit rate back to the environment is also higher resulting in an overall underestimation of pathogen concentrations on Pu.

Figure 6.15: Contamination on the uncolonized patient (Pu) over 72 hours in a system where the total available environmental surface area = 2000cm². Green=STE, Blue=ATE, Red=MTE.
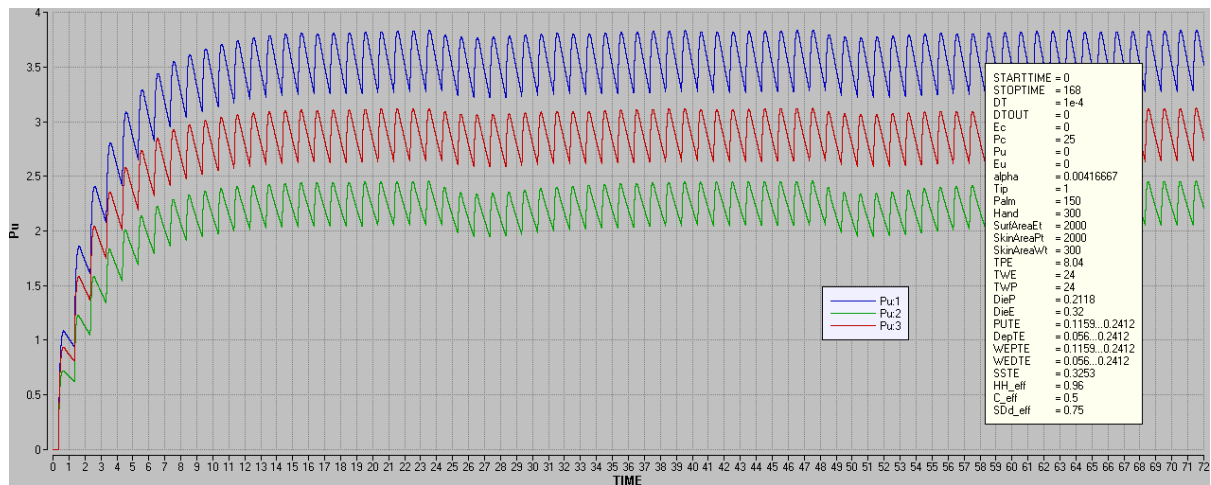
The flow of *A. baumannii* from the non-porous surfaces of Eu to Pu is overestimated by the STE model and underestimated by the MTE model. The STE model significantly overestimates the level of contamination flowing from Eu, (set at 2000 cm^2) to Pu by almost 161% (Figure 6.19). In the STE model, the environment is essentially "cleaning" the skin with every touch resulting in much higher levels of pathogen on environmental surfaces, which become available for pickup by Pu and consequently inflates the flow from Eu to Pu. In contrast, concentration levels for this flow in the MTE model are about 6% *lower* than the ATE model (Figure 6.19). This is due to the use of the mean pickup and deposit transfer efficiency value of 0.1162, which (1) reduces overall available contamination on the Eu for pickup and (2) cuts the "cleaning" effect by the environment in half. Therefore, the MTE model marginally underestimates the flow from Eu to Pu compared to the ATE model.

Figure 6.16: Flow of A. baumannii from the non-porous environmental surfaces of the uncolonized patient's room to the uncolonized patient over time where the surface area = 2000 cm^2. Red=ATE, Light blue=MTE and Black=STE.
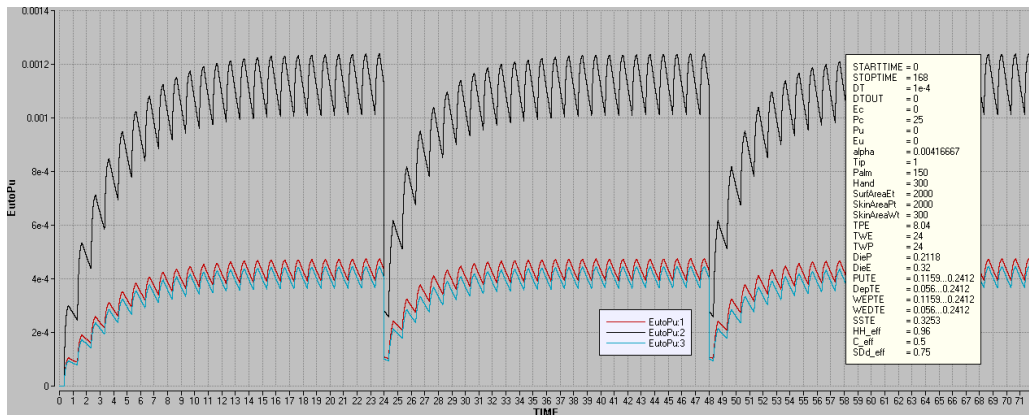
Symmetry underestimates the flow of pathogens from the HCW to the uncolonized patient (Pu) in a large environment. Since skin-to-skin transfer is a symmetrical event and the same ρ_S value is used in all three models, the underestimation here is less drastic than that seen

for the flow from Eu to Pu. The STE model underestimates the flow from the HCW to Pu by almost 21% and the MTE model by almost 11% (Figure 6.20). The decrease in HCW contamination, due to the high deposit rate to the environment, means that there is less pathogen available for transfer to the patient in the STE model. In the MTE model, there is also an overall decrease in contamination on the HCW resulting in a narrower underestimation of the flow from HCW to Pu compared to the ATE model.

Figure 6.17: Flow of A. baumannii from the healthcare worker to the uncolonized patient (Pu) over time where the surface area = 2000 cm². Red=ATE, Black=MTE and Yellow = STE.
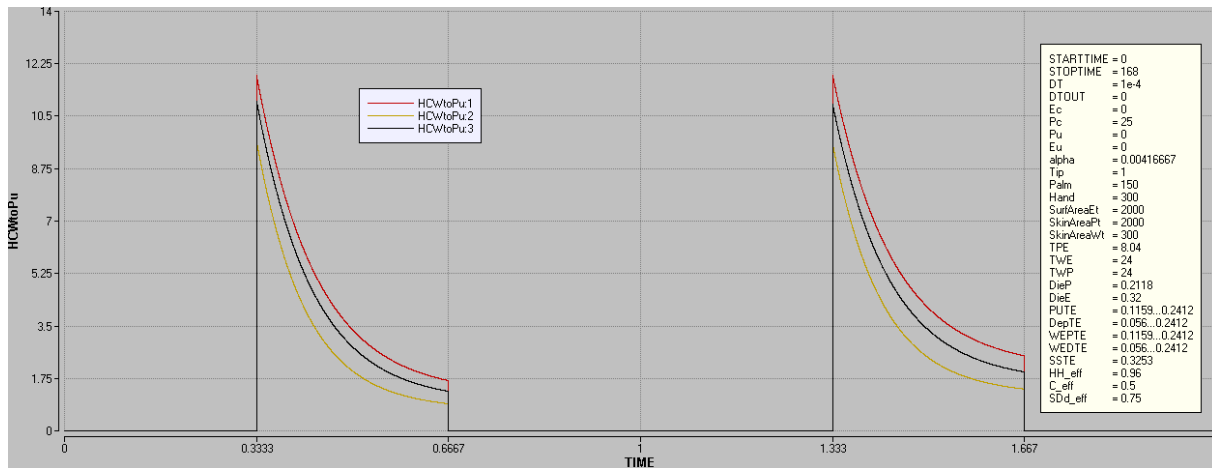
6.4.4   Small Environment (200 cm²)

The system dynamics of the asymmetrical transfer efficiency (ATE) model was compared to that of the symmetrical transfer efficiency (STE) and the mean bi-directional transfer efficiency (MTE) models, where the total available environment was reduced to 200 cm² – the size of the bed remote control or a keypad. For all compartments and flows in each model, the maximum concentration (cfu/cm²) of *A. baumannii* was calculated. The percent change in pathogen concentration for each compartment and flow for the three systems of symmetry within a small environment of 200 cm² are reported in Table 6.13.

Table 6.13: Comparing A. baumannii concentrations at 72 hours derived from the model using Asymmetrical transfer efficiencies (ATE) with that using symmetrical transfer efficiencies (STE) and the mean bi-directional transfer efficiencies (MTE) within a small environment area of 200 cm^2.

		Small Environmental Area (200 cm^2)		
		ATE CFU/cm^2	STE % Change	MTE % Change
5 Main Compartments	EC	0.419	241.73	185.78
	EU	0.144	253.60	205.10
	HCW	3.21	-7.29	-5.76
	PC	25.51	-2.65	-2.11
	PU	4.31	-14.23	-10.65
Flows	EU to PU	0.0014	253.53	46.57
	PU to EU	0.0065	269.46	85.43
	HCW to PU	13.01	-7.34	-5.79
	PU to HCW	5.05	-14.23	-10.65
	HCW to PC	25.05	-7.29	-5.75
	PC to HCW	29.87	-2.64	-2.11
	PC to EC	0.0383	319.35	103.12
	EC to PC	0.0040	281.44	56.11
	HCW to EC	2.16	299.33	95.55
	EC to HCW	1.82	241.88	37.21
	HCW to EU	1.12	299.53	95.10
	EU to HCW	0.63	253.48	45.87

HCW=Healthcare worker; PC=Colonized Patient; PU=Uncolonized Patient; EC=Environment of Colonized Patient; EU=Environment of Uncolonized Patient

Symmetry overestimates contamination levels on environmental surfaces in a reduced environmental setting of 200cm^2. As seen in the 2000cm^2 environment analysis, symmetry resulted in an overestimation of pathogen levels on environmental surfaces compared to asymmetrical transfer. Compared to the ATE model, the STE model overestimated Eu by about 254% and the MTE model overestimated by almost 205% (Table 6.13, Figure 6.21). This is because the STE and MTE models have a higher ρ_D compared to the ATE model, which grossly overestimates the amount of pathogen being removed from the skin and deposited to the environment. Thus, there is a cleaning of the skin effect with every touch in the models with symmetrical transfer efficiencies.

Figure 6.18: A. baumannii contamination on the non-porous environmental surfaces of the uncolonized patient's room (Eu) over time where the surface area = 200 cm^2. Yellow=ATE, Green=MTE and Blue=STE.
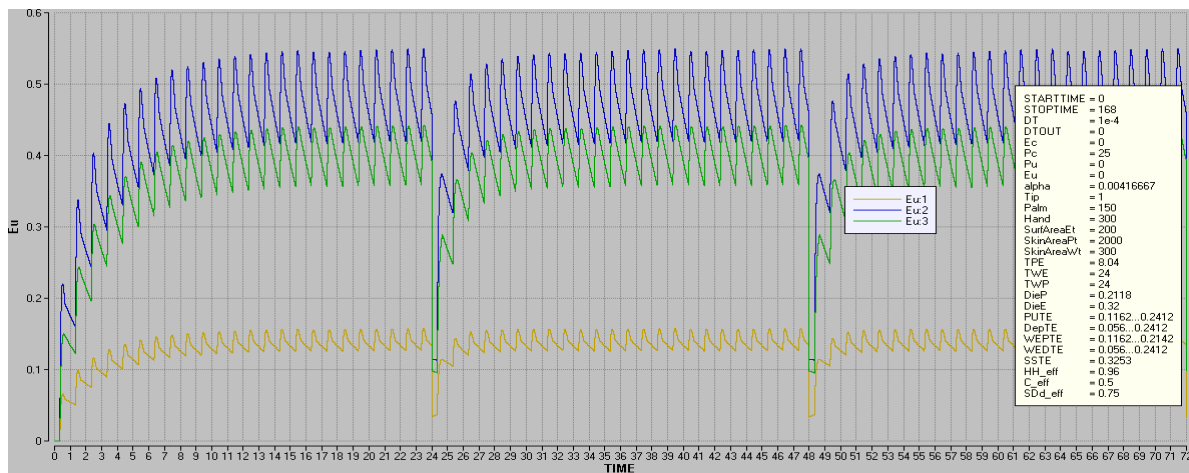
Symmetry overestimates the flows of *A. baumannii* from the non-porous surfaces to the patients in a small environment. Figure 6.22 shows the flow of contamination from the Eu to the Pu over time in a small environment. Again, the MTE model is a better approximation of the asymmetrical system, but it still overestimates this flow by more than 46%. As in the large environment system, the high rate of pick-up from the environment results in an overestimation

of contamination on the skin in both symmetric models compared to the asymmetric model, but in this small environment, the results are even more inflated. Touches between the patient and this environment occur with the fingertip of the patient, a ratio of 1cm^2/200cm^2. Touches between the HCW and the environment occur with the palm of the hand, which is a ratio of 150cm^2/200cm^2. For both the HCW and the patient, 10 times the amount of bacteria is made available for pick up in this small environment scenario compared to the large environment. For this reason, the overestimation resulting from symmetry is even greater given a much smaller environment.

Figure 6.19: Flow of A. baumannii from the non-porous environmental surfaces of the uncolonized patient's room (Eu) to the uncolonized patient (Pu) over time where the surface area = 200 cm^2. Blue=ATE, Red=MTE and Green=STE.
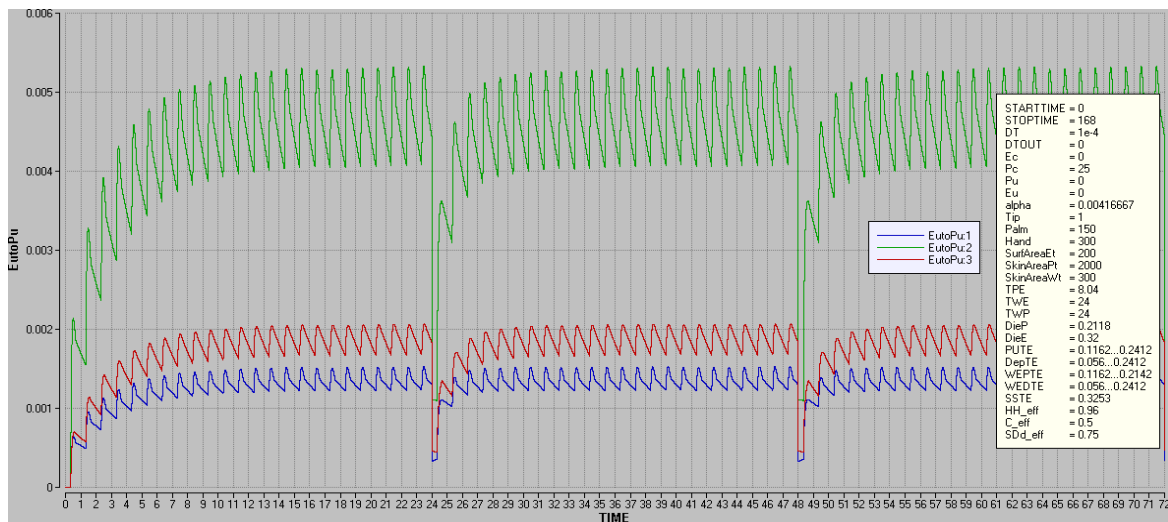
Symmetry underestimates contamination levels on the patients and HCW in a small environment. As in the large environment system, symmetry again underestimates contamination levels on both patients as well as the HCW, shown in Figure 6.23. As discussed earlier, the deposit transfer efficiencies used in the STE and MTE systems are much larger than that for the ATE system such that the environment effectively "cleans" the skin with each touch,

resulting in lower pathogen concentrations on the skin. The underestimation of contamination levels on the patients and HCW is narrower in the 200cm^2 environment compared to the 2000cm^2 environment and the MTE model is a better approximation of asymmetry.

Figure 6.20: Contamination on the uncolonized patient (Pu) over time in a system where the total available environmental surface area = 200cm^2. Blue=ATE, Green=STE, Red=MTE.
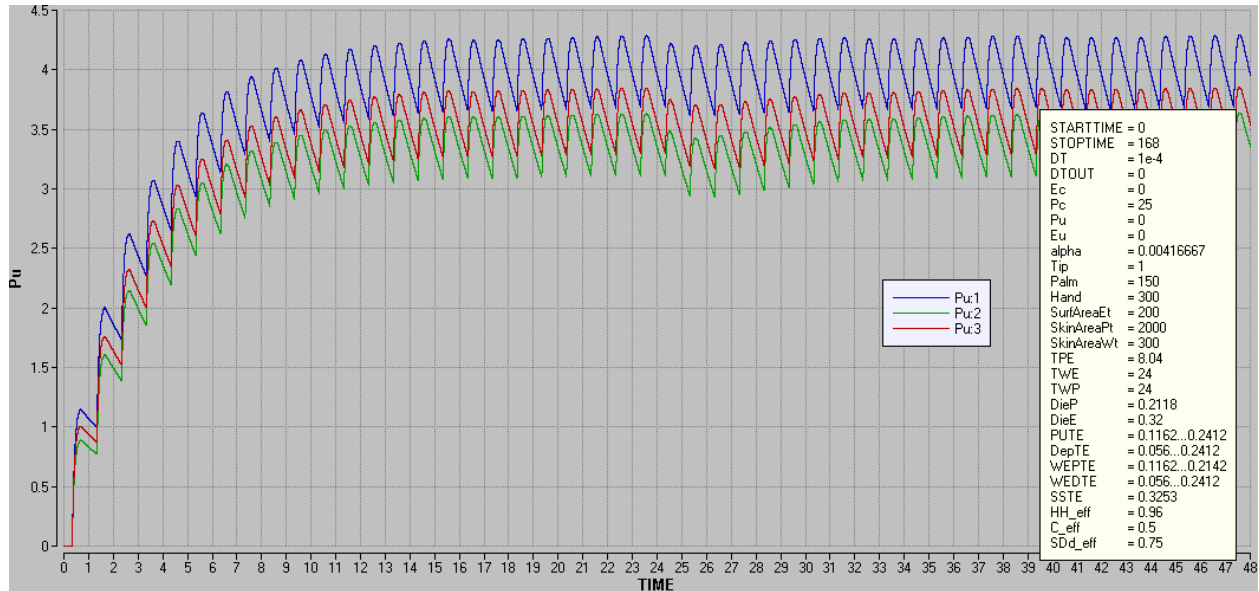
Symmetry underestimates the flow of pathogens from the HCW to Pu in a small environment. The STE model underestimates of the flow of pathogens from the HCW to Pu by about 7.3% and the MTE model by over 5.7% (Table 6.13). In the STE model, the higher deposit rates to the environment leading to the overall decrease in pathogen levels on the HCW. In the MTE model, the much smaller pickup transfer efficiency effectively reduces the level of contamination picked up from the environment by the HCW.

6.4.5 *Glove Use by the Healthcare Worker*

By exploring model behavior under a wide variety of conditions, mistakes in the model or surprising real aspects of the model may be revealed. In the previous analyses', model behavior was explored by changing the size of the environment. In this analysis, model behavior is explored by adding glove use to the healthcare worker. Previous analyses suggest that the HCW plays a prominent role in the transfer of pathogens between patients. The "cleaning effect" of the HCW due to touching the patient observed thus far appears unrealistic. This effect is due to a relatively high pick-up transfer efficiency compared to the deposit transfer efficiency. In an effort to compare symmetry vs asymmetry in a system where the HCW role is minimized, this time we simulate the model assuming that the HCW wears gloves for all direct interactions between the HCW and the patients. This reduces the skin-skin transfer efficiency. In this scenario, it is assumed that (1) the HCW uses the same pair of gloves during their entire 8-hour shift, and (2) the HCW removes the gloves for touches with the environment and then puts them back on for touches with the patient. This is entirely unrealistic, but it serves the purpose of diminishing the impact of skin-skin transfer and is therefore suitable for the sole objective of comparing symmetry models. The impact of pathogen transfer via the HCW was minimized by replacing the skin-skin transfer efficiency (ρ_S=0.3253) with the pickup transfer efficiency for glove use (ρ_S=0.1063). The total available environmental surface area is set to 2000cm^2. Using these parameters for skin-skin transfer, the ATE model is compared to the STE and the MTE models to evaluate the effects of symmetry.

The system dynamics of the baseline ATE model (hand hygiene only, total environmental area = 2000cm^2) is compared to an ATE model with a diminished HCW role (total environmental area = 2000cm^2). The purpose of this initial comparison is to evaluate the system dynamics when the HCW wears gloves compared to the baseline and to confirm that reducing the ρ_S will effectively reduce the role of the HCW in the transmission of pathogen between patients. The extra protection of gloves provides a substantially lower transfer efficiency rate for touches between the patient skin and the HCW. As a result, less contamination is picked up by the HCW from Pc during direct patient care and the contamination levels remain *higher* on Pc compared to hand hygiene only (Figure 6.24). The higher concentrations left on the Pc remain available for shedding into the environment and for transfer to the environment via touches between the Pc and their environment (Ec). Thus, the flow of pathogens from Pc to Ec is higher in the scenario where gloves are worn by the HCW during direct patient care compared to when gloves are not worn (Figure 6.25). Despite this, contamination levels in both environments (Figures 6.26 and 6.27) remain lower in the gloved HCW scenario compared to hand hygiene only. With the exception of Pc, the contamination levels in all other compartments are overall lower when the HCW wears gloves during direct patient care compared to using hand hygiene only. The results from comparing glove use with hand hygiene only in the AET system demonstrates that minimizing the effect of the HCW can be accomplished by replacing the skin-skin transfer efficiency (ρ_S=0.3253) with the pickup transfer efficiency for glove use (ρ_S=0.1063).

Figure 6.21: Contamination on the colonized patient (Pc) and the uncolonized patient (Pu) over time in a system where the total available environmental surface area = 2000cm^2; ATE. Black=Pc, gloves; Green=Pc, no gloves; Blue=Pu, no gloves; Red=Pu; gloves.
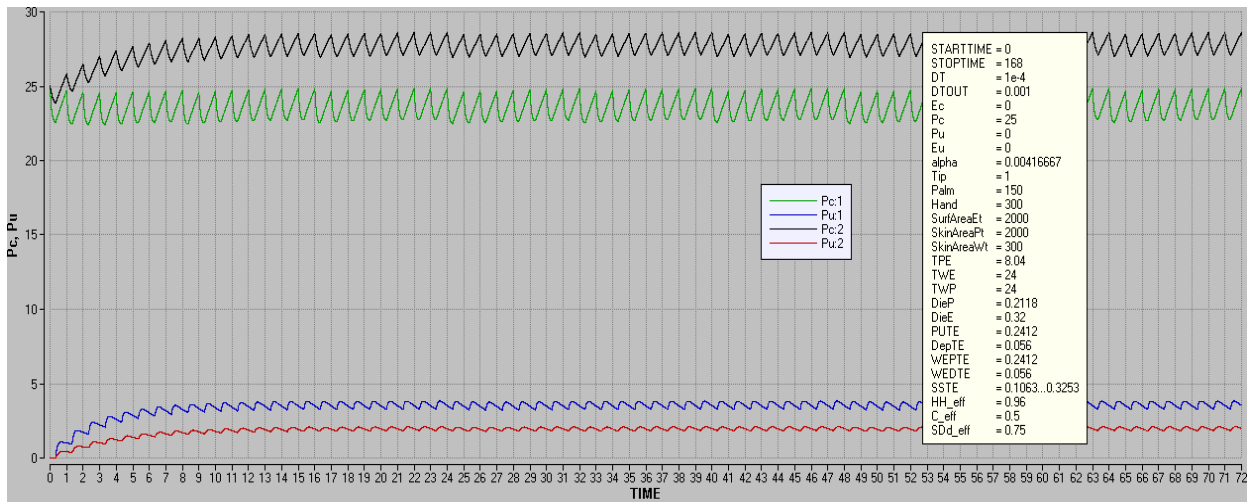

Figure 6.22: Flow of A. baumannii from the contaminated patient (Pc) to their environment (Ec) over time where the surface area = 2000 cm^2 and ATE. Pink=No Gloves, Blue=Gloves.
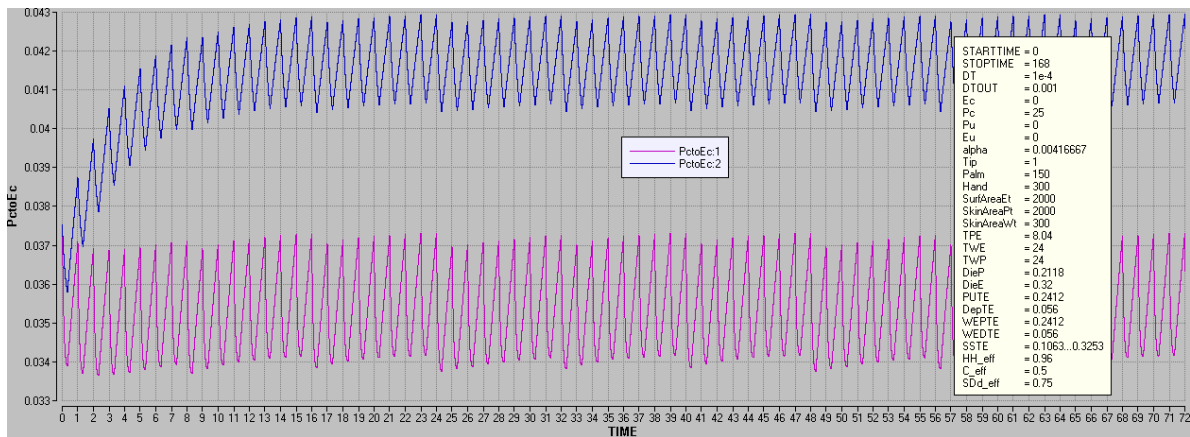
Figure 6.23: Contamination on the uncolonized patient environment (Eu) over time in a system where the total available environmental surface area, SA = 2000cm² and ATE. Black=Eu, gloves; Yellow=Eu, no gloves.
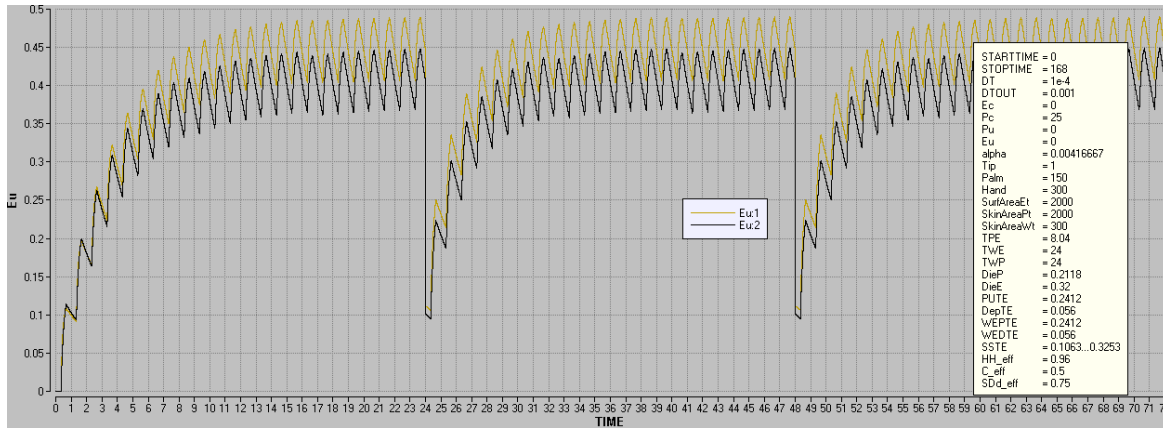
Figure 6.24: Contamination on the uncolonized patient environment (Eu) over time in a system where the total available environmental surface area, SA = 2000cm² and ATE. Black=Eu, gloves; Yellow=Eu, no gloves.
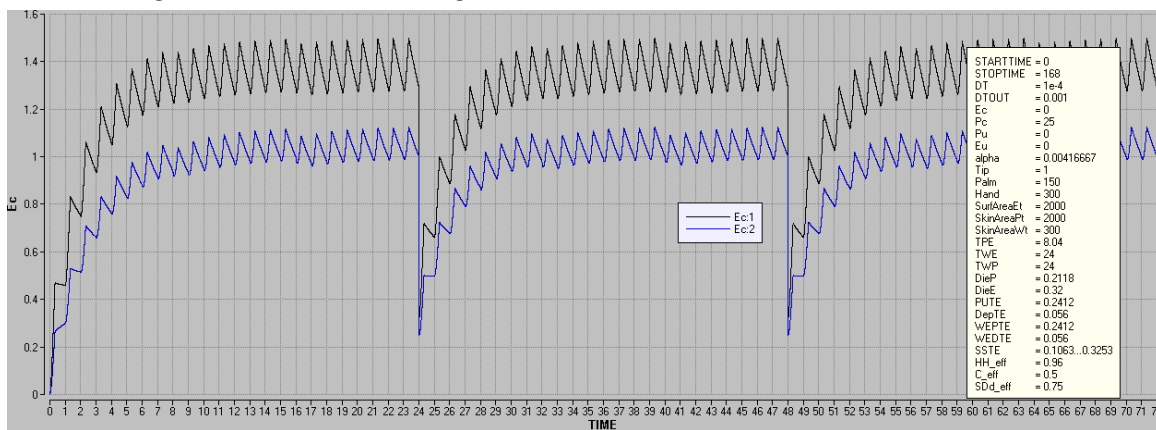
Comparing the system dynamics using asymmetrical transfer efficiencies (ATE) to using symmetrical transfer efficiencies (STE) and the mean bi-directional transfer efficiencies (MTE) after reducing the role of the HCW by adding glove use during direct patient care: The system dynamics of the ATE model was compared to that using STE and MTE models where the role of the HCW was minimized by wearing gloves as described above. For all compartments and flows in each model, the maximum concentration (cfu/cm²) of *A*.

141

baumannii was calculated. The percent change in pathogen concentration for each compartment

and flow for the three systems of symmetry with glove use by the HCW during direct patient

care are reported in Table 6.14.

Table 6.14: Comparing *A. baumannii* concentrations at 72 hours derived from the model using Asymmetrical transfer efficiencies (ATE) with that using symmetrical transfer efficiencies (STE) and the mean bi-directional transfer efficiencies (MTE) where the healthcare worker uses hand hygiene AND wears gloves during direct patient care only (ρ_S=0.1063).

		Hand Hygiene Plus Gloves During Direct Patient Care		
		ATE CFU/cm^2	STE % Change	MTE % Change
5 Main Compartments	EC	1.09	197.43	99.20
	EU	0.45	152.79	92.90
	HCW	2.27	-23.50	-12.29
	PC	28.60	-3.73	-1.78
	PU	2.08	-39.30	-20.66
Flows	EU to PU	0.0004	152.80	-7.31
	PU to EU	0.0031	161.42	64.19
	HCW to PU	3.01	-23.58	-12.33
	PU to HCW	0.80	-39.30	-20.66
	HCW to PC	5.79	-23.50	-12.29
	PC to HCW	10.37	-4.20	-2.07
	PC to EC	0.04	314.68	103.26
	EC to PC	0.0011	198.55	-4.04
	HCW to EC	1.53	229.51	81.53
	EC to HCW	0.49	198.56	-4.04
	HCW to EU	0.79	229.15	81.46
	EU to HCW	0.19	152.80	-7.31

HCW=Healthcare worker; PC=Colonized Patient; PU=Uncolonized Patient; EC=Environment of Colonized Patient; EU=Environment of Uncolonized Patient

Symmetry overestimates environmental contamination levels in a system where the HCW wears gloves during direct patient care. The symmetrical models use a larger deposit rate compared to the asymmetrical model. The ρ_D in the STE model is 4 times greater than ρ_D used in the ATE model resulting in a 197% inflation of contamination on Ec. The MTE model has a ρ_D that is 2 times greater than that used in the ATE model and overestimated Ec

contamination by more than 99% (Figure 6.28). The STE model also overestimated

contamination on Eu by more than 152% and the MTE model by about 93% (Figure 6.29). The

high ρ_D in the symmetrical models results in higher contamination levels in the environment

compared to the ATE model.

Figure 6.25: Contamination on the colonized patient environment (Ec) over time where
ρ_S=0.1063 and the total available environmental surface area = 2000cm².
Black=ATE; Light blue=STE; Purple=MTE.

Figure 6.26: Contamination on the uncolonized patient environment (Eu) over time where
ρ_S=0.1063 and the total available environmental surface area = 2000cm².
Yellow=ATE; Blue=STE; Green=MTE.
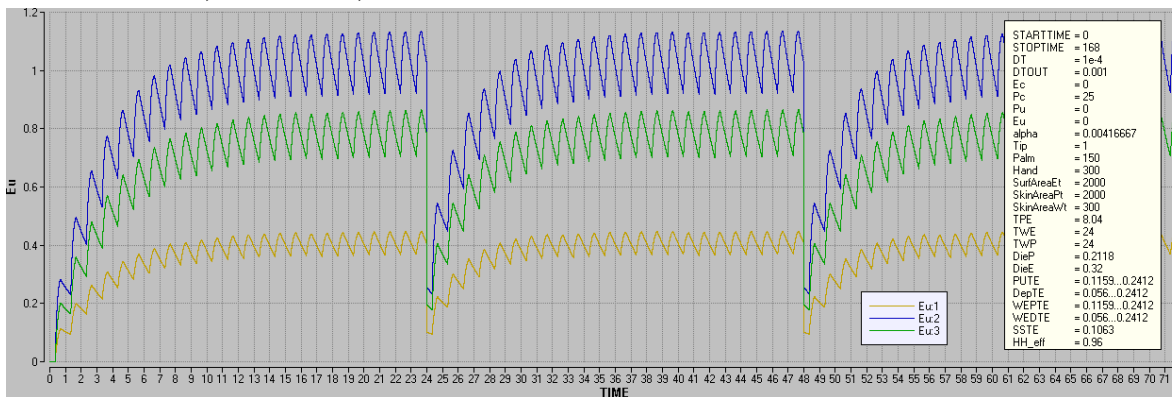
Symmetry underestimates contamination levels on the HCW and both patients

when the HCW wears gloves during direct patient care. The one aspect that ATE, STE and

MTE systems have in common is the symmetry of the skin-to-skin transfer events that occur

143

during patient care by the HCW. In all three systems, this is a symmetrical event and the value

of ρ_S remains constant. Because of this similarity, the degree of underestimation by the

symmetrical models is not excessive. For example, compared to the ATE model, the STE model

underestimates the Pu by more than 20% and the MTE model underestimates the Pu by just over

10% (Figure 6.30). As discussed earlier, the skin-to-fomite deposit transfer efficiency in the

STE system is 4 times greater than that used in the ATE model. Thus, there is a "cleaning

effect" by the environment each time the patient touches a surface. The MTE model has a

narrower underestimation because it has a deposit transfer efficiency of 0.1162 which is smaller

the STE model, but still larger than that used by the ATE model. Symmetry also results in

underestimation of contamination on the contaminated patient (Figure 6.31) and the HCW

(Figure 6.32). The STE model underestimates pathogen levels on the HCW by more than 23%

compared to the ATE model and the MTE model by just over 12%. The healthcare worker has

barehanded touches the environment, and so the "cleaning effect" by the environment applies to

the HCW as well.

Figure 6.27: Contamination on the Pu over time where $\rho_S=0.1063$ and the total available environmental surface area = 2000cm^2. Blue=ATE; Green=STE; Red=MTE.
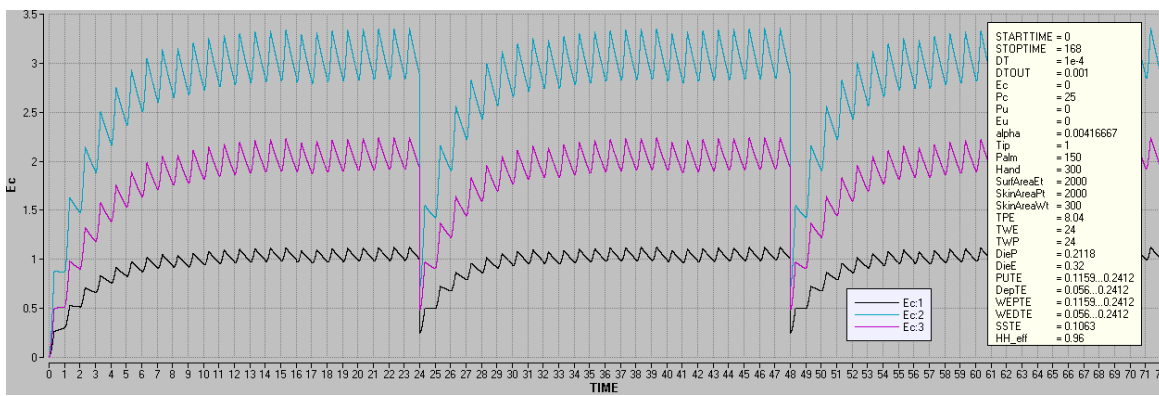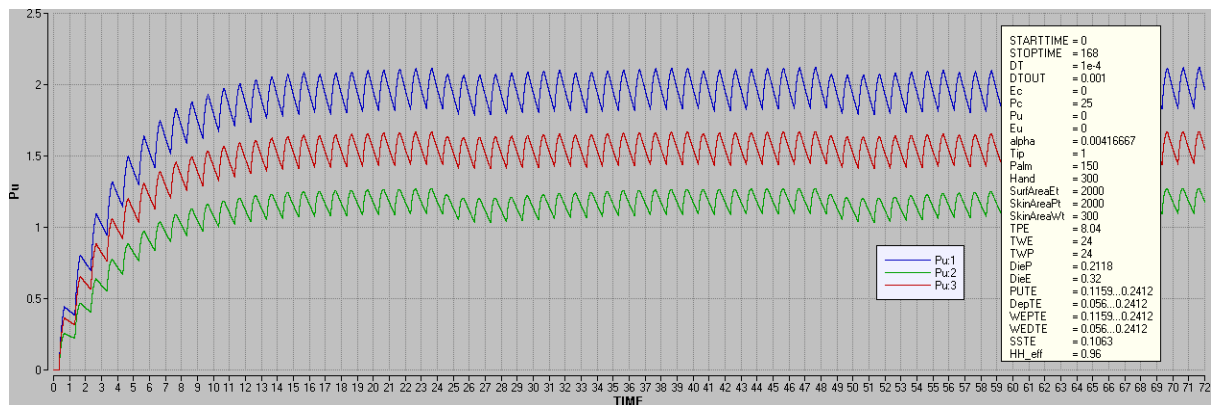
Figure 6.28: Contamination on Pc over time where ρ_S=0.1063 and the total available environmental surface area = 2000cm². Green=ATE; Red=STE; Black=MTE.
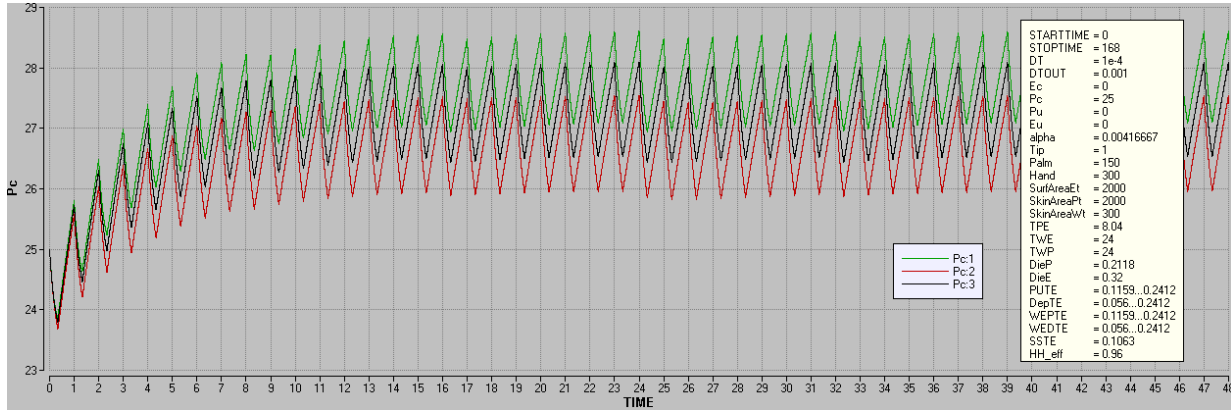
Figure 6.29: Contamination on the HCW over time where ρ_S=0.1063 and the total available environmental surface area = 2000cm². Red=ATE; Black=STE; Light Blue=MTE.
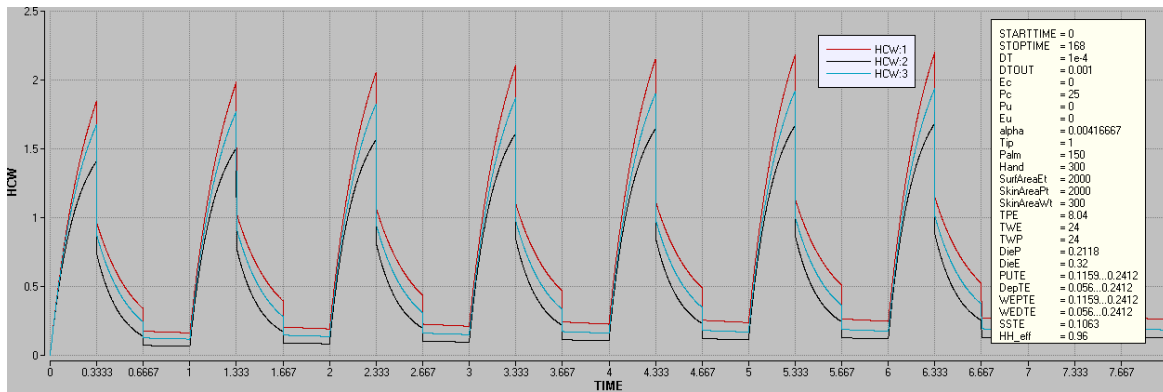
The flow of *A. baumannii* from Eu to Pu is overestimated by the STE model and underestimated by the MTE model when the HCW wears gloves during direct patient care. The overestimation/underestimation of the flow from Eu to Pu by the symmetrical models is also seen in the STE and MTE model comparison where the total available surface area was 2000cm² and only hand hygiene was used. Again, the STE model with glove use during patient care significantly overestimates the level of contamination flowing from Eu to Pu by almost 153%

145

and the MTE model underestimates this flow by more than 7% (Figure 6.33). In the STE model, the environment is essentially "cleaning" the skin with every touch, leaving exaggerated levels of pathogen on the surfaces. The flow will travel from areas of high to low concentrations thereby inflating the flow of contamination from Eu to Pu. In contrast, the underestimation by the MTE model is due to the use of the mean pickup and deposit transfer efficiency value of 0.1162, which (1) reduces overall available contamination on the Eu for pickup and (2) the cuts the "cleaning" effect by the environment in half. Therefore, the MTE model marginally underestimates the flow from Eu to Pu compared to the ATE model.

Figure 6.30: Flow of A. baumannii contamination from Eu to Pu over time where ρ_S=0.1063 and the total available environmental surface area = 2000cm². Green=ATE; Red=STE; Black=MTE.
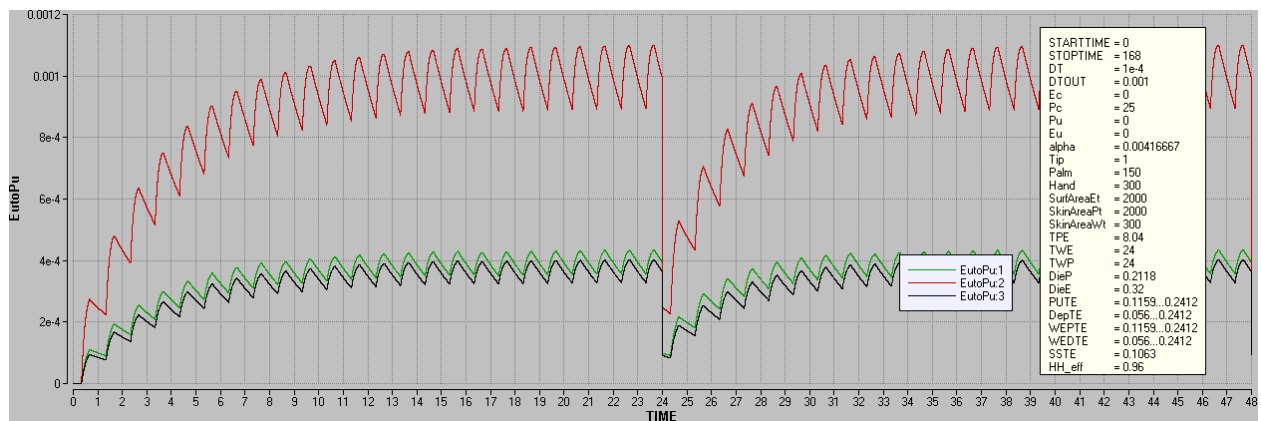
Symmetry overestimates the flow of pathogens from HCW to the uncontaminated patient environment (Eu) in a system where the HCW wears gloves during direct patient care. Both symmetrical models underestimate the flow of *A. baumannii* from the HCW to the uncontaminated patient when the HCW wears gloves during direct patient care. The STE system underestimates this flow by almost 24% and the MTE system by about 12% (Figure 6.34). This

underestimation is due to the reduced concentration level of pathogen on the HCW from the

higher deposit rates to the environment during barehanded touches compared to the AET system.

Figure 6.31: Flow of A. baumannii contamination from HCW to Eu over time where $\rho_S=0.1063$ and the total available environmental surface area = 2000cm². Blue=ATE; Green=STE; Red=MTE.
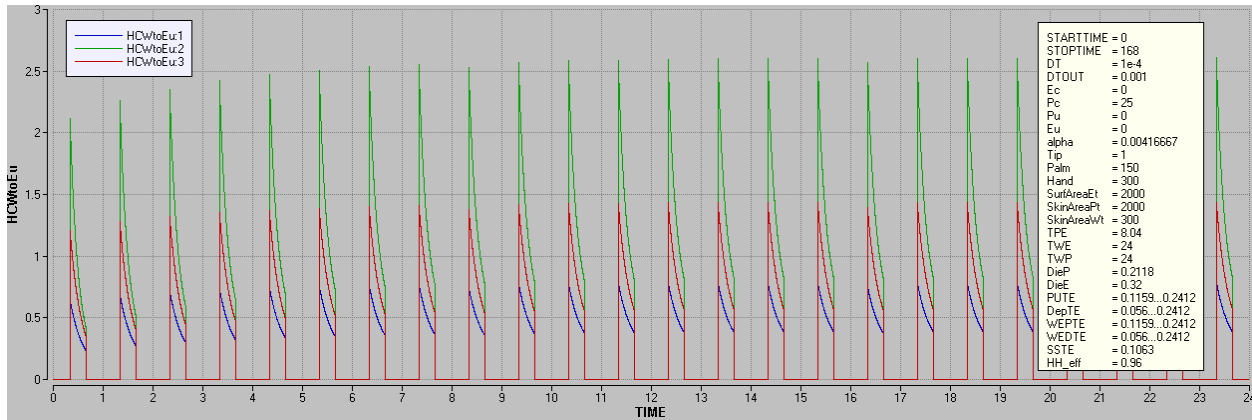

6.5.0 MODEL CONCLUSIONS

The use of asymmetric versus symmetric transport influences the relative importance of

direct and indirect contact in environmentally mediated transmission of *A. baumannii*. Both

models of symmetry (STE and MTE) consistently overestimate or underestimate the

contamination levels of *A. baumannii* compared to the asymmetrical model (ATE) regardless of

changing the level of environmental or HCW influence as follows:

1. Contamination levels in the environment are consistently and exceptionally overestimated.
2. Contamination levels on the HCW are consistently underestimated.
3. Contamination levels on both patients are consistently underestimated where the greatest underestimation occurs with the uncontaminated patient.
4. The flows of pathogen from each patient to their respective environment are grossly overestimated.

5. The flows of pathogen from the HCW to each patient as well as from each patient to the HCW are underestimated.

6. The flow of pathogen from HCW to Ec and from HCW to Eu is grossly overestimated, regardless of environment size or reduction in HCW influence.

The flows of pathogen from HCW to each patient's environment, as well as the flows of pathogen from each patient to their respective environments, are grossly overestimated regardless of environment size or glove use by the HCW. This occurs because the deposit transfer efficiency is significantly greater in the symmetrical models, creating a "cleaning effect" of the skin by the surface with each touch. Therefore, the contamination levels in both environmental areas are consistently overestimated in both models of symmetry. This also results in an underestimation of the flow of pathogen from the HCW to each patient and from each patient to the HCW because the skin is being "cleaned" with every environmental touch, effectively reducing pathogen levels on these individuals. Consequently, contamination levels on both patients are consistently underestimated. Compared to the STE model, the MTE model is a better approximation of the asymmetrical system overall.

Some of the unrealistic aspects of this model could potentially have affected the patterns presented here. In particular, in order to greatly simplify the environment the current model assumes that the contamination deposited to a surface is instantaneously and evenly distributed over the entire, available surface area. This assumption provides a constant (or total) pickup of pathogens by subsequent touches. A more realistic approach would be to assume that the contamination will stay where the first (depositing) touch actually occurred and that the second (pick-up) touch may or may not actually touch the area containing the contamination, resulting in a random pickup of pathogens. This would be the average pick up of pathogens under the assumption of instantaneous dissemination to the entire surface. If the current model were to

relax the simplifying assumption of instantaneous dissemination with constant pickup of pathogens, and assume an average pickup of pathogens, we would still expect the same pattern of over or underestimation of contamination seen using symmetry because the deposit transfer efficiencies in the symmetrical models are markedly greater than that in the asymmetrical model. With respect to the pickup transfer efficiencies, the pickup transfer efficiency in the STE and ATE model are the same (ρ_{PU}=0.2412), so relaxing the simplifying assumption of instantaneous dissemination would reduce the mean pickup of pathogens equally between these two models. The pickup transfer efficiency in the MTE model is ½ that of the ATE model (ρ_{PU}=0.1162 and 0.2412 respectively), so relaxing the simplifying assumption of instantaneous dissemination would reduce the mean pickup of pathogens proportionally between these two models. Compared to the ATE model, the deposit transfer efficiency in the STE model is 4.3 times greater than that in the ATE model and the deposit transfer efficiency in the MTE model is 2 times greater than that in the ATE model. Thus, the relaxation of this simplifying assumption would not eliminate the "cleaning effect" occurring by the environmental surfaces in the symmetrical models. Therefore, the current model is adequate for assessing the general effects of using symmetrical versus asymmetrical transfer efficiencies.

This analysis demonstrates that the simplifying assumption of symmetrical, environmental transfer will result in the underestimation of pathogen concentrations on the uncolonized patient and significantly overestimates contamination in the environment. Consequently, transfer symmetry seriously inflates the role of the environment while minimizing the true impact of HCW mediated transmission. The application of asymmetrical transfer efficiencies in environmental transmission modeling is recommended. Additional research quantifying the bidirectional transfer efficiencies of other microorganisms is needed.

6.6.0 REFERENCES

1.   Magill SS, Edwards JR, Fridkin SK. Survey of health care-associated infections. N Engl J Med 2014;370(26):2542-3.

2.   McConnell MJ, Actis L, Pachon J. Acinetobacter baumannii: human infections, factors contributing to pathogenesis and animal models. FEMS microbiology reviews 2013;37(2):130-55.

3.   Rebmann T, Rosenbaum PA. Preventing the transmission of multidrug-resistant Acinetobacter baumannii: an executive summary of the Association for Professionals in infection control and epidemiology's elimination guide. Am J Infect Control 2011;39(5):439-41.

4.   Markogiannakis A, Fildisis G, Tsiplakou S, Ikonomidis A, Koutsoukou A, Pournaras S, et al. Cross-transmission of multidrug-resistant Acinetobacter baumannii clonal strains causing episodes of sepsis in a trauma intensive care unit. Infect Control Hosp Epidemiol 2008;29(5):410-7.

5.   Cristina ML, Spagnolo AM, Cenderello N, Fabbri P, Sartini M, Ottria G, et al. Multidrug-resistant Acinetobacter baumannii outbreak: an investigation of the possible routes of transmission. Public health 2013;127(4):386-91.

6.   Dettori M, Piana A, Deriu MG, Lo Curto P, Cossu A, Musumeci R, et al. Outbreak of multidrug-resistant Acinetobacter baumannii in an intensive care unit. The New Microbiologica 2014;37(2):185-91.

7.   Wendt C, Dietze B, Dietz E, Ruden H. Survival of Acinetobacter baumannii on dry surfaces. J Clin Microbiol 1997;35(6):1394-7.

8.   Jawad A, Seifert H, Snelling AM, Heritage J, Hawkey PM. Survival of Acinetobacter baumannii on dry surfaces: comparison of outbreak and sporadic isolates. J Clin Microbiol 1998;36(7):1938-41.

9.   Morgan DJ, Liang SY, Smith CL, Johnson JK, Harris AD, Furuno JP, et al. Frequent multidrug-resistant Acinetobacter baumannii contamination of gloves, gowns, and hands of healthcare workers. Infect Control Hosp Epidemiol 2010;31(7):716-21.

10.   Li S, Eisenberg JN, Spicknall IH, Koopman JS. Dynamics and control of infections transmitted from person to person through the environment. Am J Epidemiol 2009;170(2):257-65.

11.   Plipat N, Spicknall IH, Koopman JS, Eisenberg JN. The dynamics of methicillin-resistant Staphylococcus aureus exposure in a hospital model and the potential for environmental intervention. BMC Infect Dis 2013;13:595.

12.   Greene C, Vadlamudi G, Eisenberg M, Foxman B, Koopman J, Xi C. Fomite-fingerpad transfer efficiency (pick-up and deposit) of Acinetobacter baumannii-with and without a latex glove. Am J Infect Control 2015.

13.   Weber DJ, Rutala WA, Miller MB, Huslage K, Sickbert-Bennett E. Role of hospital surfaces in the transmission of emerging health care-associated pathogens: norovirus, Clostridium difficile, and Acinetobacter species. Am J Infect Control 2010;38(5 Suppl 1):S25-33.

14.   Greene C, Vadlamudi G, Newton D, B. F, Xi C. The impact of biofilm formation and multidrug resistance on environmental survival of clinical and environmental isolates of Acinetobacter baumannii. Am J Infect Control Submitted, Sept. 5, 2015.

15.   Larson E. Skin hygiene and infection prevention: more of the same or different approaches? Clin Infect Dis 1999;29(5):1287-94.

16.   Gontijo Filho PP, Stumpf M, Cardoso CL. Survival of gram-negative and gram-positive bacteria artificially applied on the hands. J Clin Microbiol 1985;21(4):652-3.

17.   Liu WL, Liang HW, Lee MF, Lin HL, Lin YH, Chen CC, et al. The impact of inadequate terminal disinfection on an outbreak of imipenem-resistant Acinetobacter baumannii in an intensive care unit. PLoS One 2014;9(9):e107975.

18.   Montville R, Schaffner DW. A meta-analysis of the published literature on the effectiveness of antimicrobial soaps. J Food Protection 2011;74(11):1875-82.

19.   Amin N, Pickering AJ, Ram PK, Unicomb L, Najnin N, Homaira N, et al. Microbiological evaluation of the efficacy of soapy water to clean hands: a randomized, non-inferiority field trial. Am J Tropical Med and Hygiene 2014;91(2):415-23.

20.   Midturi JK, Narasimhan A, Barnett T, Sodek J, Schreier W, Barnett J, et al. A successful multifaceted strategy to improve hand hygiene compliance rates. Am J Infect Control 2015;43(5):533-6.

21.   Vynnycky E, White RG. An Introduction to Infectious Disease Modelling. Oxford New York: Oxford Uniersity Press; 2010.

Berkeley Madonna Model Code (Globals)

{Top model}

  {Reservoirs}
  d/dt (Ec) = + PctoEc - EcRemoved - EctoHCW + HCWtoEc - EctoPc - EcDieoff + ShedtoEc
    INIT Ec = 0

  d/dt (HCW) = + PctoHCW - HCWtoPu + EctoHCW - HCWtoEu - HCWtoEc + EutoHCW - HCWDieOff -
HCWtoPc + PutoHCW - HCWremoved
    INIT HCW = 0

  d/dt (Pc) = - PctoEc - PctoHCW + EctoPc + HCWtoPc + deponskin - PcDieOff - ShedtoEc
    INIT Pc = 26

  d/dt (Pu) = + HCWtoPu + EutoPu - PutoEu - PutoHCW - PuDieOff - ShedtoEu
    INIT Pu = 0

  d/dt (Eu) = - EutoPu + HCWtoEu - EutoHCW - EuRemoved + PutoEu - EuDieOff + ShedtoEu
    INIT Eu = 0

  {Flows}
  PctoEc = Pc*(Tip/Hand)*DepTE*TPE
  PctoHCW = IF MOD(TIME,1) <= 1/3 THEN Pc*SSTE*TWP*Hand/SkinAreaPt ELSE 0
  EcRemoved = pulse(Ec*SDd_eff,0,24)
  HCWtoPu = IF MOD(TIME,1) > 1/3 AND MOD(TIME,1) <= 2/3 THEN HCW*SSTE*TWP ELSE 0
  EctoHCW = IF MOD(TIME,1) <= 1/3 THEN Ec*(Palm/SurfAreaEt)*WEPTE*TWE ELSE 0
  EutoPu = Eu*PUTE*TPE*(Tip/SurfAreaEt)
  HCWtoEu = IF MOD(TIME,1) > 1/3 AND MOD(TIME,1) <= 2/3 THEN
HCW*(palm/SkinAreaWt)*WEDTE*TWE ELSE 0
  HCWtoEc = IF MOD(TIME,1) <= 1/3 THEN HCW*(Palm/SkinAreaWt)*WEDTE*TWE ELSE 0
  EutoHCW = IF MOD(TIME,1) > 1/3 AND MOD(TIME,1) <= 2/3 THEN
Eu*(palm/SurfAreaEt)*WEPTE*TWE ELSE 0
  HCWDieOff = HCW*DieP
  EuRemoved = pulse(Eu*SDd_eff,0,24)
  PutoEu = Pu*(Tip/Hand)*DepTE*TPE
  EctoPc = Ec*PUTE*TPE*(Tip/SurfAreaEt)
  HCWtoPc = IF MOD(TIME,1) <=1/3 THEN HCW*SSTE*TWP ELSE 0
  PutoHCW = IF MOD(TIME,1) > 1/3 AND MOD(TIME,1) <= 2/3 THEN Pu*SSTE*TWP*Hand/SkinAreaPt
ELSE 0
  deponskin = alpha*SkinAreaPt
  PcDieOff = Pc*DieP
  PuDieOff = Pu*DieP
  EcDieoff = Ec*DieE
  EuDieOff = Eu*DieE
  HCWremoved = pulse (HH, 0.333, 1) + pulse (HH, 0.666, 1) + pulse (alltoHCW, 8, 8)
  ShedtoEc = Pc*alpha
  ShedtoEu = Pu*alpha

  {Functions}
  HH = HCW*HSk*HH_eff*C_eff

```
{Globals}
LIMIT HCW>=0

alpha=0.1/24            ; per hour
                        ;fraction of shed squamous cells with viable bacteria = 0.1/day.
                        ;Therefore, alpha=0.1/24 hours= 0.004166667
                        ;From healthy skin, approx 10^7 particles are disseminated into air/day,
                        ;& 10% of these skin squames contain viable bacteria}

Tip = 1                 ;contact surface area of finger tip (cm2)
Palm=150                ;contact surface area of palm (cm2)

Hand = 300              ;Area of hand (cm2)
                        ; also equals "palm x 2" to represent the use of both hands by the HCW

SurfAreaEt=2000         ; total exposed surface area for all persons and surfaces (cm2)
SkinAreaPt=2000         ;total exposed skin area for patients (cm2)
SkinAreaWt=300          ;total exposed  skin area for HCW (hand only)   (cm2)

TPE=0.134*60            ;per hour:  Touching Rate of Patient with non-porous Environment  = 0.134 per
min X 60 min/hr = 8.04/hr
TWE=0.4*60              ;per hour:  Touching Rate of HCW with Environment = 8/hr i.e.24/hr only during
20mins visit
TWP=0.4*60              ;per hour:  Touching Rate of HCW with Patient = 8/hr i.e.24/hr only during 20mins
visit

DieP = 0.00353*60       ;per hour:  Attenuation rate from any person's hand/skin - per min = 0.00353 per
min X 60 min/hr = 0.2118/hr
DieE = 0.3726/24        ;per hour:  attenuation rate from non-porous surfaces according to my data:
                        ;after day 3 = 0.3726 per day => 0.3726 per day / 24 hours = 0.015525 per hour

PUTE=0.2412             ;Pick-Up Transfer Effeciency - PATIENT/ENV- Fraction transferred from Env to
Person
DepTE=0.056             ;Deposit Transfer Efficiency - PATIENT/ENV - Fraction transferred from the
Person to the Env
WEPTE=0.2412            ;Pick-Up Transfer Effeciency - HCW/ENV- Fraction transferred from Env to
Person CAN CHG FOR GLOVE USE (=0.1063 WITH GLOVES)
WEDTE=0.056             ;Deposit Transfer Efficiency - HCW/ENV - Fraction transferred from the Person to
the Env CHG FOR GLOVE USE (=0.0296 WITH GLOVES)
SSTE = 0.3253           ;Skin-Skin Transfer Efficiency-Fraction transferred from Patient skin to HCW skin
CHG FOR GLOVE USE (=0.1063 WITH GLOVES)

HH=HCW*(HSk)*HH_eff*C_eff
HSk=Hand/(SkinAreaWt)
   HH_eff = 0.75        ; efficacy for all HH time points
   C_eff = 0.66         ; % compliance with precautionary methods (i.e. handwashing)
   SDd_eff = 0.75       ; daily surface decontamination


{End Globals}
```

CHAPTER VII

Conclusion

This dissertation culminates with five primary key outcomes: First, phenotype differences between clinical and environmental isolates were identified, specifically multidrug resistance, biofilm formation and desiccation tolerance. An evaluation of these characteristics in relationship to each other revealed that environmental survival among <u>environmental</u> strains was contingent upon high biofilm formation and a multidrug *negative* phenotype, whereas environmental survival for <u>clinical</u> strains was strongest among those that were multidrug *positive*. Second, it was determined that the detached cells of the biofilm can be discriminated from their planktonic counterparts by antibiotic susceptibility profiles. Third, it was observed that *A. baumannii* cells weakly attached to hydrophilic surfaces, such as glass and polypropylene, forming poor biofilms, whereas polycarbonate, a hydrophobic surface type, was favorable for strong biofilm formation. Fourth, the transfer of *A. baumannii* between the fingerpad and a surface was shown to be an asymmetrical event, where the pickup of pathogens from a surface was statistically greater than the deposit of pathogens to the surface. Lastly, the common assumption of symmetry in the mathematical estimation of pathogen transfer was demonstrated to produce an overestimation of contamination levels in the environment and an underestimation of the role of the healthcare worker. The key outcomes from this dissertation were determined from five studies summarized below.

The first study of this dissertation evaluated the impact of biofilm formation and multidrug resistance (MDR) on environmental survival of clinical and environmental isolates of *A. baumannii*. This investigation required the collection of *A. baumannii* isolates from infected patients and from the hospital environment. A total of 132 clinical isolates from 115 patients and 54 environmental isolates were collected from the University of Michigan Hospital over an 18 month period. Select clinical and environmental isolates were compared on the basis of their rep-PCR banding patterns, biofilm formation, antibiotic resistance profiles, and desiccation tolerance. Of the isolates that shared a single rep-type, 64% were MDR positive compared to 8% of isolates with different rep-types. This study found that the high biofilm forming, clinical, MDR positive strains were 50% less likely to die of desiccation than low biofilm, non-MDR strains. In contrast, environmental, MDR positive, low biofilm forming strains had a 2.7 times *increase* in risk of cell death due to desiccation compared to their MDR negative counterparts. MDR negative, high biofilm forming environmental strains had a 60% *decrease* in risk compared to their low biofilm forming counterparts. This study demonstrates that the MDR positive phenotype imposes a fitness cost on *A. baumannii* environmental isolates by significantly decreasing desiccation tolerance, even in the presence of the high biofilm phenotype. By contrast the MDR positive phenotype does not affect desiccation tolerance among clinical isolates, and the high biofilm phenotype increases desiccation tolerance. In the absence of the MDR phenotype, biofilm formation improved desiccation tolerance in both clinical and environmental isolates but the impact on survival was significantly greater for environmental isolates. This research clarifies the current understanding of the MDR phenotype in environmental persistence and demonstrates that it is dependent upon environmental conditions.

Understanding antibiotic susceptibility patterns over the life cycle of the biofilm is important for the development of effective therapeutic strategies that minimize the emergence of antibiotic resistance. The second study compared the antibiotic susceptibilities of *A. baumannii* planktonic cells, biofilm cells, and the detached cells of the biofilm using 5 clinical and 5 environmental *A. baumannii* isolates. Eight antibiotics from different drug classes were tested. In this study, the odds of being resistant to an antimicrobial drug was 2 times greater for detached biofilm cells compared to planktonic cells (p=0.04) and biofilms were 24.6 times more likely to be resistant than detached biofilm cells (p<0.0001). These results demonstrate that that the minimum inhibitory concentration of antibiotic needed for detached biofilm cells was greater than that required for planktonic cells, yet less than that needed for biofilm cells.

Bacterial adherence to a surface is acritical step in the formation of a biofilm. The third study examined the ability for *A. baumannii* biofilms to form on several surface types common to the hospital environment. Six non-porous material types were evaluated: glass, ceramic, stainless steel, rubber, polycarbonate plastic and polypropylene plastic. The six material types were exposed to *A. baumannii* ATCC 17978 biofilms using a CDC biofilm reactor. Biofilms were visualized and quantified using fluorescent staining and imaging by confocal laser scanning microscope and by direct viable cell counts. The mean biomass values for biofilms grown on glass, rubber, porcelain, polypropylene, stainless steel and polycarbonate were 0.04, 0.26, 0.62, 1.00, 2.08 and 2.70 $\mu m^3/\mu m^2$ respectively. Polycarbonate, a hydrophobic surface type, developed statistically more biofilm mass than glass, rubber, porcelain and polypropylene, which are more hydrophilic surface types.

The fourth study estimated important unknown environmental transfer parameters of *A.baumannii*, the pick-up and deposit transfer efficiencies between the fingerpad and a surface.

This study was performed with and without latex gloves, for six non-porous material types (fomites) using *A. baumannii* ATCC 17978 and ten human volunteers (UM IRB, HUM00075484). Fomite-to-fingerpad transfer efficiency was 24.1% and the fingerpad-to-fomite transfer efficiency was 5.6%. When latex gloves were worn, the fomite-to-fingerpad transfer efficiency was reduced by 55.9% (to 10.6%) and the fingerpad-to-fomite transfer efficiency was reduced by 47.1% (to 3.0%). The average transfer efficiency between two skin surfaces was 32.5%. These results emphasize the importance of frequent glove changes during patient care for the reduction of pathogen transmission.

The fifth study evaluated the impact of the results obtained in the 4th study on the mathematical estimation of environmentally mediated pathogen transfer by comparing two different mathematical models of symmetry with a model that assumes asymmetrical transfer efficiencies (as described in Chapter V). An *A. baumannii* fate-and-transport mathematical model was developed to simulate the touching interactions between non-porous environmental surfaces, the healthcare worker (HCW) and patients. This model was first simulated with the assumption of bacterial transfer asymmetry (as measured in Chapter V). For the second round of simulations, two different variations of the traditional simplifying assumption of bacterial transfer symmetry was applied. The differences in pathogen dissemination outcomes between the simulations were compared. This study demonstrated that both models of symmetry (using either standard symmetrical methods or the mean bi-directional method) consistently overestimate or underestimate the contamination levels of *A. baumannii* compared to the asymmetrical transfer efficiency model, regardless of the level of environmental or healthcare worker influence on transmission.

This dissertation was innovative in several ways. This research is the first to evaluate the impact of biofilm formation and multidrug resistance on environmental survival of both clinical and environmental isolates of *A. baumannii*. The results suggest that detached biofilm cells have different properties than planktonic cells, thereby identifying an alternative target for the prevention and control of biofilms. With respect to biofilm attachment, this is the first study to evaluate differences in *A. baumannii* biofilm formation across a range of non-porous surface types, indicating materials that should be avoided in the manufacture of invasive devices. In addition, this is the first study to address the current simplifying assumption of bacterial transfer symmetry in the mathematical estimation of environmentally mediated pathogen transport.

Several important areas for future research have been identified. Genetic studies are needed to identify targets that can help explain the variation in survival strategies observed between clinical and environmental isolates that are multidrug resistant. Studies identifying other distinguishing characteristics of the detached biofilm cell population are needed to develop new therapies that target these cells. The bidirectional transfer efficiencies of other microorganisms that undergo transmission through the environment need to be quantified. The development of a fate-and-transport model that relaxes simplifying assumptions by using more pathogen specific parameterization is needed for more robust estimations of pathogen transport.

The significance of this dissertation is that it demonstrates that the associations between multidrug resistance, biofilm formation, and desiccation tolerance are mediated by environmental conditions and provides data needed to help mitigate environmental survival of multidrug resistant pathogens. Collectively, this research presents evidence needed to improve current methods for the treatment of biofilm-related infections and to minimize environmental persistence and transmission of *A. baumannii*. Further, this investigation improves the accuracy

of the mathematical estimation of environmental mediated infectious disease transmission and

strengthens current guidelines for the control of hospital-acquired infections.